Report No. 6

RF 2411



# Laboratory for Isotope Geology and Geochemistry



Institute of Polar Studies
and
Department of Geology
THE OHIO STATE UNIVERSITY

# ISOTOPE GEOCHEMISTRY OF STRONTIUM AND GEOCHRONOLOGY IN THE TRANSANTARCTIC MOUNTAINS

January, 1972



Submitted to:
The National Science Foundation
Grant GA-898X

# ISOTOPE GEOCHEMISTRY OF STRONTIUM AND GEOCHRONOLOGY IN THE TRANSANTARCTIC MOUNTAINS

by

John Gunner, John R. Bowman
and G. Faure

Institute of Polar Studies
and
Department of Geology and Mineralogy
The Ohio State University
Columbus, Ohio 43210

Fourth Annual Progress Report
Grant GA-898X

The National Science Foundation
Washington, D.C.

The Ohio State University
Research Foundation

TABLE OF CONTENTS

## PREFACE

This is the fourth annual progress report prepared for the National Science Foundation which has supported research on the geochronology and geochemistry of rocks from Antarctica in this laboratory since 1967. The results reported here are preliminary in nature and should be quoted only after prior consultation with the undersigned. Copies of this report will be made available free of charge upon request.

The Laboratory for Isotope Geology and Geochemistry has now issued six reports in this series, as listed below:

Report No. 1. The geochronology of the Keweenawan rocks of Michigan and origin of the copper deposits. 1967, 41p.

Report No. 2. Strontium isotope composition and trace element concentrations in Lake Huron and its principal tributaries. 1967, 109p.

Report No. 3. Geochronology of the Transantarctic Mountains. 1968, 79p.

Report No. 4. The isotope composition of strontium of Lake Vanda and Lake Bonney in Southern Victoria Land, Antarctica. 1969, 82p.

Report No. 5. Studies in the geochronology and geochemistry of the Transantarctic Mountains. 1970, 180p.

A few copies of these reports are still available upon request.

I would like to take this opportunity to thank John F. Splettstoesser of the Institute of Polar Studies for his help with the administration of the grant and acknowledge the assistance of Chester E. Ball and Mrs. Ada G. Simon in the production of this report.

Gunter Faure
January, 1972

# AGE AND ORIGIN OF THE HOPE AND IDA GRANITES, BEARDMORE GLACIER REGION, ANTARCTICA

(Excerpts of a Ph.D. dissertation by John Gunner submitted to the Department of Geology in 1971)

## Introduction

A study of the origin of the Hope and Ida Granites can contribute significantly to answering four main questions about the Basement Complex of the Transantarctic Mountains: (1) Why do these granites crop out in so extensive an area? (2) Why are the different plutons so similar petrographically? (3) What is the relationship of the Hope and Ida Granites to the Ross Orogeny? (4) What light can a study of the origin of these granites throw on processes of granite formation in general?

## Previous Work

Most previous work on the Granite Harbour Intrusives in the Beardmore Glacier region has consisted of field mapping, petrographic description and some K-Ar dating. Gunn and Walcott (1962, p. 417) noted the petrographic similarity of the granites in the region. They suggested that the separate plutons were the "surface expression of a single, large, subjacent batholith." Grindley (1963, p. 319) described similar rocks from plutons in the Queen Elizabeth and Miller Ranges. He reported that the intrusions were "completely discordant and structureless and post-date the folding of the greywackes" (Goldie Formation). He observed weak lineation and well-developed jointing in Hope Granite in the Miller Range, and inferred the presence of "rather more stress" at the time of intrusion in this area. He also suggested that the country rocks in the Miller Range had been at "higher temperature" at this time, as shown by "marginal assimilation, lit-par-lit injection effects, and extensive feldspathization and formation of sillimanite at contacts." Laird and others (in press) report the presence of a body biotite-bearing tonalite (quartz diorite) intruding Shackleton Limestone at the north-east corner of Bartrum Plateau in the Queen Elizabeth Range (Figs. 1 and 2). The presence of calcic augite near the marginal contact of this intrusion may indicate that its parent magma was more acidic but exchanged material with the country rock, which is largely marble.

Oliver (in press) described granite and granodiorite from the Commonwealth and Separation Ranges (Figs. 1 and 2). From his description, and from work in the same area by the author during 1969-70, these rocks can be included as Hope Granite. Oliver (in press) also reported the presence of quartz diorite in this area. He described an abundance of xenoliths in the rock "which appear to be predominantly of country rock metasediment." Small plugs of quartz diorite intruding folded metasediments of the Goldie Formation have been mapped by the author at Hampton

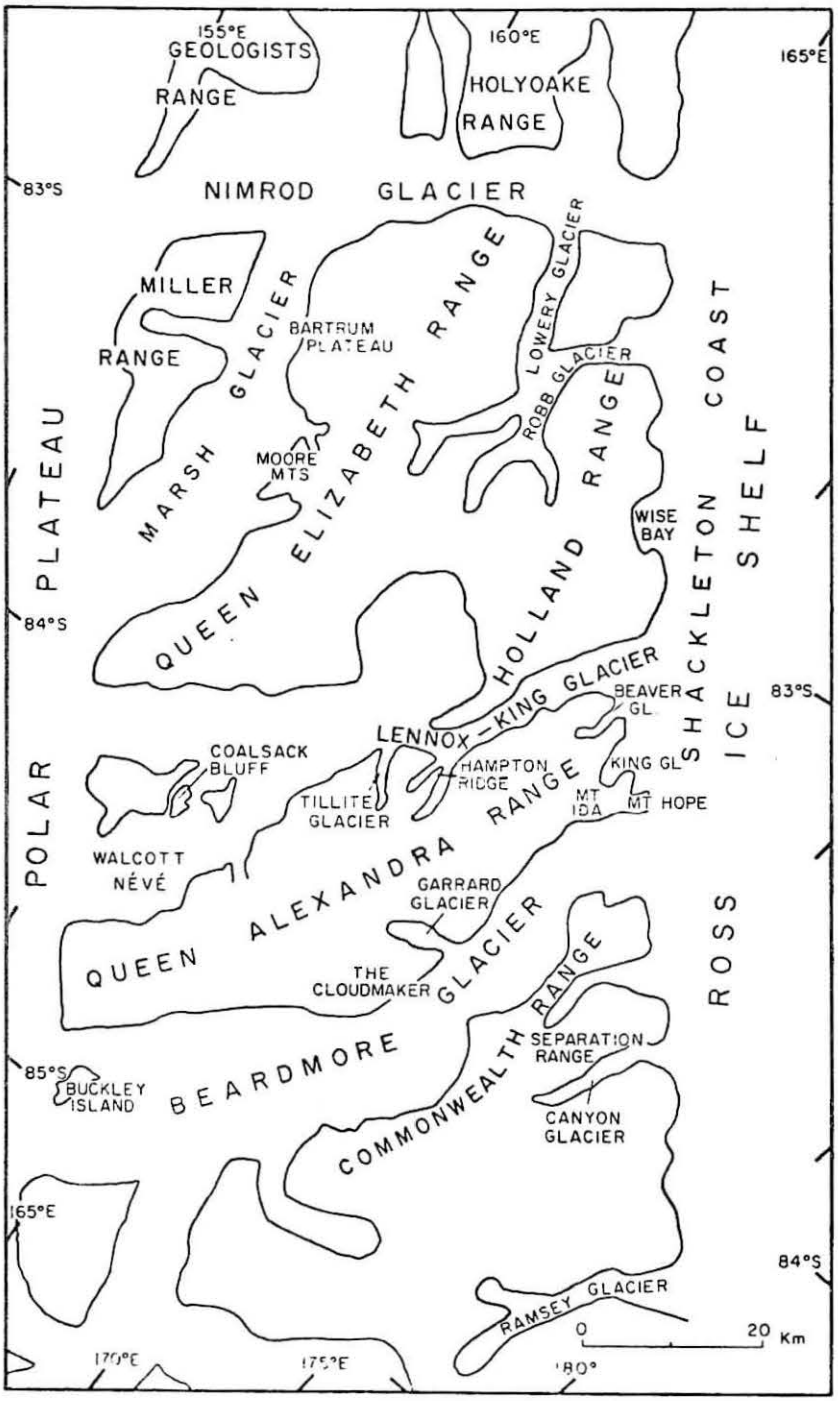
155°E
GEOLOGISTS
RANGE
160°E
HOLYOAKE
RANGE
165°E
83°S
NIMROD GLACIER
MILLER
RANGE
MARSH GLACIER
BARTRUM PLATEAU
QUEEN ELIZABETH RANGE
LOWERY GLACIER
ROBB GLACIER
HOLLAND RANGE
SHACKLETON ICE SHELF COAST
MOORE MTS
WISE BAY
POLAR PLATEAU
84°S
QUEEN
BEAVER GL
83°S
LENNOX-KING GLACIER
COALSACK BLUFF
HAMPTON RIDGE
KING GL
TILLITE GLACIER
MT IDA
MT HOPE
ALEXANDRA RANGE
WALCOTT NÉVÉ
GARRARD GLACIER
QUEEN ALEXANDRA GLACIER
THE CLOUDMAKER
ROSS
85°S
BUCKLEY ISLAND
BEARDMORE
COMMONWEALTH RANGE
SEPARATION RANGE
CANYON GLACIER
165°E
84°S
RAMSEY GLACIER
0
20 Km
170°E
175°E
180°

Figure 1

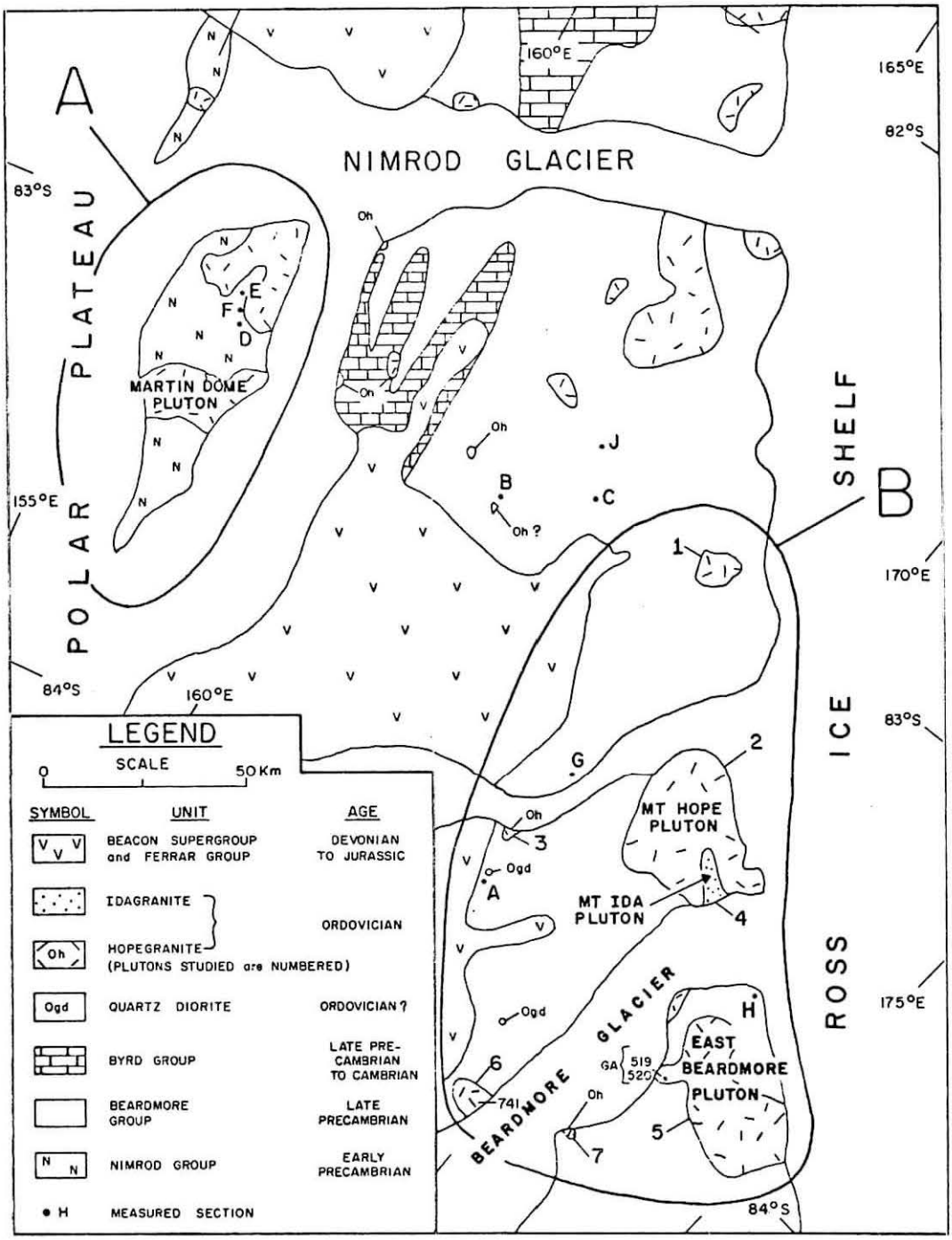
A
B
NIMROD GLACIER
POLAR PLATEAU
ROSS ICE SHELF
MARTIN DOME PLUTON
MT HOPE PLUTON
MT IDA PLUTON
EAST BEARDMORE PLUTON
BEARDMORE GLACIER
160°E
165°E
170°E
175°E
155°E
82°S
83°S
84°S
LEGEND
SCALE
0
50 Km
SYMBOL
UNIT
AGE
BEACON SUPERGROUP and FERRAR GROUP
DEVONIAN TO JURASSIC
IDAGRANITE
HOPEGRANITE
ORDOVICIAN
(PLUTONS STUDIED are NUMBERED)
QUARTZ DIORITE
ORDOVICIAN?
BYRD GROUP
LATE PRE-CAMBRIAN TO CAMBRIAN
BEARDMORE GROUP
LATE PRECAMBRIAN
NIMROD GROUP
EARLY PRECAMBRIAN
MEASURED SECTION
GA 519
GA 520
741

Figure 2

Ridge and at the Garrard Glacier (Figs. 1 and 2). These intrusions appear to be petrographically similar to those described by Oliver, except for a smaller abundance of xenoliths.

Samples of Hope Granite from a number of localities in the Beardmore Glacier region have been dated by the K-Ar method (McDougall and Grindley, 1965). The locations of the samples dated are plotted in Figures 2 and 3 and the results are given in Table 1. K-Ar dates on biotites from Hope Granite at Celebration Pass in the Commonwealth Range (two samples) and at Astro Glacier in the Miller Range (one sample) agree closely at about 460 m.y. Muscovite from a pegmatite in Hope Granite at Snowshoe Pass (Fig. 3) and biotite from Hope Granite at The Cloudmaker (Fig. 1) gave dates of 478 m.y. and 479 m.y., respectively. The K-Ar data summarized above suggest that the Hope Granite intrusions studied were emplaced during the Ordovician period (Harland et al., 1964) and cooled through the argon retention temperatures of micas about 450 to 479 m.y. ago. This is consistent with the argon loss time pattern shown by micas from the Nimrod Group (McDougall and Grindley, 1965) as mentioned above.

Table 1: K-Ar Dates on Micas from Hope Granite in the Beardmore Glacier Region

| Sample | Mineral | K (wt %) | $^{40}Ar^*/^{40}K$ | Air corr.[a] | Date (m.y.) | Rock-type & location |
|---|---|---|---|---|---|---|
| GA 766[b] | Biotite | 7.56<br>7.58 | 0.0307 | 2.2 | 463 | Hope Granite Astro Glacier |
| GA 767[b] | Muscovite | 8.46<br>8.45 | 0.0317 | 5.7 | 478 | Pegmatite in Hope Granite Snowshoe Pass |
| GA 519[b] | Biotite | 7.56<br>7.56 | 0.0307 | 2.3 | 465 | Hope Granite Celebration Pass |
| GA 520[b] | Biotite | 7.39<br>7.42 | 0.0297 | 1.9 | 450 | Hope Granite Celebration Pass |
| 741[c] | Biotite | 7.36<br>7.35 | 0.0319 | 3.3 | 479 | Hope Granite The Cloud-maker |

*Radiogenic argon
[a]Air correction in per cent
[b]Data from McDougall and Grindley (1965, p. 308)
[c]This paper. Analyst R. J. Fleck, Ohio State University

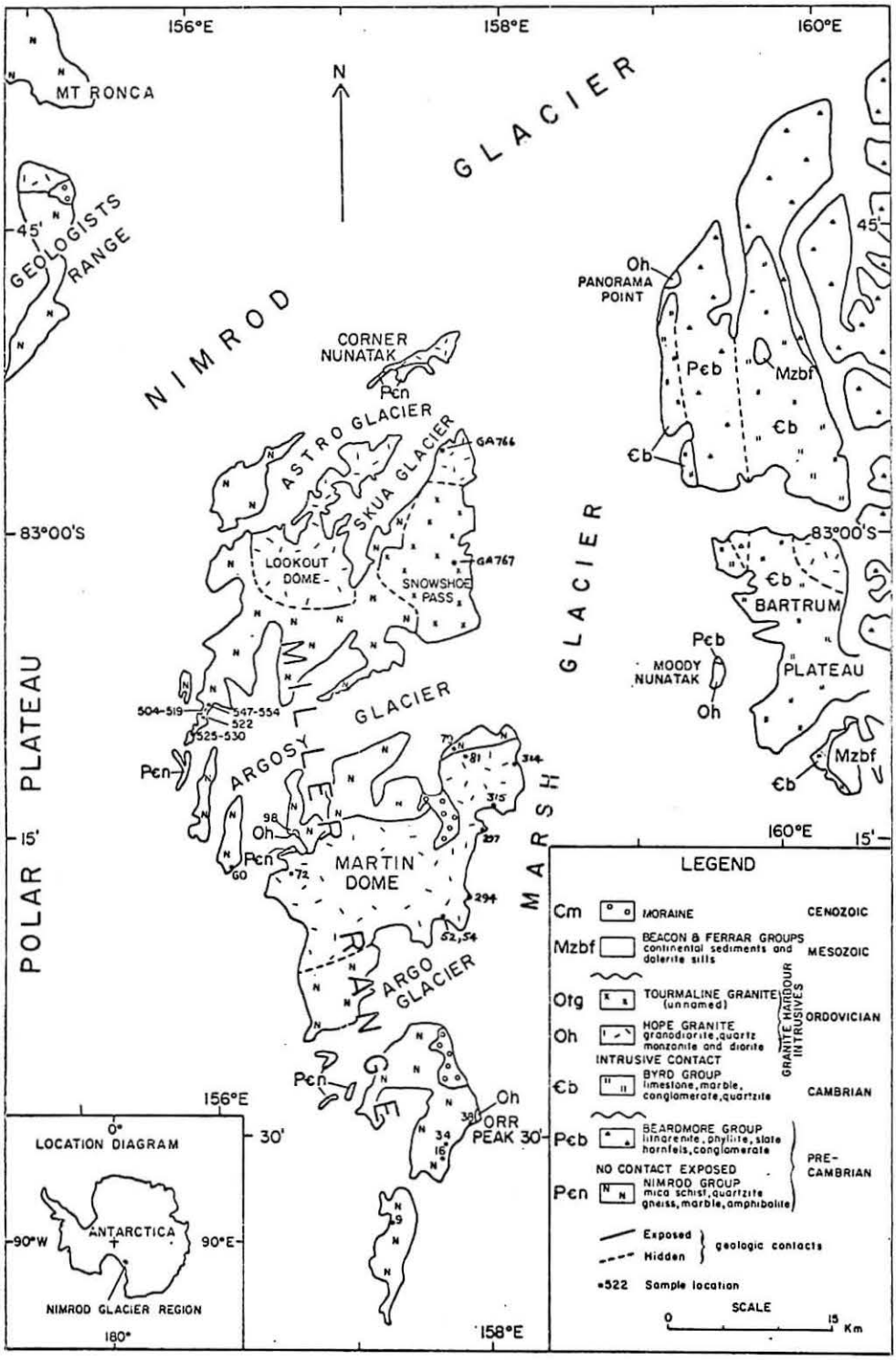
156°E
158°E
160°E
N
MT RONCA
GEOLOGISTS RANGE
45'
NIMROD GLACIER
CORNER NUNATAK
Pcn
ASTRO GLACIER
SKUA GLACIER
GA766
GA767
LOOKOUT DOME
SNOWSHOE PASS
83°00'S
POLAR PLATEAU
504-519
547-554
522
525-530
ARGOSY GLACIER
MARSH GLACIER
MARTIN DOME
RANGE
ARGO GLACIER
ORR PEAK
Oh
PANORAMA POINT
Pεb
Mzbf
εb
BARTRUM PLATEAU
MOODY NUNATAK
15'
30'
LOCATION DIAGRAM
ANTARCTICA
90°W
90°E
180°
NIMROD GLACIER REGION
LEGEND
Cm MORAINE CENOZOIC
Mzbf BEACON & FERRAR GROUPS continental sediments and dolerite sills MESOZOIC
Otg TOURMALINE GRANITE (unnamed)
Oh HOPE GRANITE granodiorite, quartz monzonite and diorite
GRANITE HARBOUR INTRUSIVES
ORDOVICIAN
INTRUSIVE CONTACT
εb BYRD GROUP limestone, marble, conglomerate, quartzite CAMBRIAN
Pεb BEARDMORE GROUP litharenite, phyllite, slate hornfels, conglomerate
NO CONTACT EXPOSED
Pcn NIMROD GROUP mica schist, quartzite gneiss, marble, amphibolite
PRE-CAMBRIAN
Exposed
Hidden
geologic contacts
•522 Sample location
SCALE
0
15 Km

Figure 3

## Objectives

The previous descriptive and K-Ar work on the Hope Granite contributed only indirectly to the solution of the four problems outlined previously. It indicated that the Hope Granite intrusions throughout the region were petrographically similar and broadly contemporaneous. But it threw little light on genetic relationships between the different intrusions and the country rock.

This study was therefore undertaken to test two major hypotheses: (1) Hope and Ida Granite intrusions in the Beardmore Glacier region have a common magmatic origin; and (2) Individual Hope Granite intrusions were derived by melting of rocks similar to those which now surround them.

## Methods

As a preliminary test, it was decided to study two plutons, intruded into country rocks of contrasting age and rock-type, to determine whether differences in initial magma composition and relationships between magma and country were detectable. The intrusions chosen were the Mt. Hope pluton, located between the Beardmore and Lennox-King Glaciers (Fig. 2) and the Martin Dome pluton, located in the Miller Range between the Argosy and Argo Glaciers (Fig. 3). Both these intrusions consist of Hope Granite, but the Mt. Hope pluton intrudes the Goldie Formation, whereas the Martin Dome pluton intrudes the Nimrod Group, as described above.

For this pilot study the Rb-Sr isochron technique was used, as described in Appendix B of Gunner (1971). A suite of whole-rock samples from each intrusion was analyzed by the Rb-Sr method and an isochron was plotted for each suite. By this method it was possible to determine three parameters: the age of each intrusion, the degree of homogeneity of strontium isotopes in each intrusion at the time of crystallization, and the initial $^{87}Sr/^{86}Sr$ ratio ($R_i$) of the magmas from which each intrusion crystallized.

For this study the Rb-Sr isochron technique has significant advantages over non-isotopic chemical methods. While it is well known that major and trace elements are fractionated by magmatic crystallization, there is no known geologic process which fractionates strontium isotopes. thus the value of $R_i$ obtained for a sample of Hope Granite should be representative of the isotopic composition of strontium in the magma from which that sample crystallized. By contrast, a non-isotopic parameter, such as the K/Rb concentration ratio of the same sample, would not be so simply related to the K/Rb ratio of the original magma. It would depend on the mineralogy of the sample, and hence on the degree of crystal fractionation which the magma had undergone. It would depend also on the distribution coefficients of trace elements between the liquid and solid phases, and these, in turn, are temperature-dependent.

After the pilot study produced significant results, the second phase of this part of the project was started. This consisted of two parts: (1) Rb-Sr analysis of samples from five other Hope Granite plutons in the Shackleton Coast ranges and from the Mt. Ida pluton (Fig. 4); and (2) An attempt to obtain representative values of $R_i$ for the Goldie Formation and the Nimrod Group.

During the 1969-70 field season the author measured six stratigraphic sections in the Goldie Formation and three in the Nimrod Group (locations, Fig. 2; descriptions, Appendix A of Gunner(1971)). Samples of each lithologic unit recognized in these sections were collected. In order to obtain the best approximation to representative samples of the Goldie Formation and the Nimrod Group, composite samples of each of a number of selected stratigraphic sections were prepared, as described in Appendix A of Gunner (1971). Only fresh samples free of quartz and calcite veins were taken. For each section the samples were ground to pass through a 120 mesh screen and homogenized. The powders were then mixed together in weight proportion to the thickness of the units which they represented. The composite thus obtained was homogenized. In sections A and D the boundaries of many lithologic units were obscured by snow or scree cover. The samples from these sections were grouped by rock-type, for example arenite and argillite. Arenite and argillite composites were then prepared by mixing all the samples of each type in equal weight proportion. These arenite and argillite composites were then mixed in proportion to the estimated thickness of arenite and argillite in the section, to form the combined composite. Composites are identified by the letter of the stratigraphic section followed by a hyphen and a number (e.g. C-1). Details of preparation and numbering of composites are given in Appendix A of Gunner (1971).

In addition to the Rb-Sr work, chemical analyses of major elements in selected samples were performed by Andrew McCreath and Sons Inc., Harrisburg, Pennsylvania. Whole-rock samples from the Mt. Hope, Mt. Ida and Martin Dome plutons were analyzed in order to make compositional comparisons between them and to obtain information on the crystallization histories of the magmas involved. Selected composites of the Nimrod Group and the Goldie Formation were analyzed to determine whether such rocks could be melted to form the magmas from which the plutons crystallized.

## Rb-Sr Analyses

### Hope and Ida Granites

The Rb-Sr analytical results on Hope and Ida Granite samples are presented in Table 2. The data are plotted in Figure 4. It is evident from Figure 4 that the Hope and Ida Granite samples define two isochrons (A and B). All the samples (Group A) from the Martin Dome pluton plot close to Isochron A; all the samples (Group B) from the remaining six

Table 2: Rb-Sr Analyses, Whole-rock Samples, Hope and Ida Granites

| Sample | Unit | $^{87}Sr/^{86}Sr$[a] | $^{87}Rb/^{86}Sr$[b] | Location |
|---|---|---|---|---|
| 52 | Hope | 0.7594 | 3.456 | Strawberry Cirque |
| 54[c] | Hope | 0.9170<br>0.9254 | 28.37 | Strawberry Cirque |
| 72 | Hope | 0.7769<br>0.7799 | 6.475 | Hockey Cirque |
| 81 | Hope | 0.7452<br>0.7465 | 3.065 | Kreiling Mesa |
| 292 | Hope | 0.7518 | 2.530 | Macdonald Bluffs |
| 297 | Hope | 0.7401 | 1.178 | Macdonald Bluffs |
| 314 | Hope | 0.7486 | 2.769 | Kreiling Mesa |
| 315 | Hope | 0.7509 | 2.694 | Dike Cirque |
| 576 | Ida | 0.8165<br>0.8183 | 16.41 | Granite Pillars |
| 593 | Hope | 0.7257 | 2.097 | Mt. Hope |
| 605 | Hope | 0.7280 | 2.816 | Yeates Bluff |
| 630 | Hope | 0.7210 | 1.966 | Threshold Nunatak |
| 647 | Hope | 0.7405 | 4.450 | Mt. Harcourt |
| 654 | Hope | 0.7292 | 2.784 | Cleft Peak |
| 672 | Hope | 0.7219 | 1.775 | Beetle Spur |
| 707 | Hope | 1.160<br>1.148 | 69.39 | Wise Bay |
| 719 | Ida | 0.8337<br>0.8295<br>0.8172 | 18.85 | King Glacier |
| 738 | Hope | 0.7715<br>0.7664 | 9.645 | Sirohi Point |
| 741 | Hope | 0.7237 | 2.248 | The Cloudmaker |

[a]Fractionation corrected assuming $^{86}Sr/^{88}Sr = 0.1194$

[b]By x-ray fluorescence

[c]Pegmatite dike

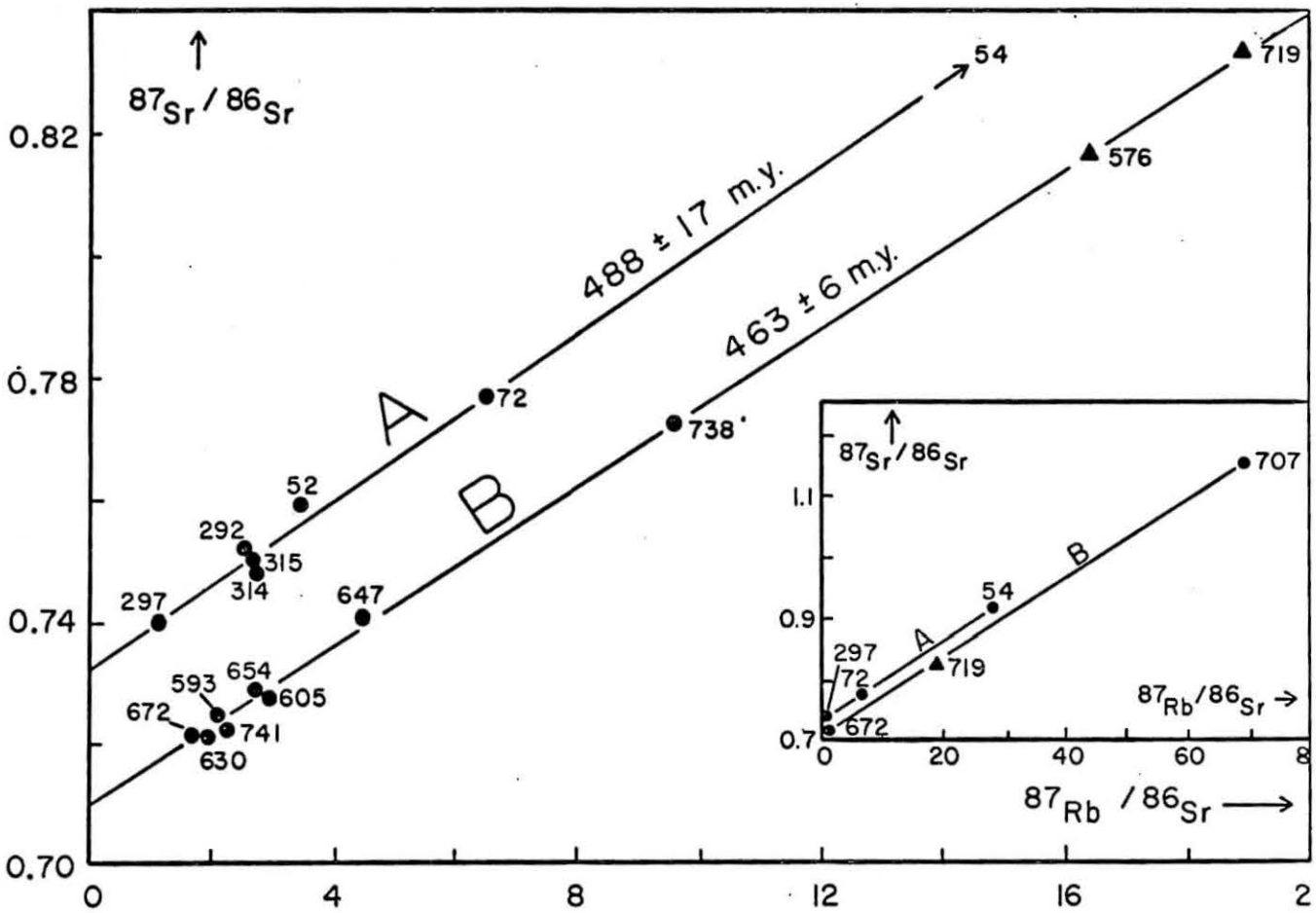


Figure 4. Rb-Sr Isochron Diagram - Whole-Rock Samples: Hope Granite (Circles) and Ida Granite (Triangles). Inset at Reduced Scale.

plutons (Fig. 2) plot close to Isochron B. The two Isochrons have similar slopes but significantly different values of $R_i$.

Seven samples from Group A define an isochron date of 486 ± 23 m.y. with $R_i$ of 0.734 ± 0.001. Eleven samples from Group B define an isochron date of 463 ± 7 m.y. with $R_i$ of 0.710 ± 0.001. Both isochrons were computed by least squares regression analysis (York, 1966; described in Appendix B of Gunner (1971).

In computing Isochron A the analysis of sample 81 was omitted. This sample has a cataclastic texture, visible in thin section, which suggests that recrystallization of quartz, feldspar and biotite occurred after the sample first crystallized. Loss of radiogenic $Sr^{87}$ during such an event would move the position of the sample on the isochron diagram and could explain why it is not colinear with the other points.

The Rb-Sr results suggest three inferences: (1) the samples in Groups A and B became closed to migration of Rb and Sr about 475 m.y. ago; (2) the strontium in each Group was isotopically homogeneous at this time; (3) the magmas from which the samples in Groups A and B crystallized had distinct strontium isotopic compositions at their time of crystallization; the $^{87}Sr/^{86}Sr$ ratios were 0.734 (Group A) and 0.710 (Group B).

The difference between the dates determined from isochrons A and B is not statistically significant, since it is smaller than the sum of the standard deviations of the dates. What is significant is the striking contrast between the initial $^{87}Sr/^{86}Sr$ ratios of the two Groups of samples, as discussed in the following section.

## Nimrod Group and Goldie Formation

### Results

Rb-Sr analyses of 13 whole-rock composites from the Nimrod Group and Goldie Formation are listed in Table 3. These data are plotted in Figure 5, together with Isochrons A and B. The point labelled N-1 is an estimate of the initial $^{87}Sr/^{86}Sr$ ratio which 17 previously analyzed metasedimentary samples of the Nimrod Group would have had 475 m.y. ago. This was calculated by averaging the values of this ratio for the 17 samples, weighing each in proportion to the strontium content of the sample, as determined by XRF. None of these samples show any petrographic evidence of a molten history. Details of composite N-1 are given in Appendix A of Gunner (1971).

The composites of the Nimrod Group and the Goldie Formation form markedly different patterns in Figure 5. The Goldie samples show a strong correlation between $^{87}Sr/^{86}Sr$ and $^{87}Rb/^{86}Sr$ ratios and plot in a narrow band which trends approximately parallel to Isochrons A and B.

Table 3: Rb-Sr Analyses, Composite Samples, Nimrod Group and Goldie Formation

| Sample | Unit | $^{87}Sr/^{86}Sr$[a] | $^{87}Rb/^{86}Sr$[b] | Location |
|---|---|---|---|---|
| A-1 | Goldie | 0.7473 | 4.176 | Hampton Ridge |
| C-1 | Goldie | 0.7195 | 1.021 | Masquerade Ridge |
| C-1[c] | Goldie | 0.7148 | - | Masquerade Ridge |
| D-1 | Nimrod | 0.7122<br>0.7100 | 0.1969 | Aurora Heights |
| D-2 | Nimrod | 0.7068<br>0.7063 | 0.0[d] | Aurora Heights |
| D-3 | Nimrod | 0.7333 | 1.423 | Aurora Heights |
| D-4 | Nimrod | 0.7492 | 1.005 | Aurora Heights |
| D-5 | Nimrod | 0.7098 | 0.2309 | Aurora Heights |
| D-6 | Nimrod | 0.7165 | 0.4855 | Aurora Heights |
| D-7 | Nimrod | 0.7106 | 0.1206 | Aurora Heights |
| G-10 | Goldie | 0.7258 | 1.706 | Vertigo Bluff |
| G-20 | Goldie | 0.7204 | 1.018 | Vertigo Bluff |
| G-30 | Goldie | 0.7539 | 5.743 | Vertigo Bluff |
| H-1 | Goldie | 0.7656 | 7.262 | Lands End Nunatak |

[a]Fractionation corrected assuming $^{86}Sr/^{88}Sr = 0.1194$
[b]By x-ray fluorescence
[c]Acid leach: analysis of soluble material
[d]Rb not detectable

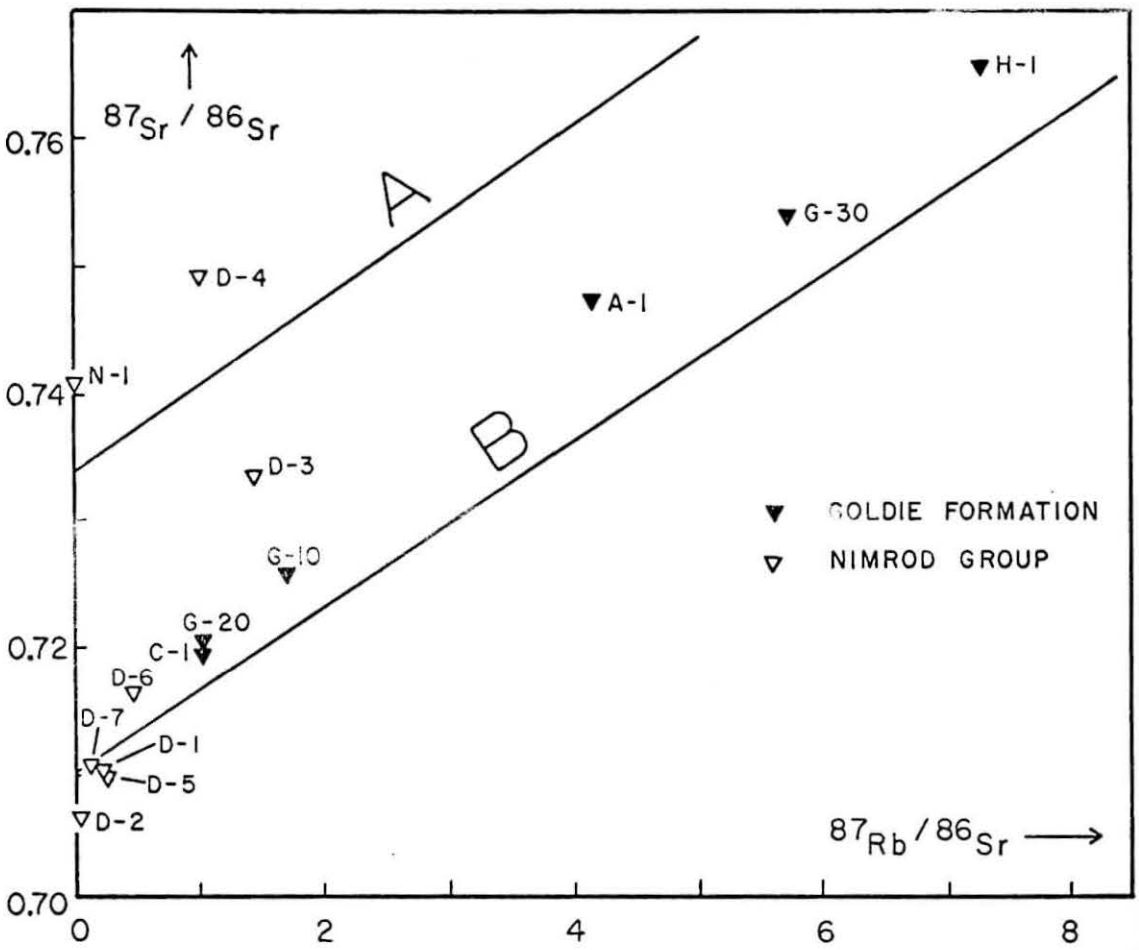


Figure 5. Rb-Sr Isochron Diagram - Whole-Rock Composites of Nimrod Group and Goldie Formation. Isochrons A and B (Figure 4) Included.

By contrast, the Nimrod samples show no significant correlation between the two ratios. The $^{87}Sr/^{86}Sr$ ratios which each sample would have had 475 m.y. ago can be constructed on the diagram. It is given by the intercept on the ordinate of a line drawn through the sample points with a slope of about 0.0066, which is the average of the slopes of Isochrons A and B. Computed by this method, the 475 m.y. initial $^{87}Sr/^{86}Sr$ ratios ($R_{475}$) of the six Goldie composites range from 0.712 to 0.720, and those of the eight Nimrod composites range from 0.707 to 0.742. This greater spread of $R_{475}$ in the case of the Nimrod Group is probably a reflection of the more varied lithologies of this unit and the consequent greater difficulty of obtaining a representative composite. Each of samples D-2 through D-7 is a composite prepared from a separate rock-type within Section D, as described in Appendix A of Gunner (1971). Sample D-1 is the combined composite which was prepared by combining samples D-2 through D-6 in proportion to the thickness in Section D of the units which they represent.

## Discussion

It has been shown that there is a significant contract in $R_i$ between the Hope Granites in Areas A and B. The question now is whether this contrast would be reflected in the isotopic compositions of the strontium which would enter the magmas if the metasedimentary rocks in Areas A and B were partially melted.

The stratigraphic and geochronological evidence discussed in Chapters III and IV of Gunner (1971) indicates that the Nimrod Group is significantly older than the Goldie Formation. Since rocks with a more prolonged crustal history should contain more radiogenic $^{87}Sr$, it should be expected that the Nimrod Group would have higher average $^{87}Sr/^{86}Sr$ ratios than the Goldie Formation. It may be significant to this discussion that the Goldie composites, A-1, C-1, G-10, G-20, G-30 and H-1, form a nearly linear array in Figure 5. A Rb-Sr isochron has been fitted to these points by the method of York (1966). It gives a date of 538 ± 28 ($\sigma$) m.y. and an initial $^{87}Sr/^{86}Sr$ ratio of 0.713 ± 0.002 ($\sigma$). The Goldie Formation is overlain unconformably by the Cambrian Byrd Group, which must be at least 550 m.y. old. The 538 m.y. date cannot therefore be the age of sedimentation of the Goldie Formation. It probably represents a time of partial isotopic homogenization of the Formation, although it is difficult to explain how rocks so widely separated geographically could be homogenized in this way. In the absence of more stratigraphic and structural data, one can only speculate that the event occurred during the early phases of the Ross Orogeny. If the Goldie Formation had a nearly homogeneous $^{87}Sr/^{86}Sr$ ratio of 0.713 about 538 m.y. ago, there is little probability that it contained significant quantities of material with $^{87}Sr/^{86}Sr$ ratios of the order of 0.734 less than 100 m.y. later.

The narrow range of $R_{475}$ values which the Goldie composites show suggests that the strontium in the Goldie Formation, as represented by the stratigraphic sections A, C, G and H, was isotopically relatively homogeneous at this time and had average $^{87}Sr/^{86}Sr$ ratios in the range 0.712 to 0.720.

The Nimrod Group shows no such isotopic homogeneity. The two combined composites, D-1 and N-1, which were prepared from samples collected at different stratigraphic and geographic locations, have markedly different values of $R_{475}$. This suggests that the Nimrod Group was spatially, as well as lithologically, heterogeneous in strontium isotopic composition 475 m.y. ago. It is therefore not possible to infer what the $^{87}Sr/^{86}Sr$ ratio of a partial melt of the Nimrod Group at this time would have been.

Nevertheless, the Nimrod Group contains a significant quantity of material which had $^{87}Sr/^{86}Sr$ ratios comparable to that in the magma represented by isochron A at its time of crystallization. There are not sufficient data to justify speculation as to the most probable strontium isotopic composition of a partial melt of any specific part of the Nimrod Group. However, it may be significant that a major part of the strontium in the combined composite D-1 was contributed by sample D-2, which is a composite of two marble samples. Such rocks would be among the most refractory under conditions of anatexis, and it is debatable whether much of their strontium would enter any but the most complete melts. A reduction in the contribution of strontium from sample D-2 would significantly increase the $^{87}Sr/^{86}Sr$ ratio of the combined composite of Section D.

In contrast to the Nimrod Group, none of the six composites of the Goldie Formation had a $^{87}Sr/^{86}Sr$ ratio comparable to that of the Martin Dome pluton at its time of crystallization. There is no evidence that melting of rocks of the Goldie Formation alone could have produced a magma with a $^{87}Sr/^{86}Sr$ ratio of 0.734. On the other hand, samples C-1 and G-20 both plot close to isochron B, and it seems likely that rocks in Sections C and G had $^{87}Sr/^{86}Sr$ ratios less than 0.710, 463 m.y. ago (isochron B). The strontium isotopic composition of the magma represented by isochron B is therefore quite compatible with an origin of this magma by partial melting of rocks of the Goldie Formation, as represented in Sections A, C, G and H.

## Major Element Chemical Analyses

### Results

Chemical analyses and norms of whole-rock single and composite samples from the Martin Dome and Shackleton Coast plutons are presented in Table 4. Samples MD-1 and SC-1 are composites of selected samples from the Martin Dome and Shackleton Coast plutons, respectively. Only petrographically normal Hope Granite samples which fit Isochrons A or B were used in preparing these composites, as described in Appendix A.

Table 4: Chemical Analyses and Norms: (1) Whole-rock Samples, Hope and Ida Granites

| Sample | Chemical Analyses | | | | | | Sample | CIPW Norms | | | | | |
|---|---|---|---|---|---|---|---|---|---|---|---|---|---|
| | [a]295 | [a]MD-1 | [b]593 | [b]SC-1 | [c]575 | [d]637 | | 295 | MD-1 | 593 | SC-1 | 575 | 637 |
| $SiO_2$ | 69.39 | 67.81 | 63.20 | 67.54 | 73.65 | 74.11 | Quartz | 29.02 | 28.06 | 21.73 | 23.73 | 36.41 | 42.35 |
| $TiO_2$ | 0.79 | 0.46 | 0.79 | 0.45 | 0.25 | 0.32 | Orthoclase | 19.53 | 24.39 | 25.14 | 29.16 | 30.17 | 22.23 |
| $Al_2O_3$ | 15.91 | 15.56 | 16.66 | 15.34 | 14.00 | 13.83 | Albite | 21.74 | 23.17 | 24.43 | 25.29 | 24.26 | 23.59 |
| $Fe_2O_3$ | 0.66 | 1.29 | 2.14 | 0.90 | 0.70 | 0.14 | Anorthite | 16.61 | 14.40 | 15.24 | 11.89 | 3.30 | 4.15 |
| FeO | 4.17 | 2.64 | 3.37 | 2.93 | 0.80 | 1.39 | Diopside | 0.0 | 0.0 | 0.0 | 0.0 | 0.0 | 0.0 |
| MnO | 0.05 | 0.05 | 0.06 | 0.06 | 0.03 | 0.04 | Hypersthene | 8.50 | 5.38 | 5.93 | 6.48 | 1.05 | 2.49 |
| MgO | 1.11 | 0.88 | 1.04 | 0.96 | 0.20 | 0.18 | Magnetite | 0.94 | 1.90 | 3.17 | 1.32 | 1.03 | 0.21 |
| CaO | 3.69 | 3.02 | 3.44 | 2.55 | 0.98 | 1.01 | Ilmenite | 1.47 | 0.89 | 1.53 | 0.87 | 0.48 | 0.62 |
| $Na_2O$ | 2.62 | 2.70 | 22.83 | 2.95 | 2.83 | 2.72 | Apatite | 0.43 | 0.28 | 0.47 | 0.33 | 0.23 | 0.14 |
| $K_2O$ | 3.37 | 4.07 | 4.17 | 4.87 | 5.04 | 3.67 | Calcite | 0.04 | - | 0.30 | - | 0.35 | 0.21 |
| $H_2O^+$ | 1.01 | 0.99 | 1.02 | 1.00 | 0.69 | 0.74 | Corundum | 1.71 | 1.53 | 2.06 | 0.93 | 2.73 | 4.00 |
| $H_2O^-$ | 0.12 | 0.10 | 0.14 | 0.11 | 0.06 | 0.09 | Total | 100.00 | 100.00 | 100.00 | 100.00 | 100.00 | 100.00 |
| $P_2O_5$ | 0.19 | 0.12 | 0.20 | 0.14 | 0.10 | 0.06 | Opx (En %<br>(Ps % | 2.71<br>5.79 | 2.22<br>3.16 | 2.64<br>3.29 | 2.42<br>4.06 | 0.50<br>0.54 | 0.46<br>2.03 |
| $CO_2$ | 0.02 | n.d.* | 0.13 | n.d.* | 0.15 | 0.09 | Norm Plaq. % An | 43.3 | 38.3 | 38.4 | 32.0 | 12.0 | 15.0 |
| Total | 103.10 | 99.69 | 99.19 | 99.80 | 99.48 | 98.39 | | | | | | | |

[a]Hope Granite, Martin Dome
[b]Hope Granite, Shackleton Coast
[c]Ida Granite aplite dike, Granite Pillars
[d]Ida Granite plutonic sample, Granite Pillars
*No data

The analyses of the two groups of Hop Granite samples do not differ significantly for any element, which indicates that their parent magmas were chemically similar, at least with respect to the major elements. However, there is a significant chemical contrast between Hope Granite samples (295, 593, MD-1, SC-1) and Ida Granite samples (575, 637). The Ida Granite samples are significantly richer in silica and poorer in lime, magnesia and total iron, differences which are consistent with the more felsic appearance of the Ida Granite. The significance of the chemical contrasts is discussed in detail in the next paper in this report.

The contrasts in lime, magnesia and iron content between the Hope and Ida Granite samples are reflected in marked differences in normative anorthite and hypersthene contents. The normative anorthite concentrations of the Hope Granite samples and the composites are between 11.9 and 16.6 percent, whereas those of the Ida Granite samples are 3.3 and 4.2 percent. Of the six samples analyzed, only the Ida Granite samples have total normative quartz + orthoclase + albite contents greater than 80 percent.

The normative concentrations of quartz, albite and orthoclase computed for samples 295, 575, 593, 637, MD-1 and SC-1 have been recalculated to 100 percent and plotted on a triangular $SiO_2$-AB-OR diagram in Figure 6. Samples 295, 593, MD-1 and SC-1 contain significant amounts of normative anorthite. This shifts their effective positions on the $SiO_2$-AB-OR diagram by small distances away from the albite corner (Fig. 6). All six samples plot near the center of the diagram in a near linear array, which lies within the area in which the 571 granitic plutonic rocks plotted by Tuttle and Bowen (1958, Fig. 42) are concentrated. The cotectic curves determined by Tuttle and Bowen (1958, p. 75) for the system $SiO_2$-$NaAlSi_3O_8$-$KAlSi_3O_8$-$H_2O$ at 500 and 4000 bars water vapor pressure are also plotted on the diagram. Reference to Figures 22 and 25 of Tuttle and Bowen (1958) shows that samples 575, 295 and MD-1 plot near the thermal minimum in the system at a water pressure of about 500 bars. Samples 593 and SC-1 plot near the cotectic curve on the orthoclase side of the ternary eutectic at about 4000 bars water pressure. All six samples lie near a line which is approximately at right-angles to the isotherms in the system.

Since normative anorthite is also significant, especially in the Hope Granite samples, the normative anorthite, albite and orthoclase contents of the same six samples, recalculated to 100 percent are plotted on a triangular AN-AB-OR diagram in Figure 7. The samples again form a near linear array, which lies in the plagioclase field approximately at right-angles to the isotherms in the system $CaAl_2Si_2O_8$-$NaAlSi_3O_8$-$H_2O$ (Yoder et al., 1957). The influence of increased normative anorthite is shown in the location of sample 295 at a greater distance from the 500 bar cotectic than in the $SiO_2$-AB-OR system (Fig. 6). The bearing of these diagrams on the magmatic development of the Hope and Ida Granites is discussed in the next paper in this report.

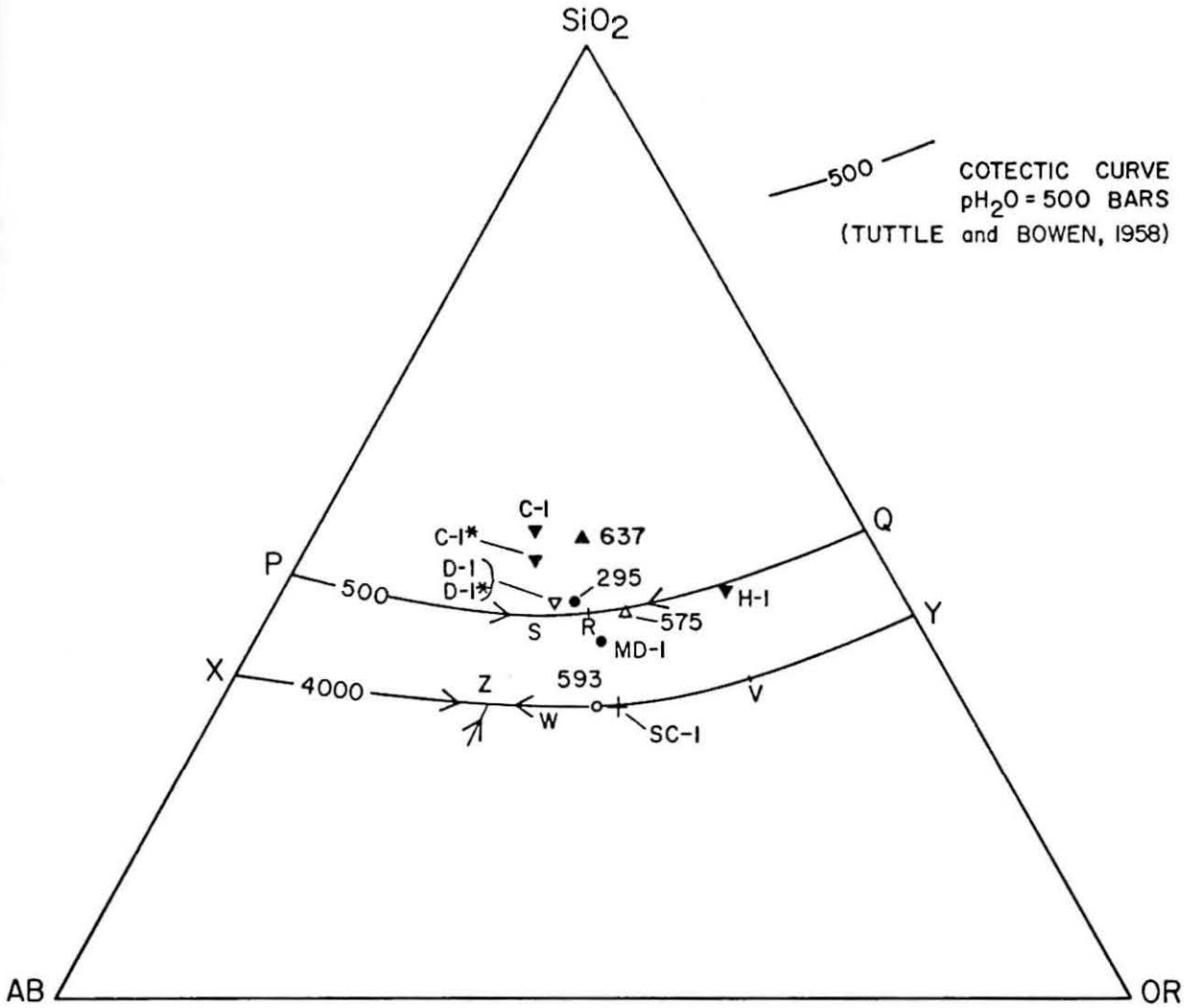


Figure 6. Normative Quartz, Albite and Orthoclase Analyses. Whole-Rock Samples of Hope and Ida Granites and Metasedimentary Composite Samples of Nimrod Group and Goldie Formation. Cotectic Curves at 500 and 4000 bars Water Vapor Pressure from Tuttle and Bowen (1958). Symbols as in Figure 6, p. 47.

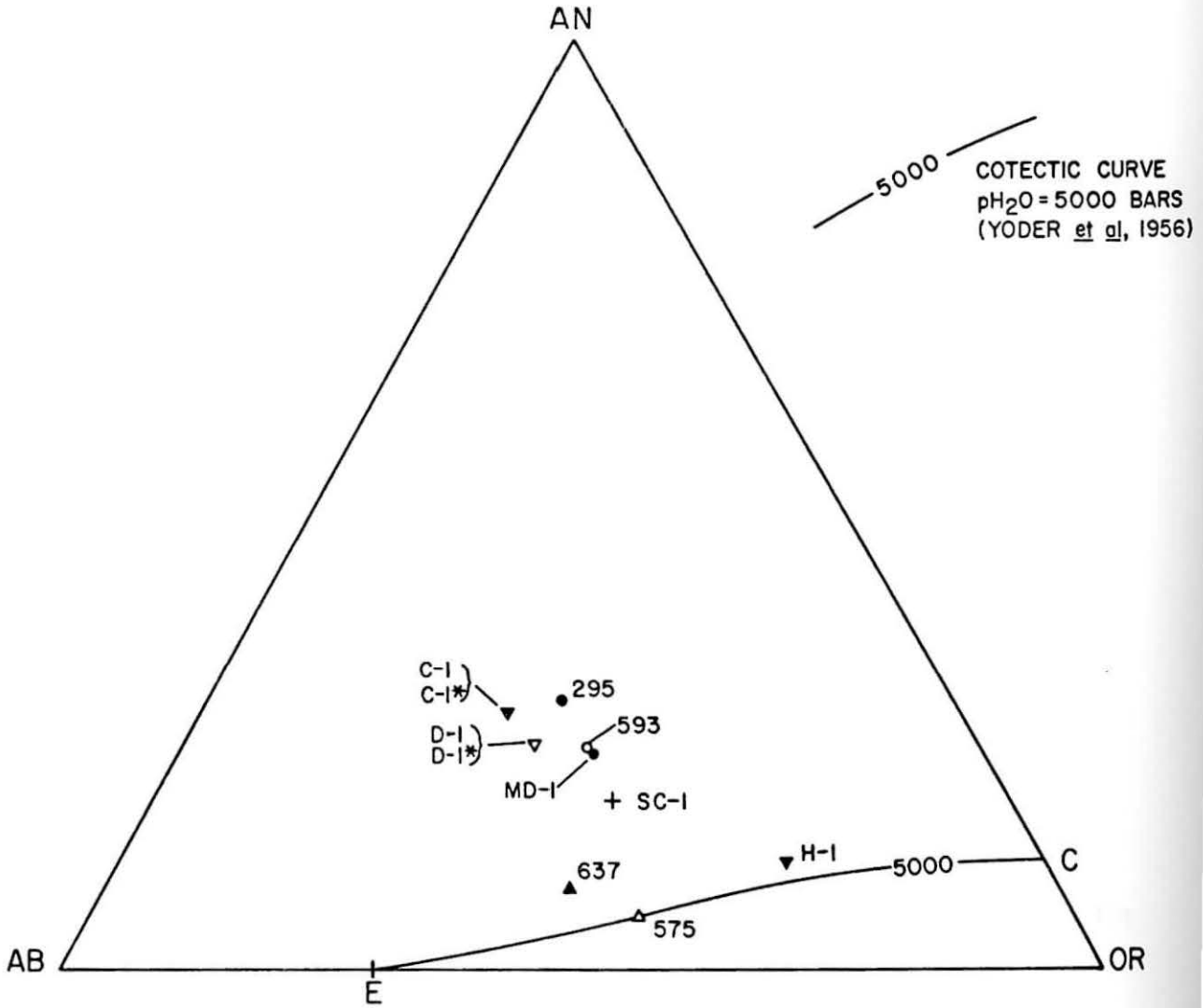


Figure 7. Normative Anorthite, Albite and Orthoclase Analyses. Whole-Rock Samples of Hope and Ida Granite and Metasedimentary Composite Samples of Nimrod Group and Goldie Formation. Cotectic Curve at 5000 bars Water Vapor Pressure from Yoder et al. (1957). Symbols as in Figure 6 of the next paper in this report.

Chemical analyses and norms of two composites of the Goldie Formation (C-1 and H-1) and of one composite of the Nimrod Group (D-1) are given in Table 5. In order to consider the silicate chemistry of samples C-1 and D-1, which contain significant concentrations of carbonate, their analyses have been recalculated to 100 percent, after elimination of carbon dioxide ($CO_2$) and its equivalent in lime and magnesia. For sample D-1, the $CO_2$ was arbitrarily assumed to be combined entirely in calcite, and for sample C-1 it was assumed to be combined with equal molecular proportions of CaO and MgO. The recalculated $CO_2$-free analyses, denoted C-1* and D-1* are also listed in Table 5.

The normative contents of quartz, albite and anorthite and of anorthite, albite and orthoclase in samples C-1, C-1*, D-1, D-1* and H-1 have also been recalculated to 100 percent and plotted in Figures 6 and 7. In the $SiO_2$-AB-OR diagram (Fig. 6) samples C-1, C-1*, D-1 and D-1* lie within the field of quartz at any water pressure above 500 bars. Sample H-1 plots within the feldspar field at 500 bars and would plot within the quartz field at a slightly higher pressure. In the AN-AB-OR diagram all the samples plot in the two-feldspar field.

## Discussion

The question at this stage is whether the Nimrod Group and the Goldie Formation, as represented by the composite samples D-1, and C-1 and H-1 respectively, could be melted in bulk to form liquids which would crystallize samples of the Hope and Ida Granites such as 295, 593, MD-1, SC-1, 575 and 637. The discussion which follows is limited by the simplified nature of the phase systems considered and by the number of unknown factors, such as water vapor pressure at the supposed site of melting.

On the AN-SB-OR diagram samples C-1 and D-1 plot close together and near to sample 295, which is the most calcic of the intrusive samples analyzed. The errors involved in the process of compositing imply that the locations of these three points are not significantly different. Thus, if samples C-1 and D-1 were totally melted a magma with anorthite, albite and orthoclase components similar to those of sample 295 would be formed. Fractional crystallization of such a magma could form a suite of rocks with a pattern similar to that shown by the six intrusive samples in Figure 7, as discussed in the next paper of this report. If samples C-1 and D-1 were partially melted in the AN-AB-OR system the phase diagram of Yoder and others (1957) would predict an initial liquid of composition between E and sample 575, dpending on the AB/AN ratio. Continued melting of the samples would cause the liquid composition to move up the cotectic curve towards C while plagioclase and K-feldspar melted and the plagioclase became progressively more calcic, the reverse of the crystallization sequence discussed by Turner and Verhoogen (1960, pp. 114-115). If equilibrium melting continued, K-feldspar would be completely melted when the liquid reached some point nearly mid-way

Table 5: Chemical analyses and norms: (2) Composite samples of the Nimrod Group and the Goldie Formation

| Chemical Analyses | | | | | |
|---|---|---|---|---|---|
| Sample | C-1 | C-1* | H-1 | D-1 | D-1* |
| $SiO_2$ | 60.98 | 70.70 | 60.90 | 51.55 | 67.82 |
| $TiO_2$ | 0.62 | 0.72 | 0.83 | 0.65 | 0.86 |
| $Al_2O_3$ | 12.23 | 14.18 | 16.87 | 11.05 | 14.53 |
| $Fe_2O_3$ | 1.07 | 1.24 | 1.04 | 0.46 | 0.60 |
| FeO | 3.32 | 3.85 | 5.58 | 3.60 | 4.74 |
| MnO | 0.07 | 0.08 | 0.08 | 0.09 | 0.12 |
| MgO | 2.60 | 0.05 | 3.47 | 2.07 | 2.72 |
| CaO | 6.38 | 3.37 | 1.79 | 14.24 | 2.77 |
| $Na_2O$ | 2.47 | 2.86 | 1.19 | 2.01 | 2.65 |
| $K_2O$ | 2.41 | 2.79 | 4.36 | 2.30 | 3.03 |
| $H_2O^+$ | 2.12 | 0.0 | 2.56 | 1.16 | 0.0 |
| $H_2O^-$ | 0.09 | 0.0 | 0.18 | 0.11 | 0.0 |
| $P_2O_5$ | 0.16 | 0.18 | 0.18 | 0.12 | 0.15 |
| $CO_2$ | 5.58 | 0.0 | 0.50 | 9.52 | 0.0 |
| Total | 100.10 | 100.02 | 99.53 | 98.93 | 99.99 |

| CIPW Norms | | | | |
|---|---|---|---|---|
| Sample | C-1* | H-1 | D-1 | D-1* |
| Quartz | 34.31 | 27.31 | 21.88 | 28.05 |
| Orthoclase | 16.48 | 26.62 | 13.92 | 17.91 |
| Albite | 24.20 | 10.40 | 17.42 | 22.43 |
| Anorthite | 15.54 | 4.70 | 9.91 | 12.76 |
| Diopside | 0.0 | 0.0 | 0.0 | 0.0 |
| Hypersthene | 5.13 | 17.36 | 10.73 | 13.79 |
| Magnetite | 1.80 | 1.56 | 0.68 | 0.87 |
| Ilmenite | 1.37 | 1.63 | 1.26 | 1.63 |
| Apatite | 0.42 | 0.43 | 0.28 | 0.35 |
| Calcite | 0.0 | 1.17 | 22.17 | 0.0 |
| Corundum | 0.76 | 8.81 | 1.75 | 2.21 |
| Total | 100.00 | 100.00 | 100.00 | 100.00 |
| OPX En % | 0.12 | 8.93 | 5.28 | 6.77 |
| OPX Fs % | 5.00 | 8.44 | 5.45 | 7.01 |
| Norm. plag. % An | 39.1 | 31.1 | 36.3 | 36.3 |

between C and E. The liquid would then leave the cotectic and would follow a curved path, concave towards anorthite, to the location of C-1 and D-1, by which time all the plagioclase would have melted.

Sample H-1 (Goldie formation) is richer in normative orthoclase than are samples C-1 and D-1. It plots nearer the cotectic curve for the AN-AB-OR system at 4000 bars water pressure and at some distance from the trend of the remaining samples. This sample was composited from an outcrop of Goldie Formation rocks which are closer to the outcrop of a Hope Granite stock and are more highly metamorphosed than those composited in sample C-1. For this reason it may contain metasomatic material. A metasomatic increase in potassium at the expense of sodium, as has been suggested for granite contact zones by Orville (1962), could cause sample H-1 to change in composition towards the orthoclase corner of the AN-AB-OR triangle from a composition closer to that of samples C-1 and D-1. However, if sample H-1 is representative of the Goldie Formation at the location of Section H (Lands End Nunatak), fractional melting of such rocks at 5000 bars water pressure could produce an initial liquid of normative feldspar composition between E and sample 575 (Fig. 7). Continued melting under equilibrium conditions would cause the liquid to follow the cotectic curve to a composition slightly more orthoclase-rich than H-1. By this time the sample would be completely liquid, except for a small quantity of plagioclase, which would melt when the liquid moved from the cotectic to the position of H-1. At about the halfway point between E and H-1, the liquid would have a composition similar to that of the Ida Granite, as represented by samples 575 and 637. Thus, partial melting of rocks with the normative feldspar composition of sample H-1 could produce a magma which would form rocks of Ida Granite composition.

On the $SiO_2$-AB-OR diagram (Fig. 6) samples C-1, C-1*, D-1 and D-1* also plot in a small area which is close to the location of samples 637 and 295. Thus, total melting of samples C-1 and D-1 or of their $CO_2$-free equivalents would form a magma with silica, albite and anorthite components similar to those of samples 295 and 637. The first crystals formed from such a magma in the $SiO_2$-AB-OR system would be quartz. However the stage at which feldspar would start to crystallize would be strongly affected by the water vapor pressure. At 500 bars water pressure, formation of alkali feldspar would begin after very little quartz crystallization. The liquid would then follow the cotectic curve PQ to R (Fig. 6), where the remaining liquid would crystallize eutectically. At a water pressure of 4000 bars or over, more extensive crystallization of quartz would occur before the magma reached the cotectic XY, at a point between Z and sample 593. Simultaneous crystallization of K-feldspar would ensue while the liquid moved the short distance to the ternary eutectic Z. A parent magma of composition similar to samples C-1 and D-1 is not consistent with the lack of quartz phenocrysts in in the Hope and Ida Granite outcrops and with the evidence discussed in the next paper of this report which strongly suggests that the Ida Granite is a magmatic differentiate of the Hope Granite.

Partial melting of samples C-1 and D-1 at 500 and 4000 bars water pressure would produce initial liquids of compositions R and Z, respectively. Subsequent equilibrium melting would cause the liquids to follow the reverse paths to those for crystallization. Thus the same rock composition would form a liquid similar to samples 295, 575 and MD-1 in silica content if partially melted at 500 bars water pressure, and another liquid similar to samples 593 and SC-1 if partially melted at 4000 bars water pressure. A liquid similar to samples 295, 575 and MD-1 could also be produced by nearly total melting of samples C-1 and D-1 at 4000 bars water pressure. These relationships are summarized in Table 6.

Table 6: Melting Relationships in the $SiO_2$-AB-OR-$H_2O$ System: Samples C-1, D-1 and H-1

| Sample | $P_{H_2O}$ (bar) | Composition of liquid[a] | | | |
|---|---|---|---|---|---|
| | | Total melting | Considerable melting | Moderate melting | First melt |
| C-1 and D-1 | 500 | C-1 or D-1 | "S" $Q_{40}AB_{35}OR_{25}$ | "R" $Q_{40}AB_{30}OR_{30}$ | "R" |
| | 4000 | C-1 or D-1 | "S" | "W" $Q_{30}AB_{40}OR_{30}$ | "Z" $Q_{30}AB_{45}OR_{25}$ |
| H-1 | 500 | H-1 $Q_{42}AB_{17}OR_{41}$ | H-1 | "R" | "R" |
| | 4000 | H-1 | "V" $Q_{39}AB_{19}OR_{48}$ | 593 $Q_{30}AB_{35}OR_{35}$ | "Z" |

[a]See Figure 6

Partial melting of sample H-1 would also produce initial liquids of compositions R and Z, respectively. However, continued isobaric equilibrium melting would cause the liquids to follow different paths from those described previously. At 500 bars water pressure the liquid would move along the cotectic curve PQ from R towards H-1, with simultaneous melting of quartz and feldspar. At 4000 bars the liquid would move along the cotectic XY to V, where the feldspar would be exhausted, and continued melting of quartz would cause the liquid to move along the line V-$SiO_2$ to H-1. These relationships are summarized in Table 6.

The previous discussion has assumed that melting and crystallization were isobaric. If, however, a magma generated at Z (Fig. 6) by partial melting at 4000 bars water pressure were subjected to a pressure reduction, as might be caused by intrusion to a higher crustal level, its crystallization behavior would be greatly changed. A magma of composition Z at 500 bars water pressure would crystallize alkali feldspar and would follow a curved path, away from the feldspar boundary (Fig. 6). Such a path could produce liquids compositionally somewhat similar to samples 593 and SC-1.

## Summary

The following paragraphs summarize the ways in which liquids with the compositions of samples 295, 575, 593, 637, MD-1 and SC-1 can be produced by melting samples C-1, D-1 and H-1 in the AN-AB-OR and $SiO_2$-AB-OR systems. An attempt is made to determine which of the possible alternatives fits the chemistry and mineralogy of the Hope and Ida Granites best.

### Martin Dome Pluton

A liquid compositionally similar to the Hope Granite samples from Martin Dome (295 and MD-1) can be produced directly by melting samples C-1 or D-1 at 500 bars water pressure. In the $SiO_2$-AB-OR system a considerable amount of melting will have relatively little effect on the composition of this melt. However, to obtain a sufficiently calcic melt, a large amount of melting is necessary (AN-AB-OR diagram, Fig. 7).

A liquid with the normative alkali feldspar content of samples 295 and MD-1 can also be produced by limited partial melting of sample H-1. However, the high normative anorthite content of the Martin Dome samples is incompatible with this model.

A third method of obtaining a magma with the $SiO_2$-AB-OR normative composition of the Martin Dome samples is by limited partial melting of samples C-1, D-1 or H-1 at a higher water vapor pressure, followed by fractional crystallization. But such a model would not produce rocks with high enough calcium contents, even at water pressures of 5000 bars.

### Shackleton Coast Plutons

Magmas with the compositions of the Mt. Hope pluton and of the other Hope Granite plutons in the Shackleton Coast ranges (samples 593 and SC-1) can not be produced directly by melting samples C-1, D-1 or H-1 at water vapor pressures less than 4000 bars. At pressures of this order a moderate amount of melting would give liquids with quartz compositions similar to those of samples 593 and SC-1, but samples C-1 and

D-1 would not provide sufficient potassium. A considerable degree of melting of samples C-1 or D-1 would be necessary to provide the calcium in sample SC-1, and near total melting would be necessary for sample 593 (Fig. 7). No amount of melting of sample H-1 alone could give a liquid with the calcium contents of samples SC-1 and 593.

## Ida Granite

A magma with the composition of sample 575 (Ida Granite) could be obtained from samples C-1, D-1 or H-1 in two ways: (1) by partial melt- at 500 bars water pressure, or (2) by fractional crystallization at this pressure of a less siliceous and more calcic melt generated by partial melting at higher water pressures. This second alternative is more consistent with the geochemical and mineralogical evidence quoted in the next paper in this report, which indicates that the Ida Granite was derived by fractional crystallization of a more calcic, less siliceous Hope Granite magma. The anomalously high silica content of the Ida Granite sample 637 (Fig. 6) is difficult to explain in terms of the $SiO_2$-AB-OR system. Such a composition would crystallize at a very considerable temperature, even at waterpressures as low as 500 bars, whereas all the other evidence indicates that the Ida Granite crystallized from a highly differentiated residual magma. The most probable explanations are analytical error, or contamination by silica-rich material.

## Water Vapor Pressure at the Sites of Melting

The suggested contrast in water pressure at the sites of melting in Areas A and B (Fig. 2) may be due to a difference either in depth of magma generation or in amount of water available. The second alternative is consistent with the contrast in water contents between the Nimrod Group and the Goldie Formation, as represented by samples D-1, and C-1 and H-1, respectively. The concentrations of combined water in these samples are: -- D-1: 1.16%; C-1: 2.12%; H-1: 2.56% (Table 5). Although the data are limited, this contrast would fit a structural model in which the Goldie Formation comprises the relatively wet and recently deposited sediments of the Ross Geosyncline, and the Nimrod Group forms part of the older, drier craton on the Polar Plateau side.

## Conclusions

The isotopic and chemical data presented in this report suggest seven conclusions:

(1) The Hope and Ida Granites sampled in Area B (Shackleton Coast) were comagmatic.

(2) The magmas from which the plutons in Areas A (Miller Range) and B were derived crystallized at about the

same time (475 m.y. ago) but had significantly different $^{87}Sr/^{86}Sr$ ratios.

(3) These differences in $^{87}Sr/^{86}Sr$ ratios are consistent with the interpretation that the strontium in the magmas was largely derived from rocks similar to those which now surround the plutons.

(4) Derivation of these magmas in Areas A and B by partial melting of rocks of the Nimrod Group and the Goldie Formation, as represented by composites D-1 and C-1, respectively, is compatible with the known phase relations in the $SiO_2$-AB-OR-$H_2O$ and AN-AB-OR-$H_2O$ systems.

(5) The chemical data suggest that the magma in Area A could have been generated by nearly total melting of material chemically similar to the Nimrod Group (composite D-1) under relatively dry conditions (of the order of 500 bars water vapor pressure).

(6) The parent magma of the Hope and Ida Granites in Area B could have been generated by a moderate degree of melting of material chemically similar to the Goldie Formation (composite C-1) under relatively high water vapor pressures (4000 bars or more). More potassic material, such as sample H-1, could also have contributed to the melt.

(7) The suggestion that the Nimrod Group was melted under drier conditions than the Goldie Formation is entirely compatible with the available data on water contents of samples from the two units. It is consistent with a model in which the Goldie Formation composed the relatively wet sediments of the Ross Geosyncline while the Nimrod Group formed part of an older, drier cratonic area.

## References

rindley, G. W., 1963, The geology of the Queen Alexandra Range, Beardmore Glacier, Ross Dependency, Antarctica. N. Z. Jour. Geol. Geophys., 6, 307-347.

unn, B. M. and Walcott, R. I., 1962, The geology of The Mount Markham Region, Ross Dependency, Antarctica. N. Z. Jour. Geol. Geophys., 5, 407-426.

unner, J. D., 1971, Age and origin of the Nimrod Group and of the Granite Harbour Intrusives, Beardmore Glacier Region, Antarctica. Ph.D. dissertation, Dept. of Geology, The Ohio State University, Columbus, Ohio, 231p.

Harland, W. B., Smith, A. G. and Wilcock, B., 1964, The Phanerozoic Time Scale. Quart. Jour. Geol. Soc. Lond., 120s, 458p.

McDougall, I. and Grindley, G. W., 1965, Potassium-argon dates on micas from the Nimrod-Beardmore-Axel Heiberg region, Ross Dependency, Antarctica. N. Z. Jour. Geol. Geophys., 8, 304-313.

Orville, P. M., 1962, Alkali metasomatism and feldspars. Norsk. Ocol. Tidoskr., 42, 283.

Turner, F. J. and Verhoogen, J., 1960, Tgneous and metamorphic petrology. McGraw-Hill, New York, Second Edition, 694p.

Tuttle, O. F. and Bowen, N. L., 1958, Origin of granite in the light of experimental studies in the system $NaAlSi_3O_8$-$KAlSi_3O_8$-$SiO_2$-$H_2O$. Geol. Soc. Amer. Mem., 74, 153p.

Yoder, H. S., Stewart, D. B. and Smith, J. R., 1957, Ternary feldspars. Carnegie Inst. Wash. Year Bk., Ann. Rept. Director Geophys. Lab., 206-214.

York, D., 1966, Least squares fitting of a straight line. Canad. Jour. Phys., 44, 1079-1086.

# MAGMATIC DEVELOPMENT OF THE HOPE AND IDA GRANITES, BEARDMORE GLACIER REGION, ANTARCTICA

(Excerpt of a Ph.D. dissertation by John Gunner submitted to the Department of Geology in 1971)

## Introduction

As a second part of the study of the Hope and Ida Granites, an attempt was made to investigate the evolution of their parent magmas after their generation. This study was designed to answer two main questions: (1) to what extent does geochemical and mineralogical evidence support the existence of a common parent magma for the Hope and Ida Granite intrusions in the region? (2) can the chemical and mineralogical variations within and between these intrusions be explained by fractional crystallization of a common parent magma.

## Methods

Emphasis was placed on four principal areas of study: (1) major element chemical analysis of selected whole-rock samples, (2) chemical analysis of K, Na, Ca, Rb, Sr and Ba in K-feldspar separates, (3) optical analysis of albite-anorthite composition in plagioclase, (4) petrographic modal analysis. Samples were analyzed from the Martin Dome pluton, the Mt. Ida pluton, the pluton east of the mouth of the Beardmore Glacier (East Beardmore pluton) and from a number of aplite and pegmatite dikes intruding the Mt. Hope pluton (Fig. 2 of the preceding paper). For each sample a number of geochemical and mineralogical parameters were determined, for example K/Rb concentration ratio of K-feldspar, anorthite content of plagioclase and modal biotite content. Variation diagrams for a number of pairs of parameters were then used to interpret the magmatic history of the rocks.

## Analytical Techniques

### Analyses of Whole-rocks

Analyses of 9 powdered samples of selected whole-rocks were carried out by Andrew McCreath and Sons. A total of 14 major elements were determined. The samples were prepared as described in Appendix C of Gunner (1971).

### Analyses of K-feldspars

K-feldspars were separated from crushed and ground samples as described in Appendix C of Gunner (1971). Petrographic examination showed that almost all the samples analyzed were non-perthitic. They

did contain inclusions of other minerals, such as quartz, plagioclase and biotite. However, most of the significant inclusions were larger than the opening (250 micron) of the 60 mesh screen through which the samples were sieved. The good general agreement of most of the K, Na and Ca analyses with K-feldspar stoichiometry indicates that most of the samples were of high purity.

## Representativeness of K-feldspar Separates

The chemical analyses of the K-feldspars were interpreted on the assumption that the separates were representative of all the K-feldspar present in the rock. The presence of internal chemical zoning in the K-feldspars or of chemical variations with crystal size -- many of the rock samples are porphyritic -- would negate this assumption. As a preliminary test, two samples containing K-feldspar phenocrysts were analyzed by electron microprobe and separates of phenocryst and groundmass K-feldspar of another sample were analyzed chemically.

For the electron microprobe study, 2-1/2 cm wide slabs of material, containing K-feldspar as well-formed phenocrysts and groundmass crystals were prepared from samples 315 and 573. At least two phenocrysts about 1 cm across and two groundmass crystals about 1 mm across were scanned in each sample. Variations in x-ray fluorescent intensity of K, Na, Ca, Al and Si were recorded on a triple-pen chart recorder coupled to the three spectrometers. Continuous traverses of from 800 to 3300 microns in length were made at the rate of 60 micron/min. Because of time limitations, complete traverses could not be made across individual crystals. Instead, broken traverses along the same line were made near the phenocryst margins, near the centers and in between. Neither K, Na, Ca, Al or Si showed any systematic concentration variations within phenocrysts or between phenocrysts and groundmass crystals in the same samples. The variations in signal intensity from K-feldspars were about ten percent or less for each sample, except for narrow zones a few microns across which were interpreted as fractures.

The potassium spectrometer of the instrument was calibrated approximately by traversing a sample of pure potassium chloride (KCl). 'Model' K concentration variations calculated on this basis, neglecting matrix effects, are presented in Table 1 for seven scans of K-feldspar crystals. None of the scans show internal K variations of more than 1.9% model K, and neither sample shows a variation of more than 2.0% model K, or about 13% of the average concentration. No information is available on long-term fluctuations of the instrument on the scale of hours. The K calibrations was made only once, so that it is probable that at least part of the variations observed were due to instrumental fluctuation.

Table 1: Electron Microprobe Results: Variations in K Concentrations in Scans across K-feldspar crystals

| Sample | [a]K (%) | | δK[b] (%) | Length of scan (micron) |
|---|---|---|---|---|
| | Maximum | Minimum | | |
| 573[c] | 15.89 | 14.15 | 1.74 | 3260 |
| 573M[d] | 14.91 | 14.23 | 0.68 | 810 |
| 315P[e] | 14.35 | 13.61 | 0.74 | 1000 |
| | 15.00 | 13.82 | 1.18 | 900 |
| 315M[f] | 14.39 | 13.72 | 0.67 | 1102 |
| | 15.15 | 13.27 | 1.88 | 1012 |
| | 13.93 | 13.12 | 0.81 | 1410 |

[a]'Model' concentration neglecting matrix effects. Based on a single calibration.

[b]Range of variation

[c]Phenocryst

[d]Matrix

[e]Two scans in single crystal. First near margin, second near center.

[f]Three scans, two crystals.

Analyses of K, Na, Ca, Rb, Sr and Ba in separates of matrix and phenocryst K-feldspar from sample 709 are presented in Table 2. The K and Rb analyses of the two seem to be in moderately good agreement, but the remaining four elements show differences of between 18% (Ca) and 80% (Ba) of average concentration. This sample is very coarsely porphyritic and K-feldspar phenocrysts form at least 50 percent of its volume. Since any chemical differences between phenocrysts and matrix K-feldspar will be at their greatest where phenocrysts are large and have had lengthy magmatic histories, sample 709 can be regarded as an extreme case. The K, Na and Ca analyses of K-feldspars from sample 709 contrast with those obtained on sample 315 and 573, both of which are more typical of most Hope Granite outcrops in the Martin Dome, Mt. Hope and East Beardmore plutons.

This preliminary study suggests that K and Rb analyses of K-feldspar separates prepared for this study are representative of the rocks sampled, but that some caution should be applied in the interpretation of Na, Ca, Sr and Ba analyses, especially from coarsely and strongly porphyritic samples.

Table 2: Sample 709: Analyses of matrix and phenocryst K-feldspar separates

| Sample | Matrix | Phenocryst |
|---|---|---|
| K (%) | 12.4 | 11.1 |
| Na (%) | 1.15 | 1.74 |
| Ca (ppm) | 1130 | 1360 |
| Ba (ppm) | 542 | 1270 |
| Rb (ppm) | 739 | 633 |
| Sr (ppm) | 148 | 228 |

## Chemical Analyses

Analytical procedures are described in Appendix C of Gunner (1971). Flame photometry was used for K and Na, x-ray fluorescence for Rb and Sr, and atomic absorption spectrophotometry for Ca and Ba.

## X-ray Diffraction Analyses

A limited number of K-feldspar separates were analyzed by x-ray diffraction (XRD), as described in Appendix C of Gunner (1971). This study served two purposes: (1) determination of the structural state of the K-feldspar, (2) independent determination of the orthoclase content, as a check on the flame photometric measurement of K. The samples were prepared as described in Appendix C of Gunner (1971), using fluorite ($CaF_2$), previously heated at 800°C for one hour, as an internal standard.

The structural state of a K-feldspar relative to the microcline - low albite, orthoclase and high sanidine - high albite solid solution series affects the $2\theta$ positions of certain K-feldspar x-ray diffraction peaks, as discussed by Wright (1968). The three series can be distinguished on a plot of the $2\theta$ ($CuK_\alpha$) values of the reflections (060) and ($\bar{2}04$) as reproduced in Figure 1. Average values of these angles obtained from five scans over the diffraction spectrum of twelve samples are presented in Table 3 and plotted in Figure 1. The data points are closely grouped on the diagram. The maximum differences in $2\theta$ between samples are: -- $2\theta(060)$: 0.09°; $2\theta(\bar{2}04)$: 0.13°. These differences are comparable to the analytical uncertainty in the measurments, as determined from variations between different scans on the same sample. The structural states of the twelve samples analyzed are therefore intermediate between microcline and orthoclase, but no significant differences between the samples are detectable from the data.

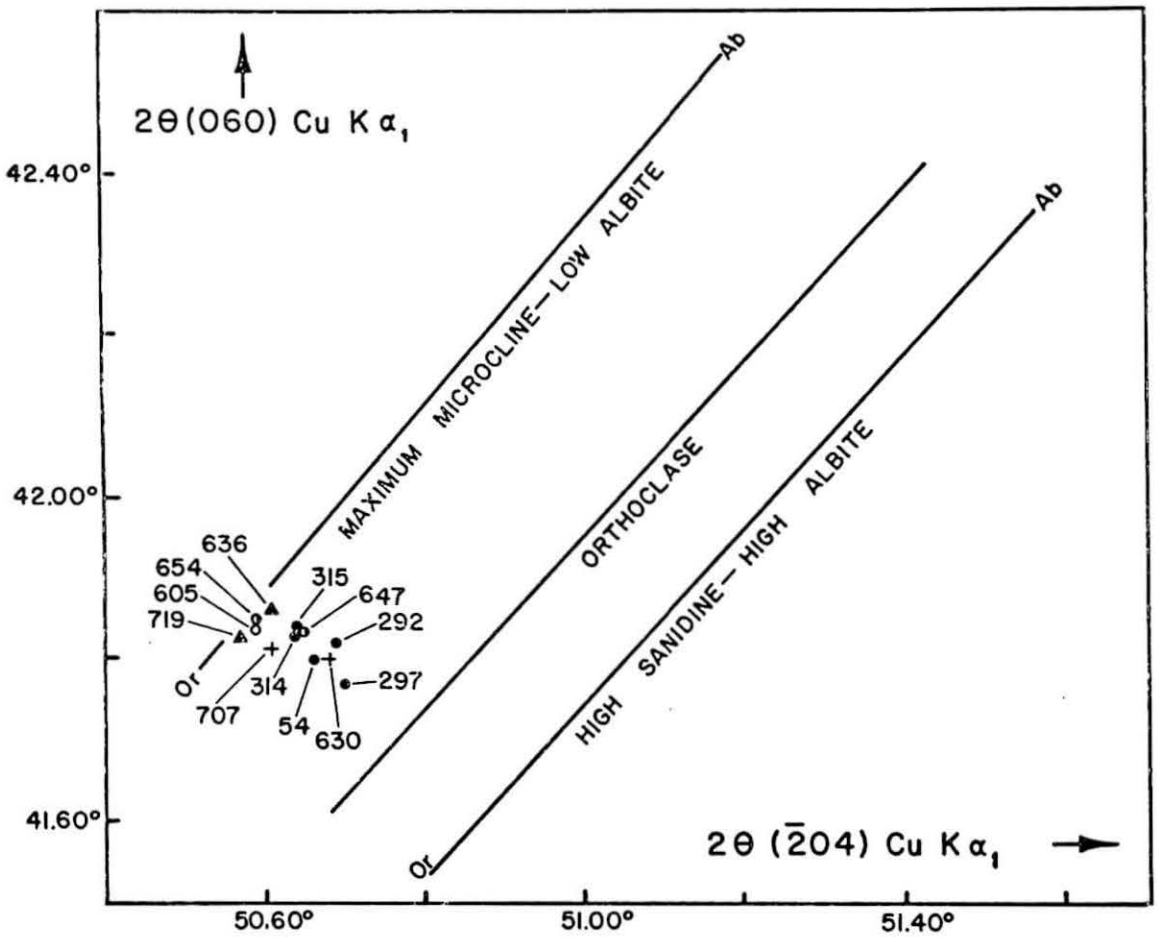


ure 1. Twelve K-feldspar Separates from Hope and Ida Granite Samples Plotted on a (060) - ($\bar{2}$04) Diagram, Simplified from Wright (1968). Lines 'MAXIMUM MICROCLINE - LOW ALBITE' and 'HIGH SANIDINE - HIGH ALBITE' Represent the solid Solution Series of Orville (1967). The Line 'ORTHOCLASE' Represents Alkali-Exchanged Orthoclase (P50-56) of Wright (1968). Symbols as in Figure 6.

Table 3: Orthoclase Contents of 12 K-feldspar Separates, Determined by X-ray Diffraction (XRD) and Flame Photometry (FP)

| Sample | $2\theta(\bar{2}01)$ $CuK_{\alpha_1}$ (degrees) | Weight percent orthoclase | |
|---|---|---|---|
| | | XRD[a] | FP |
| 54 | 20.91 | 100.62 | - |
| 292 | 21.05 | 88.03 | 84.14 |
| 297 | 21.00 | 92.53 | 65.78 |
| 314 | 21.09 | 84.44 | 86.35 |
| 315 | 21.08 | 85.33 | 86.49 |
| 605 | 21.05 | 88.03 | 92.40 |
| 630 | 21.03 | 89.83 | 84.00 |
| 636 | 21.04 | 88.93 | 92.90 |
| 647 | 21.02 | 90.73 | 89.48 |
| 654 | 21.06 | 87.13 | 85.00 |
| 707 | 21.00 | 92.53 | 88.77 |
| 719 | 21.04 | 88.93 | 92.26 |

[a]Calculated from the equation, $y = -89.94x + 1981.27$ (Wright, 1968, p. 97)

Wright (1968) also showed that the $2\theta$ angle of the $(\bar{2}01)$ reflection is a nearly linear function of the orthoclase content of a K-feldspar, as reproduced in Figure 2. The average values (five scans) of $2\theta(\bar{2}01)$ for the twelve samples are listed in Table 3, together with the computed orthoclase contents. These were calculated from the equation $y = mx + b$, where y = weight percent orthoclase and $x = 2\theta(\bar{2}01)CuK_{\alpha}$. Values of the parameters m and b were obtained by averaging the values given by Wright (1968, p. 97) for the orthoclase and microcline - low albite series. Comparison of the orthoclase contents calculated from XRD and flame photometric K analyses shows general good agreement.

## Petrographic Analyses

Plagioclase composition was determined with a Leitz five-axis universal stage and microscope. Extinction angles on (010) were measured in crystals oriented with a-axes vertical and anorthite content was determined from the plots of van der Kaaden (1951) assuming the plagioclase to be of the low temperature variety. At least four crystals were measured in each section where practicable, and the maximum and minimum extinction angles were noted for each crystal.

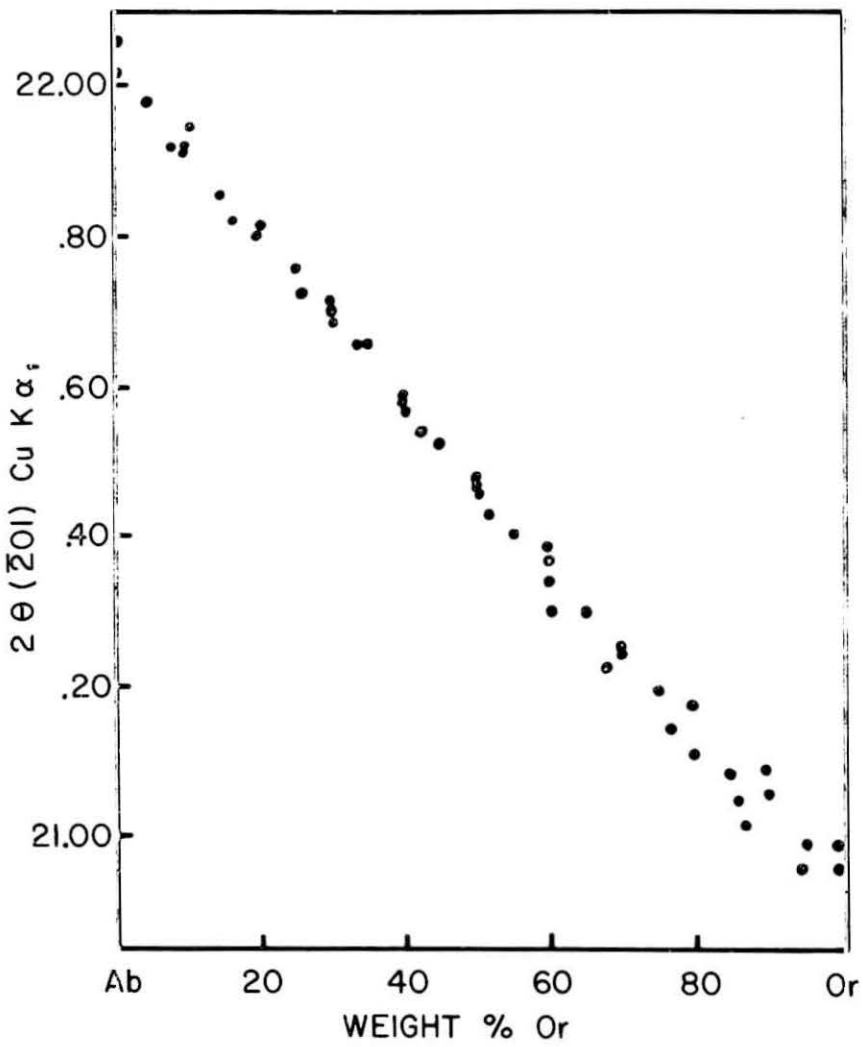


Figure 2. Orthoclase Contents of K-feldspars Plotted Versus $2\theta(\bar{2}01)$. Data from Wright (1968, Fig. 4).

Modal analyses were carried out with a Swift Ltd. point counter and an automatic stage, using increments of 0.33 mm on each traverse and traverse separations of 1.0 mm. About 1000 points were counted for each thin section, which gives an accuracy of about 3% at the 95% confidence level for minerals with abundances between 20 and 40 percent, assuming correct identification (van der Plas and Tobi, 1965). Secondary alteration products were counted as the parent mineral where this was determinable.

## Results

Major element analyses of four whole-rock samples and of two composite samples of Hope and Ida Granite are presented in Table 4 of the preceding paper. As discussed previously, the Hope Granite samples show little significant variation in major element contents. Concentrations of potash, soda, lime and magnesia are plotted as a function of silica content and of "Larsen Index", which equals (1/3Si + K) - (Ca + Mg) (Nockolds and Allen, 1953) in Figures 3 and 4. These diagrams show a progressive reduction in lime and magnesia content with increasing felsic character of the samples. Soda content shows no significant variation, and potash appears to have a slight tendency towards enrichment with increasing Larsen Index.

Analyses of K, Na, Ca, Rb, Sr and Ba in 40 K-feldspar separates from 39 samples of Hope and Ida Granite are presented in Table 4, together with the concentration ratios K/Rb, Ba/Rb, Ca/Sr, Rb/Sr and Ba/Sr and the orthoclase, albite and anorthite stoichiometric contents calculated from the data. The orthoclase, albite and anorthite contents, recalculated to 100 percent, are plotted in Figure 5. The K-feldspars analyzed show relatively little variation in orthoclase content. The recalculated values range from 74% to 93%. Albite and anorthite contents are somewhat variable, ranging from 7% to 22% and from 0.4% to 4.0%, respectively. The trace elements Rb, Sr and Ba are much more variable. Their concentrations range from 251, 17.2 and 57.9 ppm to 1510, 710 and 4350 ppm, respectively.

Plagioclase composition ranges in samples and modal analyses of thin sections of Hope and Ida Granite samples are listed in Tables 5 to 8. Plagioclase anorthite content shows a high degree of variability between samples, ranging from 0% to 56%. Compositional variations within samples of 20% anorthite are common, and a maximum variation of 38% was recorded for sample 651. Plagioclase in many samples, especially those of Hope Granite, is compositionally zoned. The crystals are generally more sodic at the margins than at the centers (normal zoning), although occasional small-scale reversale (oscillatory zoning) were noted in a few samples. Discontinuous composition changes are common in Hope Granite samples. In some crystals, rounded and embayed contacts are visible between more calcic cores and more sodic overgrowths. Compositional variation of individual crystals in Hope Granite samples is commonly 20%, and ranges up to 38% (sample 651). Ida Granite samples,

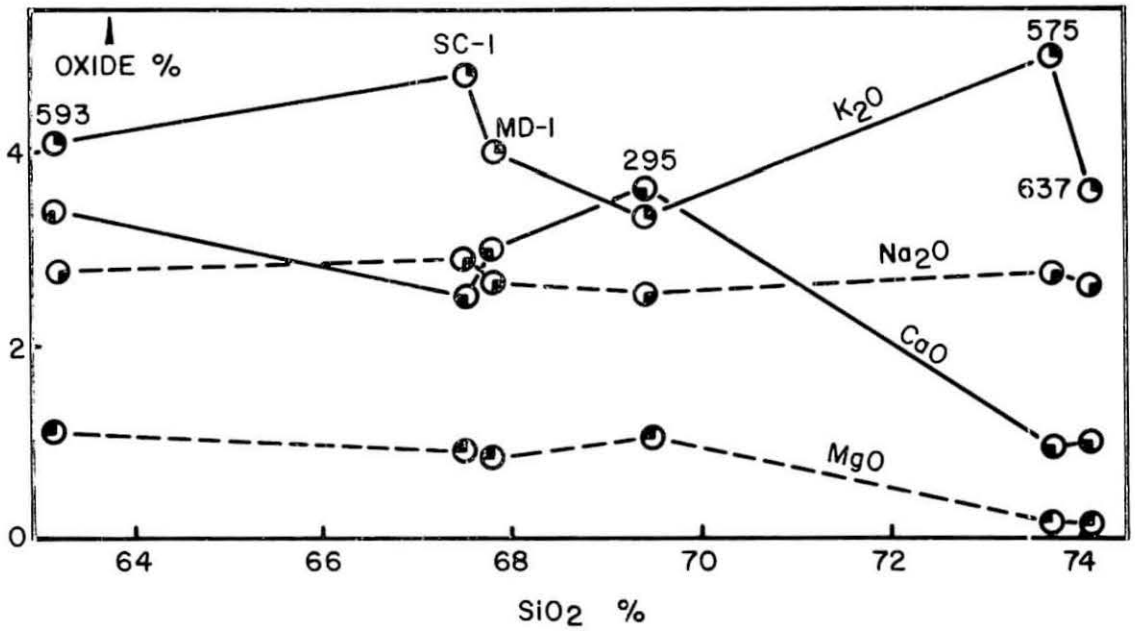


Figure 3. Variation of $K_2O$, CaO and MgO with $SiO_2$ Contents. Hope and Ida Granites - Whole-Rock Samples. Sectors: NE - $K_2O$, SE - $Na_2O$, SW - CaO, NW - MgO.

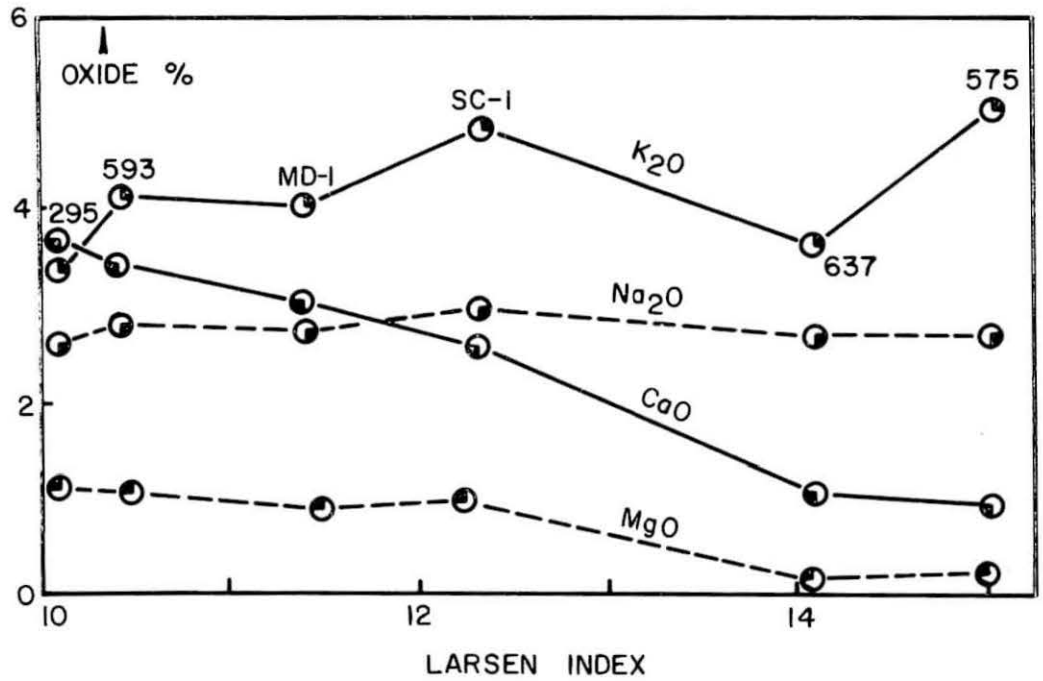


Figure 4. Variation of $K_2O$, $Na_2O$, CaO and MgO Contents with Larsen Index (Nockolds and Allen, 1953). Samples and Symbols as in Figure 3.

Table 4: Analyses of K, Na, Ca, Ba, Rb and Sr in K-feldspar Separates, Hope and Ida Granites

| Sample | K % | Na % | Ca ppm | Ba ppm | Rb ppm | Sr ppm | K/Rb | Ba/Rb | Rb/Sr | Ca/Sr | Ba/Sr | Weight % | | |
|---|---|---|---|---|---|---|---|---|---|---|---|---|---|---|
| | | | | | | | | | | | | Or | Ab | An |
| 292 | 11.8 | 1.06 | 3970 | 3100 | 370 | 340 | 319 | 8.37 | 1.09 | 11.7 | 9.12 | 84.1 | 12.4 | 2.8 |
| 294 | 11.0 | 1.29 | -- | -- | 322 | 387 | 342 | -- | 0.83 | -- | -- | 78.4 | 15.1 | -- |
| 295 | 12.8 | 0.86 | -- | -- | -- | -- | -- | -- | -- | -- | -- | 91.0 | 10.0 | -- |
| 297 | 9.24 | 1.63 | 5120 | 4530 | 291 | 710 | 317 | 15.6 | 0.41 | 7.22 | 6.38 | 65.8 | 19.0 | 3.6 |
| 314 | 12.1 | 0.93 | 1870 | 2050 | 363 | 271 | 334 | 5.64 | 1.34 | 6.88 | 7.56 | 86.4 | 10.8 | 1.3 |
| 315 | 12.2 | 0.97 | 2130 | 2410 | 415 | 313 | 293 | 5.80 | 1.33 | 6.81 | 7.70 | 86.5 | 11.3 | 1.5 |
| 573 | 12.5 | 1.05 | 993 | 2530 | 394 | 307 | 318 | 6.41 | 1.28 | 3.23 | 8.24 | 89.3 | 12.2 | 0.7 |
| 575 | 13.2 | 0.58 | 867 | 269 | 961 | 94.9 | 138 | 0.28 | 10.1 | 9.14 | 2.83 | 94.1 | 6.7 | 0.6 |
| 578A | 12.7 | 0.84 | 1070 | 319 | 978 | 110 | 129 | 0.33 | 8.88 | 9.74 | 2.90 | 90.1 | 9.9 | 0.7 |
| 583 | 12.6 | 0.88 | 1270 | 1560 | 357 | 276 | 354 | 4.37 | 1.29 | 4.60 | 5.65 | 89.8 | 10.3 | 0.9 |
| 587 | 12.0 | 0.98 | 1770 | 2440 | 329 | 363 | 364 | 7.42 | 0.90 | 4.86 | 6.72 | 85.1 | 11.4 | 1.2 |
| 594 | 12.8 | 0.61 | 614 | 84.0 | 1510 | 58.9 | 84.8 | 0.06 | 25.7 | 27.4 | 1.43 | 91.3 | 7.1 | 0.4 |
| 596 | 11.7 | 0.85 | 803 | 225 | 985 | 101 | 119 | 0.23 | 9.74 | 7.94 | 2.23 | 83.6 | 10.0 | 0.6 |
| 597 | 12.5 | 0.87 | 603 | 292 | 976 | 109 | 128 | 0.30 | 8.92 | 5.51 | 2.68 | 88.7 | 10.2 | 0.4 |
| 601 | 12.3 | 1.16 | -- | -- | 572 | 203 | 215 | -- | 2.82 | -- | -- | 87.4 | 13.6 | -- |
| 604 | 10.9 | 1.91 | 2650 | 584 | 423 | 73.6 | 258 | 1.38 | 5.76 | 36.1 | 7.93 | 77.7 | 22.3 | -- |
| 605 | 13.0 | 0.82 | 998 | 1040 | 565 | 493 | 230 | 1.84 | 1.15 | 2.03 | 2.11 | 92.4 | 9.6 | 0.7 |
| 608A | 12.4 | 1.18 | 915 | 82.1 | 1230 | 57.8 | 101 | 0.07 | 21.2 | 15.8 | 1.42 | 88.3 | 13.8 | 0.6 |
| 608B | 12.5 | 1.05 | 855 | -- | 1510 | 17.2 | 82.5 | -- | 87.7 | 49.6 | -- | 88.7 | 12.3 | 0.6 |
| 630 | 11.8 | 1.19 | 1800 | 668 | 674 | 437 | 175 | 0.99 | 1.54 | 4.13 | 1.53 | 84.0 | 13.9 | 1.3 |

Table 4 - Continued

| Sample | K % | Na % | Ca ppm | Ba ppm | Rb ppm | Sr ppm | K/Rb | Ba/Rb | Rb/Sr | Ca/Sr | Ba/Sr | Weight % Or | Ab | An |
|---|---|---|---|---|---|---|---|---|---|---|---|---|---|---|
| 635 | 12.3 | 1.19 | 1120 | 513 | 421 | 86.5 | 292 | 1.22 | 4.87 | 13.0 | 5.93 | 87.5 | 13.9 | 0.8 |
| 636 | 13.0 | 0.91 | 1460 | 158 | 943 | 100 | 138 | 0.17 | 9.44 | 14.7 | 1.58 | 92.5 | 10.6 | 1.0 |
| 637 | 12.8 | 0.77 | 1330 | 242 | 1000 | 84.8 | 127 | 0.24 | 11.8 | 15.6 | 2.85 | 90.8 | 8.9 | 0.9 |
| 638 | 12.5 | 1.20 | 1150 | 330 | 907 | 104 | 138 | 0.36 | 8.74 | 11.1 | 3.17 | 89.3 | 14.0 | 0.8 |
| 639 | 13.0 | 0.71 | 1480 | 199 | 706 | 67.3 | 185 | 0.28 | 10.5 | 22.0 | 2.96 | 92.8 | 8.3 | 1.0 |
| 640 | 12.5 | 0.99 | 523 | 314 | 758 | 84.9 | 165 | 0.41 | 8.93 | 6.16 | 3.70 | 88.8 | 11.5 | 0.4 |
| 646 | 12.1 | 1.08 | 598 | 505 | 744 | 94.6 | 162 | 0.68 | 7.87 | 6.33 | 5.34 | 86.0 | 12.6 | 0.4 |
| 647 | 12.6 | 0.83 | 914 | 2050 | 429 | 179 | 293 | 4.79 | 2.40 | 5.12 | 11.5 | 89.5 | 9.7 | 0.6 |
| 651 | 12.2 | 0.92 | 844 | 1490 | 481 | 174 | 254 | 3.09 | 2.76 | 4.84 | 8.56 | 86.9 | 10.7 | 0.6 |
| 654 | 11.9 | 1.05 | 1060 | 2440 | 400 | 297 | 299 | 6.09 | 1.35 | 3.55 | 8.22 | 85.0 | 12.2 | 0.7 |
| 658 | 12.3 | 1.25 | 652 | 3970 | 251 | 448 | 490 | 15.8 | 0.56 | 1.46 | 8.86 | 87.6 | 14.6 | 0.5 |
| 707 | 12.5 | 0.92 | 598 | 57.9 | 1190 | 39.0 | 106 | 0.05 | 30.4 | 15.3 | 1.48 | 88.8 | 10.7 | 0.4 |
| 709m | 12.4 | 1.15 | 1130 | 542 | 739 | 148 | 168 | 0.73 | 4.98 | 7.60 | 3.66 | 88.3 | 13.4 | 0.8 |
| 709p | 11.1 | 1.74 | 1360 | 1270 | 633 | 228 | 176 | 2.01 | 2.78 | 5.98 | 5.57 | 79.3 | 20.3 | 0.9 |
| 719 | 13.0 | 0.71 | -- | -- | 1130 | 88.9 | 115 | -- | 10.3 | -- | -- | 92.3 | 8.3 | -- |
| 721 | 11.9 | 1.02 | 883 | 386 | 962 | 123 | 123 | 0.40 | 7.79 | 7.15 | 3.14 | 84.4 | 11.8 | 0.6 |
| 722 | 12.8 | 0.79 | 1300 | 316 | 1220 | 102 | 104 | 0.26 | 12.0 | 12.7 | 3.10 | 90.8 | 9.2 | 0.9 |
| 724 | 12.5 | 0.79 | 569 | 482 | 859 | 143 | 146 | 0.56 | 6.01 | 3.98 | 3.37 | 89.1 | 9.3 | 0.4 |
| 726 | 12.4 | 0.98 | 1090 | 949 | 758 | 157 | 163 | 1.25 | 4.83 | 6.97 | 6.04 | 88.1 | 11.5 | 0.8 |
| 739 | 11.9 | 1.50 | 622 | 762 | 602 | 75.1 | 197 | 1.27 | 8.01 | 8.29 | 10.2 | 84.4 | 17.5 | 0.4 |

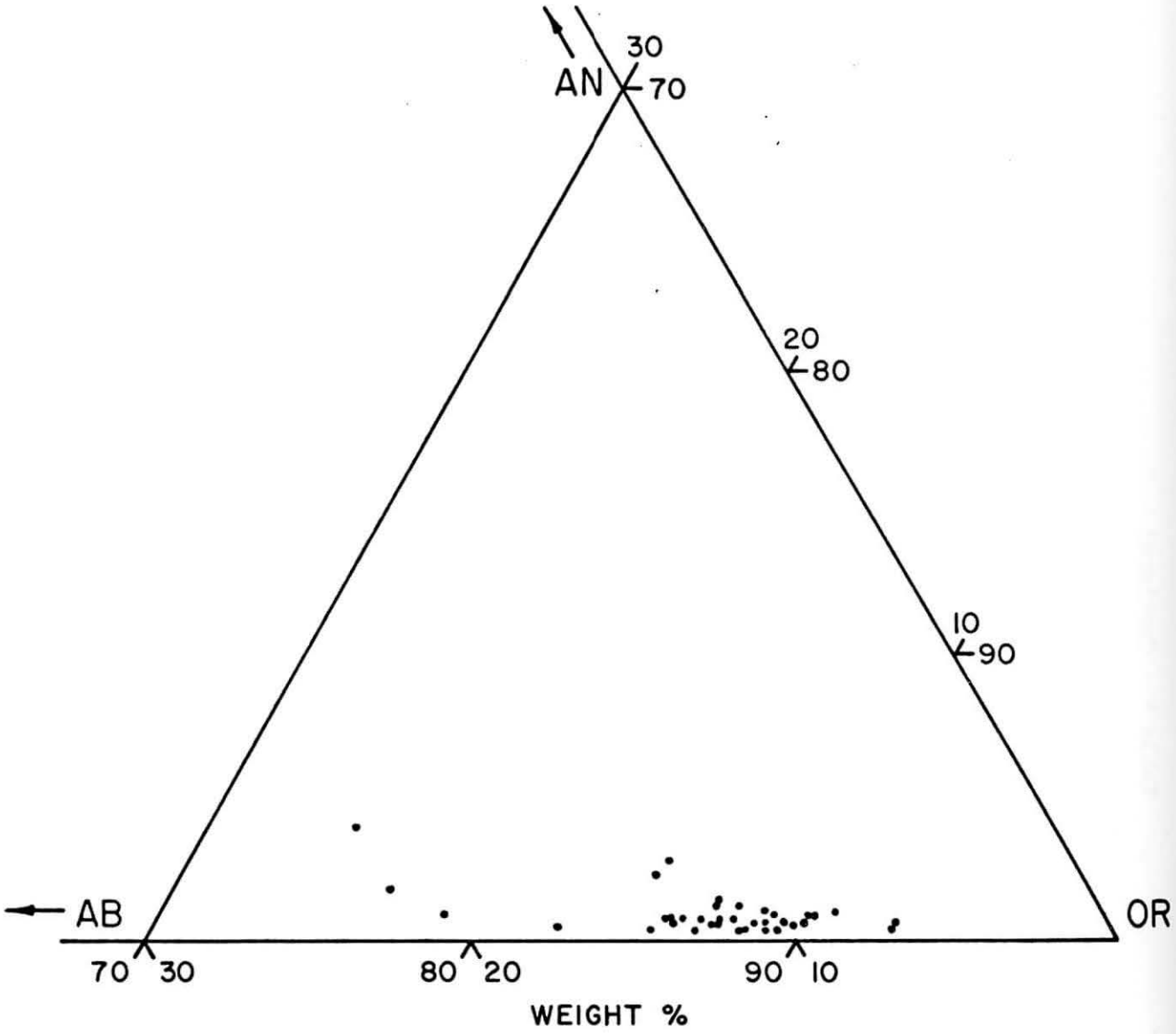


Figure 5. Orthoclase, Albite and Anorthite Contents - K-feldspar Separates, Hope and Ida Granites. Analyses Recalculated to 100 Percent.

Table 5: Petrographic Data: Hope Granite

| Location | Martin Dome | | | | | Shackleton Coast | | | | | |
|---|---|---|---|---|---|---|---|---|---|---|---|
| Sample | 40 | 81 | 292 | 295 | 314 | 573 | 587 | 604 | 647 | 654 | 707 |
| Quartz | 29 | 22 | 37 | 32 | 25 | 40 | 40 | 41 | 32 | 10 | 27 |
| K-feldspar | 9 | 24 | 5 | 24 | 27 | 13 | 25 | 34 | 26 | 63 | 43 |
| Plagioclase | 42 | 42 | 40 | 28 | 32 | 34 | 22 | 23 | 26 | 11 | 28 |
| Biotite | 19 | 11 | 18 | 16 | 15 | 11 | 13 | 2 | 14 | 8 | 3 |
| Hornblende | - | - | - | - | - | Acces.[a] | - | Tr.[b] | Acces. | 5 | - |
| Plagioclase composition[d] | n.d.[c] | zoned | zoned | zoned | zoned | zoned | zoned | zoned | zoned | zoned | zoned |
| % An | n.d. | 25-48 | 31-56 | 33-46 | 29-48 | 27-56 | 21-55 | 20-27 | 31-36 | 21-29 | 2-25 |

[a]Accessory
[b]Trace
[c]No data
[d]Determined by measurement of extinction angle on (010) in sections oriented normal to a-axis (van der Kaaden, 1951)

Table 6: Petrographic data: Ida Granite

| Sample | 575 | 580 | 608B | 636 | 637 | 719 |
|---|---|---|---|---|---|---|
| Quartz | 28 | 40 | 36 | 32 | 26 | 36 |
| K-feldspar | 42 | 35 | 25 | 39 | 45 | 21 |
| Plagioclase | 28 | 24 | 38 | 24 | 21 | 37 |
| Biotite | 3 | Tr | Tr[a] | 3 | Acces.[b] | 4 |
| Muscovite | - | Tr | Tr | Acces. | 3 | Acces. |
| Plagioclase | n.d.[c] | n.d. | unzoned | unzoned | unzoned | unzoned |
| Composition[d] % An | n.d. | n.d. | 2-22 | 4-11 | 11-15 | 25-29 |

[a]Trace
[b]Accessory
[c]No data
[d]Determined by measurement of extinction angle on (010) in sections oriented manual to a-axis (van der Kaader, 1951)

Table 7: Plagioclase Compositions: Hope Granite

| Sample | Number of Crystals Studied | Variation | % Anorthite[a] | | | |
|---|---|---|---|---|---|---|
| | | | Unzoned Crystals | Zoned Crystals | | All Crystals |
| | | | | Margin | Center | |
| 40 | 4 | Min | - | 39 | 40 | 39 |
| | | Max | | 44 | 53 | 53 |
| 81 | 10 | Min | [b]30 | 25 | 31 | 25 |
| | | Max | 30 | 38 | 48 | 48 |
| 292 | 9 | Min | 34 | 31 | 40 | 31 |
| | | Max | 51 | 45 | 56 | 56 |
| 294 | 10 | Min | 31 | 38 | 43 | 31 |
| | | Max | 46 | 43 | 51 | 51 |
| 295 | 6 | Min | 34 | [b]37 | 46 | 34 |
| | | Max | 54 | 37 | 46 | 54 |
| 297 | 6 | Min | 21 | 20 | 25 | 21 |
| | | Max | 23 | 28 | n.d.[c] | 28 |
| 314 | 8 | Min | 33 | 29 | 40 | 29 |
| | | Max | 43 | 41 | 48 | 48 |
| 315 | 10 | Min | 35 | 37 | 48 | 35 |
| | | Max | 45 | 37 | 48 | 48 |
| 573 | 5 | Min | - | 27 | 39 | 27 |
| | | Max | | 37 | 56 | 56 |
| 578A | 2 | Min | 24 | - | - | 24 |
| | | Max | 25 | | | 25 |
| 583 | 4 | Min | 14 | 23 | 28 | 14 |
| | | Max | 40 | 33 | 38 | 40 |
| 587 | 4 | Min | [b]26 | 21 | 23 | 21 |
| | | Max | 26 | 39 | 55 | 55 |
| 593 | 4 | Min | 26 | 37 | 45 | 26 |
| | | Max | 29 | 37 | 45 | 45 |
| 596 | 9 | Min | 12 | 6 | 16 | 6 |
| | | Max | 21 | 16 | 30 | 30 |
| 601 | 4 | Min | - | [d]9(26) | 28 | 9 |
| | | Max | | 31 | 34 | 34 |

Table 7 - Continued

| Sample | Number of Crystals Studied | Vari-ation | % Anorthite[a] | | | |
|---|---|---|---|---|---|---|
| | | | Unzoned Crystals | Zoned Crystals | | All Crystals |
| | | | | Margin | Center | |
| 604 | 4 | Min | 20 | [b]22 | 27 | 20 |
| | | Max | 23 | 22 | 27 | 27 |
| 605 | 7 | Min | [b]48 | 24 | 30 | 24 |
| | | Max | 48 | 38 | 54 | 54 |
| 630 | 3 | Min | [b]32 | 23 | 36 | 23 |
| | | Max | 32 | 26 | 43 | 43 |
| 635 | 2 | Min | [b]21 | - | - | 21 |
| | | Max | 21 | | | 21 |
| 646 | 4 | Min | - | 15 | 24 | 15 |
| | | Max | | 22 | 28 | 28 |
| 647 | 3 | Min | 31 | - | - | 31 |
| | | Max | 36 | | | 36 |
| 651 | 10 | Min | 26 | 18 | 27 | 18 |
| | | Max | 37 | 35 | 56 | 56 |
| 654 | 1 | Min | - | [b] 4 | 35 | 4 |
| | | Max | | 4 | 35 | 35 |
| 707 | 5 | Min | [b]13 | 2 | 19 | 2 |
| | | Max | 13 | 13 | 25 | 25 |
| 726 | 4 | Min | - | 25 | 29 | 25 |
| | | Max | | 27 | 35 | 35 |
| 738 | 5 | Min | 4 | 11 | 18 | 4 |
| | | Max | 4 | 18 | 24 | 24 |

[a]Determined by measurement of extinction angle on (010) in sections oriented normal to a-axis (van der Kaaden, 1951)

[b]Single crystal

[c]No data

[d]Crystal overgrown by more sodic material. Composition of inner margin in parentheses.

Table 8: Plagioclase Compositions: Ida Granite

| Sample | Number of Crystals Studied | Variation | % Anorthite[a] | | | |
|---|---|---|---|---|---|---|
| | | | Unzoned Crystals | Zoned Crystals | | All Crystals |
| | | | | Margin | Center | |
| [c]594 | 2 | Min | [b]17 | [b]5 | 17 | 5 |
| | | Max | 17 | 5 | 17 | 17 |
| 597 | 2 | Min | 21 | - | - | 21 |
| | | Max | 29 | | | 29 |
| [c]608B | 7 | Min | 2 | - | - | 2 |
| | | Max | 22 | | | 22 |
| 636 | 2 | Min | 4 | - | - | 4 |
| | | Max | 11 | | | 11 |
| 637 | 3 | Min | 11 | - | - | 11 |
| | | Max | 15 | | | 15 |
| 638 | 4 | Min | 0 | - | - | 0 |
| | | Max | 14 | | | 14 |
| [c]639 | 3 | Min | 9 | - | - | 9 |
| | | Max | 17 | | | 17 |
| 719 | 4 | Min | 25 | - | - | 25 |
| | | Max | 29 | | | 29 |
| 721 | 5 | Min | 22 | - | - | 22 |
| | | Max | 26 | | | 26 |
| 722 | 4 | Min | [b]29 | 13 | 18 | 13 |
| | | Max | 29 | 22 | 28 | 29 |
| 724 | 4 | Min | [b]33 | 19 | 27 | 19 |
| | | Max | 33 | 28 | 33 | 33 |

[a]Determined by measurement of extinction angle on (010) in sections oriented normal to a (van der Kaaden, 1951)

[b]Single crystal

[c]Dike

[d]Reverse zoning present

including aplite and pegmatite dikes contain plagioclase which is generally more sodic and less strongly zoned than that in the Hope Granite.

Samples of Hope Granite for which modal analyses are available vary from granodiorite to quartz monzonite (Williams et al., 1954). Ida Granite samples tend to have higher modal K-feldspar/plagioclase ratios and vary from quartz monzonite to granite. Modal contents of mafic minerals, biolite and occasionally hornblende, are consistently higher in Hope Granite than in Ida Granite samples, in some of which they are only present in trace amounts.

## Theoretical Aspects of Magmatic Differentiation

The interpretation of the chemical and mineralogical data on the Hope and Ida Granites is based on several theoretical concepts. These are discussed briefly in this section.

It is well known that a body of magma tends to become chemically fractionated during crystallization, due to preferential concentration of certain elements in the first-formed minerals. In granitic magmas the crystallization of mafic minerals, for example biotite and hornblende, and of calcic plagioclase tends to enrich the residual magma in silica and in some cases in alkalis and to impoverish it in iron, magnesium and calcium. If disequilibrium conditions prevail, plagioclase crystallizing from such a magma will be normally zoned. Only when the magma begins to crystallize eutectically will fractionation cease.

Trace elements also tend to be fractionated by non-eutectic crystallation, commonly more strongly than major elements. The behavior in a magma of a trace element which is competing with another element for a site in a crystal lattice can in most cases be predicted in terms of two empirical rules formulated by Goldschmidt (1937). These state that in such a case the ion having the smaller ionic radius and the greater charge will tend to enter the lattice site more readily. Thus if $K^+$ and $Rb^+$ ions are competing for an alkali site in a K-feldspar lattice the smaller $K^+$ ion will tend to be more successful. However, in the case of $K^+$ and $Ba^{+2}$, the doubly charged $Ba^{+2}$ ion will tend to be favored. Each substitution of $K^+$ by $Ba^{+2}$ is accompanied by coupled substitution of $Si^{+4}$ by $Al^{+3}$. This means that, in a magma from which K-feldspar is crystallizing, $Ba^{+2}$ will tend to be concentrated in the early-formed K-feldspar and $Rb^+$ in the residual magma. The same holds true for other potassium minerals such as biotite and muscovite. Consequently, the potassium minerals which crystallize from the later-stage 'residual' magmas tend to be enriched in Rb relative to their earlier counterparts, since Rb forms no minerals of its own. The K/Rb and Ba/Rb ratios of K-feldspars crystallizing under these conditions tend to decrease as crystallization proceeds. These ratios can therefore be used as parameters to monitor the degree of fractional crystallization which a suite of granitic rocks has undergone.

The anorthite content of plagioclase can also be used as a measure of magmatic differentiation. Ideally, a plagioclase crystal should have a homogeneous anorthite content which is directly related to that of the magma with which it is in equilibrium. However, in most granitic magmas, disequilibrium conditions cause incomplete reaction of plagioclase and the development of normally zoned crystals, as found in the Hope Granite. In such a crystal, the center and margin provide measures of the anorthite content of the first and last magmas with which the crystal was in contact, respectively. If a plagioclase crystal comes into contact with a more calcic liquid, for example by convective movement in a chemically heterogeneous magma, some or all of the crystal may be resorbed. Later contact with a more sodic magma will cause crystallization of an overgrowth of more sodic plagioclase, separated from the resorbed core by an irregularly shaped compositional discontinuity. Such features are present in some of the Hope Granite samples studied.

Finally, the mineralogical composition of the rock, as determined by modal analysis, provided another measure of the degree of fractionation of the magma from which it crystallized. A low content of mafic minerals and an abundance of quartz and K-feldspar tend to indicate a strongly fractionated magma.

These three parameters, K-feldspar chemistry, plagioclase composition and petrographic mode, are reliable measures of magmatic fractionation only if two conditions are fulfilled: (1) the mineral assemblages studied reflect the course of fractional crystallization of the magma and contain no xenocrysts, and (2) the chemistry and mineralogy of the rocks sampled have not been affected significantly by later alteration.

## Discussion of Results

In this section the relationships between variations of the three parameters, K-feldspar chemistry, plagioclase composition and petrographic mode, in the samples analyzed are discussed. The behavior of the parameters as a function of rock-type and geographic location of the samples is examined. Three lithologic groups of samples, Hope Granite, Ida Granite plutonic and Ida Granite aplite and pegmatite dike samples are distinguished. In addition, the Hope Granite samples are grouped geographically under those from Martin Dome, the Mt. Hope pluton, the intrusions east of the mouth of the Beardmore Glacier and other intrusions in the Shackleton Coast. Different symbols are used for each of these six sample groups in the diagrams which follow. Finally, it is shown that (1) the chemical results support the strontium isotopic evidence (preceding paper) that the Hope and Ida Granites in the Shackleton Coast were derived from a common parent magma, and (2) the chemical and mineralogical variations in the Hope and Ida Granites are explicable by differentiation of this parent magma.

## Rb in K-feldspars

### Results

Concentrations of K and Rb in 39 K-feldspar samples are plotted in Figure 6. The samples show a continuous pattern of variation in K/Rb ratio, from 83 (sample 608B) to 490 (sample 658). Samples from the three lithologic units occupy more restricted areas of the diagram. Hope Granite samples tend to have relatively high K/Rb ratios (101 to 490). Ida Granite plutonic samples have intermediate ratios (104 to 146), and Ida Granite dike samples include ratios as low as 83. There is no detectable difference in the K/Rb pattern of Hope Granite samples from the four geographic areas.

In Figure 7 the ranges of plagioclase anorthite content of 32 samples are plotted versus the K/Rb ratios of K-feldspar separates from the same samples. The diagram shows a definite trend towards decreasing maximum, average and minimum anorthite content of plagioclase as K-feldspar K/Rb ratio decreases. The three lithologic groups again occupy more restricted overlapping areas of the diagram. The Ida Granite plutonic and dike samples tend to have more sodic plagioclase as well as more Rb-rich K-feldspar than the Hope Granite. As before, there is no detectable difference in plagioclase composition pattern for Hope Granite samples from the four locations.

Two modal parameters, K-feldspar and total mica (biotite and muscovite) contents are plotted versus K/Rb ratio for 12 samples in Figures 8 and 9. Although there is no detectable pattern in the K-feldspar modes, there appears to be a distinct trend towards increasing K-feldspar K/Rb ratio in the samples which have higher mica contents. The diagram also shows the general lower mica content of the Ida Granite samples.

### Interpretation

The relationship between K-feldspar K/Rb ratio and rock-type, sample mica content and composition of coexisting plagioclase support the strontium isotope evidence that the rocks sampled from the Shackleton Coast belong to the same magma differentiation series. The most basic magma which the samples record crystallized K-feldspar with a K/Rb ratio of 490 (sample 658). As crystallization proceeded the Rb content of the crystallized magma increased to the point where it was crystallizing K-feldspar with a K/Rb ratio of 83 (sample 608B).

## Ba in K-feldspars

### Results

Concentrations of Ba and Rb in 34 K-feldspar samples are plotted in Figure 10. The Ba/Rb ratio shows a continuous pattern of variation from

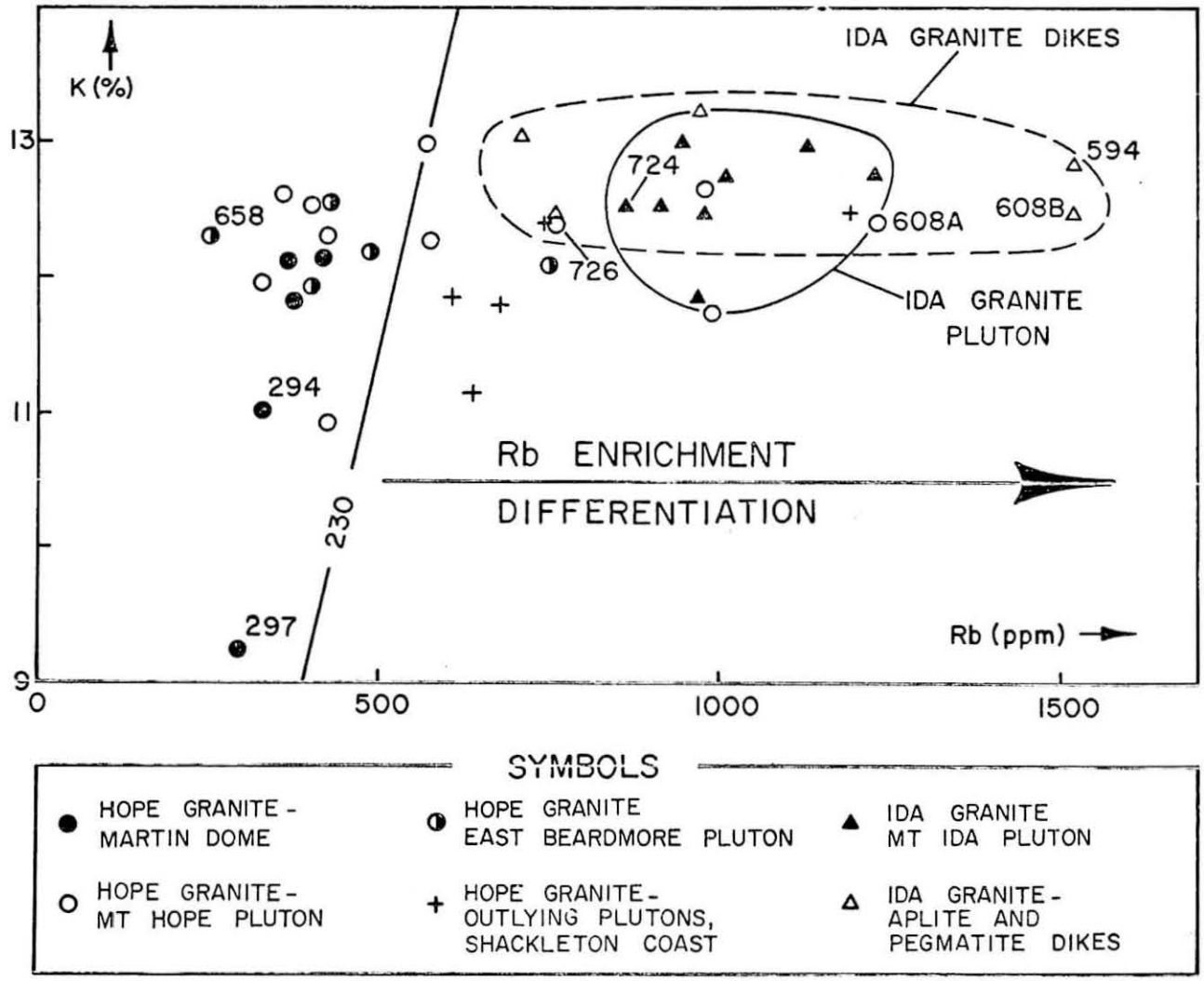


Figure 6. K and Rb in K-feldspar Separates - Hope and Ida Granites. Areas of Ida Granite Plutonic and Dike Samples Outlined. Crustal Average K/Rb Ratio 230 Indicated. Selected Samples Numbered.

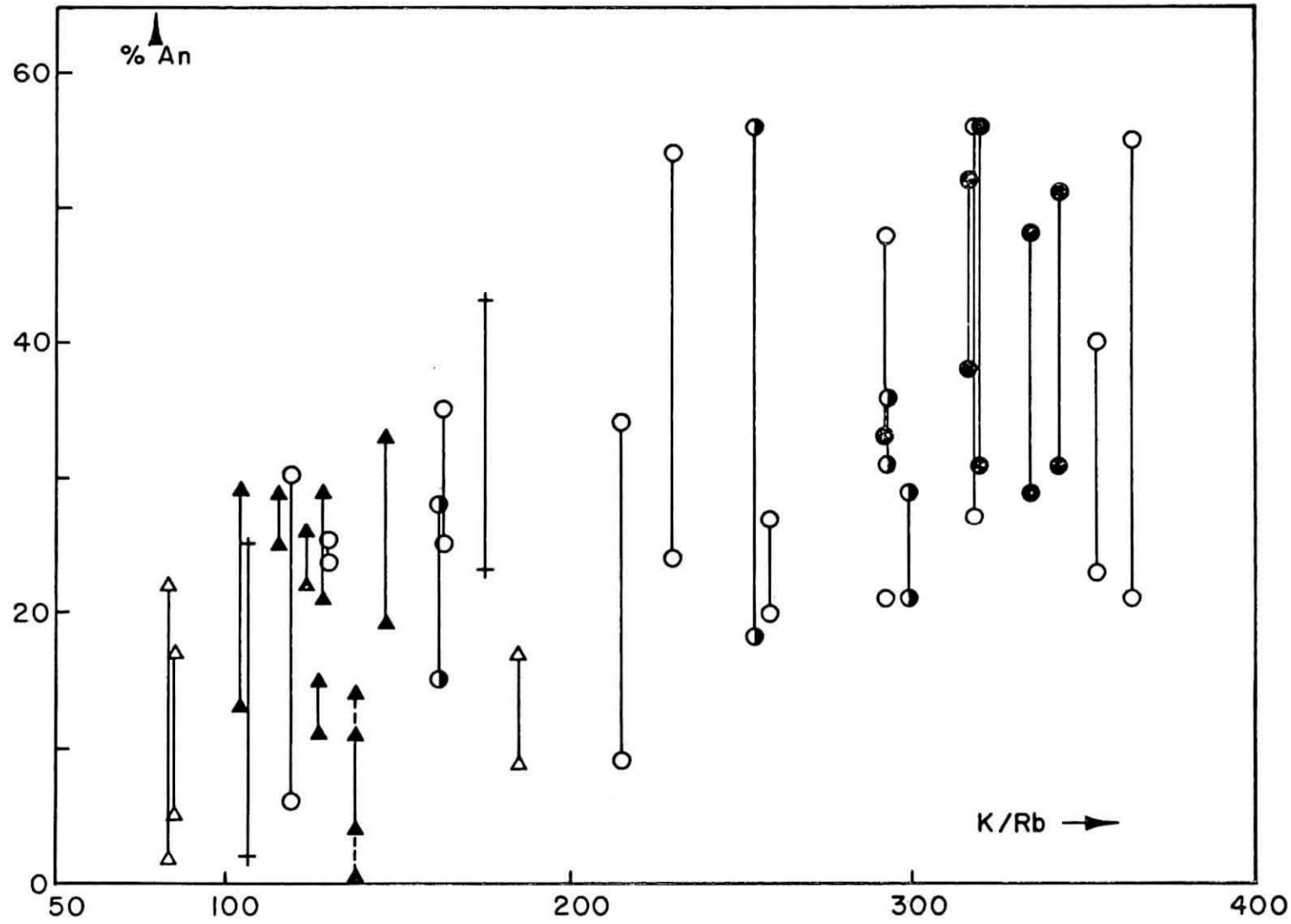


Figure 7. Ranges in Plagioclase Anorthite Content Plotted Versus K/Rb Ratios in Coexisting K-feldspars - Hope and Ida Granites. Symbols as in Figure 6.

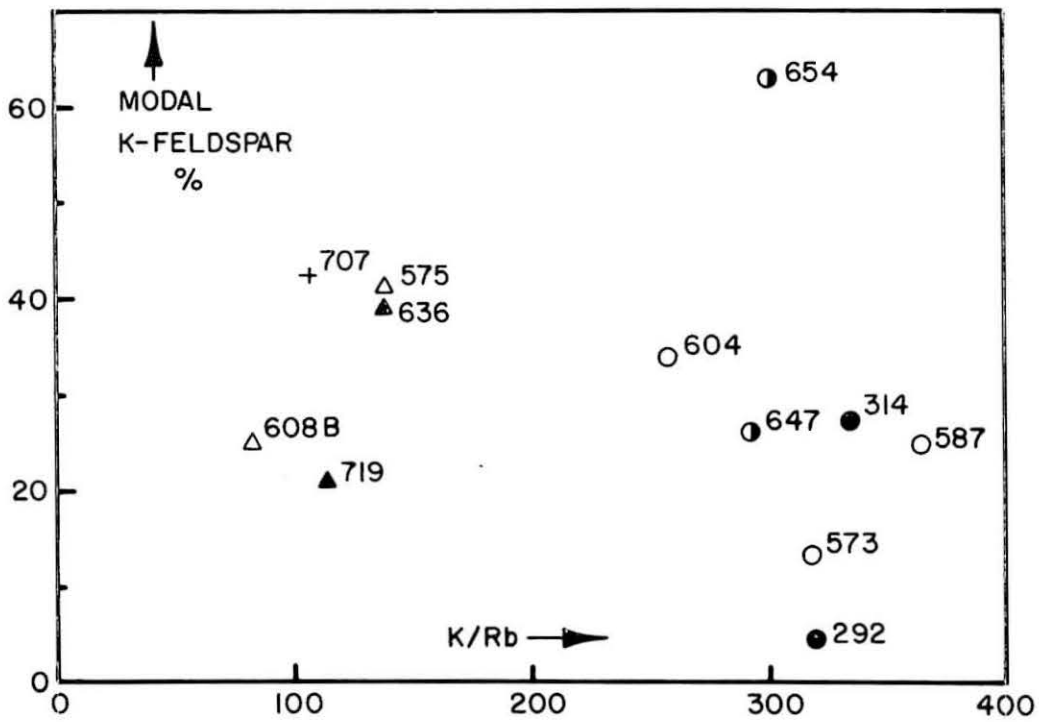


Figure 8. K/Rb Ratios of K-feldspar Separates Plotted Versus Modal K-feldspar Contents in the Same Samples - Hope and Ida Granites. Symbols as in Figure 6.

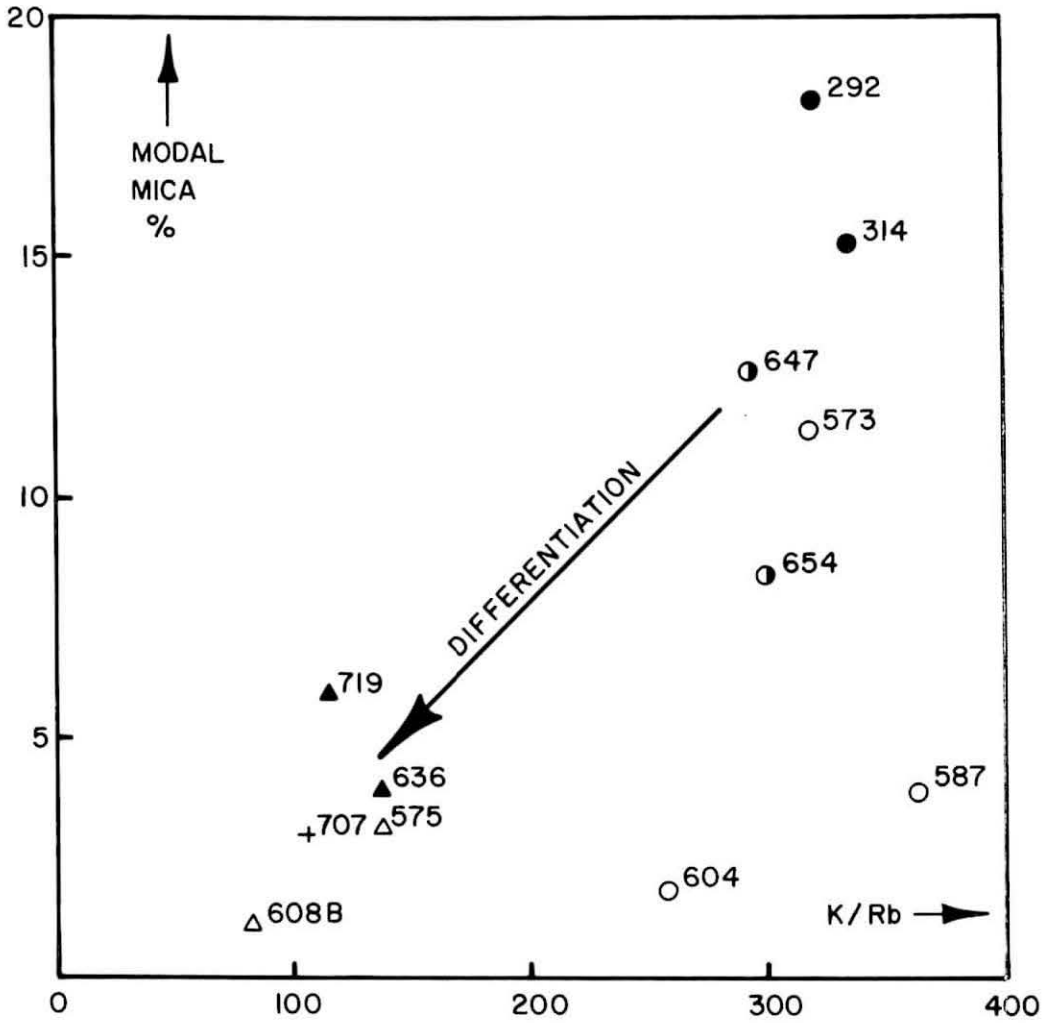


Figure 9. K/Rb Ratios of K-feldspar Separates Plotted Versus Modal Total Mica Contents (Biotite + Muscovite) - Hope and Ida Granites. Symbols as in Figure 6.

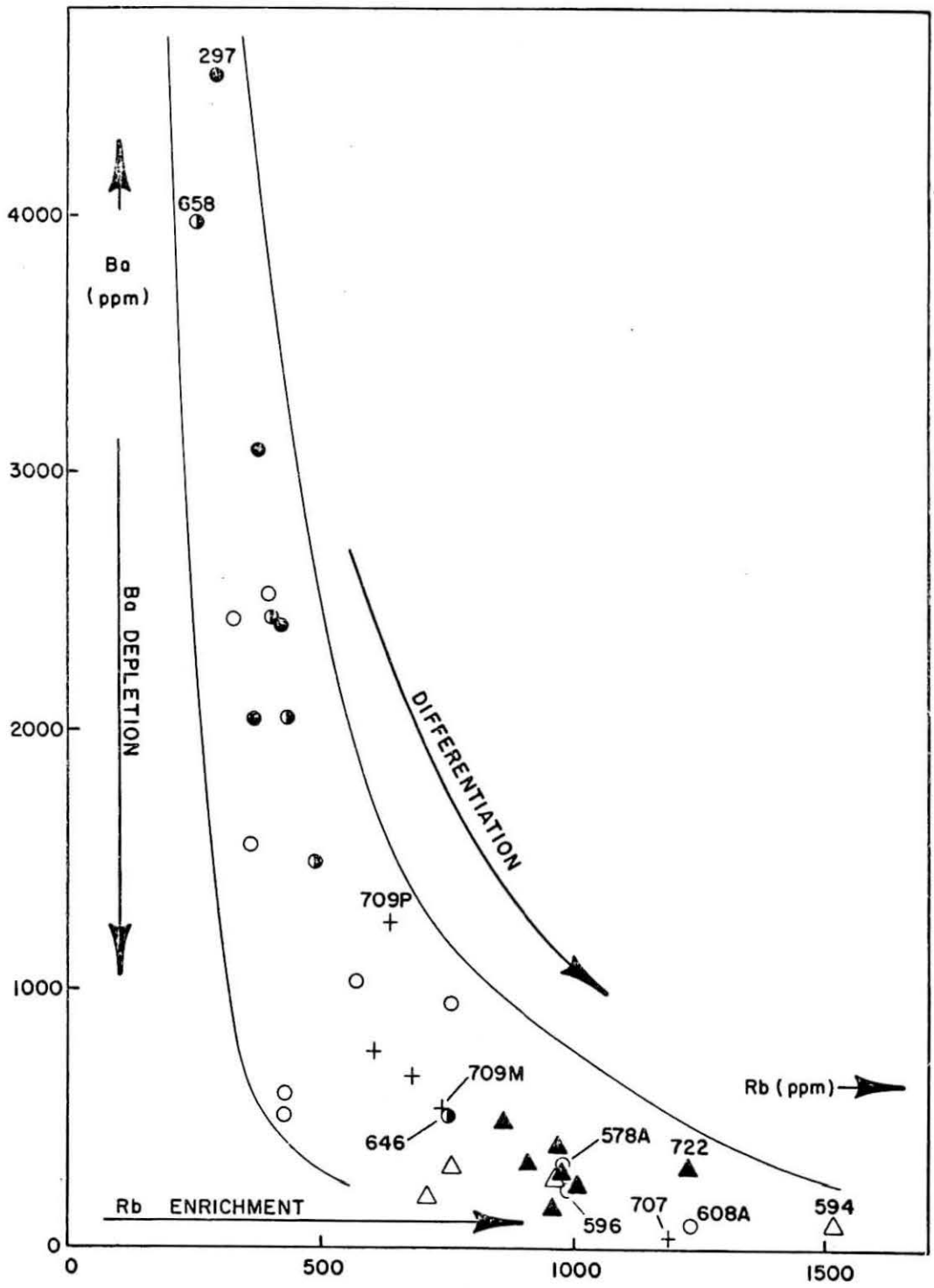


Figure 10. Ba and Rb in K-feldspar Separates - Hope and Ida Granites. Selected Samples Numbered. Symbols as in Figure 6.

0.05 (sample 707) to 15.8 (sample 658), similar to that of the K/Rb ratio. The Ida Granite samples, of both plutonic and dike rocks, are concentrated in the lower part of the diagram and have K-feldspar Ba/Rb ratios between 0.06 and 0.56. However, the Hope Granite samples span the whole range of Ba/Rb variation. Again there is no detectable difference in Ba/Rb pattern for Hope Granite samples from the four locations. The trend of increasing plagioclase anorthite content with increasing K-feldspar Ba/Rb ratio (Fig. 11) matches the K/Rb pattern. Hope Granite samples 578A, 596, 646 and 707 which have low K-feldspar Ba/Rb ratios (less than 0.7) have plagioclase which is consistently less calcic than that in the remaining Hope Granite samples. Comparison of Figures 9 and 10 shows that the samples with high modal mica tend to have high Ba/Rb ratios.

### Interpretation

Notwithstanding the previously expressed caution about the representativeness of K-feldspar Ba analyses, the Ba/Rb ratios tend to match the trends shown by the same K-feldspar samples. This supports the interpretation of the K/Rb and strontium isotope evidence in terms of a single magma fractionation series for the samples from the Shackleton Coast. The progressive reduction in Ba content of the K-feldspars with increasing K-feldspar Rb and plagioclase Na content suggests that the magma was progressively depleted in Ba as crystallization proceeded. The relatively small increase in K-feldspar Rb content and in plagioclase Na content with a decrease in K-feldspar Ba content from 4000 ppm to 1000 ppm (Figs. 10 and 11) suggests that gradual Ba depletion covered much of the range of crystallization of the Hope Granite samples. However, during crystallization of the Ida Granite plutonic and dike samples depletion of Ba in the magma proceeded at a lower rate relative to Rb enrichment.

## Sr in K-feldspars

### Results

Concentrations of Sr are plotted versus Rb, Ca and Ba concentrations in K-feldspar samples in Figures 12, 13 and 14, respectively. The pattern of Sr/Rb variation is similar to that shown by Ba/Rb in the same samples (Fig. 10). Hope Granite samples span the whole range of Rb/Sr ratios from 0.56 (sample 658) to 30 (sample 707). Ida Granite plutonic samples are restricted to a small area of the diagram and have relatively high K-feldspar Rb/Sr ratios. Ida Granite dikes also have high K-feldspar Rb/Sr ratios which range up to 88 (sample 608B).

Neither Ba nor Ca show the inverse relationship with Sr which is typical of the Rb/Sr and Ba/Rb variation patterns in the K-feldspars. On the Ca/Sr diagram (Fig. 13) the Ida Granite samples are clustered in

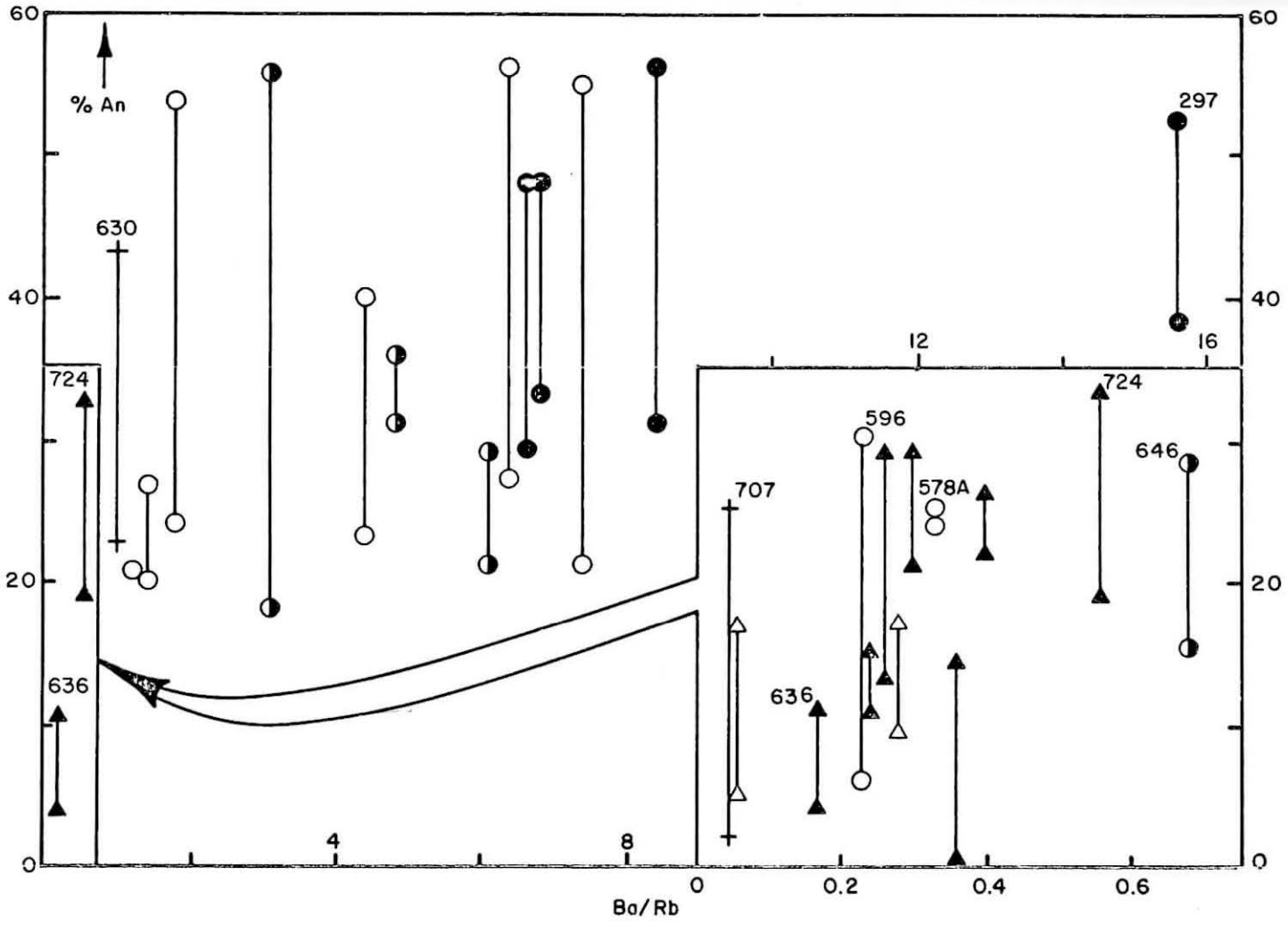


Figure 11. Ranges in Plagioclase Anorthite Content Plotted Versus Ba/Rb Ratios in Coexisting K-feldspars - Hope and Ida Granites. Inset - Low Ba/Rb Samples with Expanded Ba/Rb Scale. Symbols as in Figure 6.

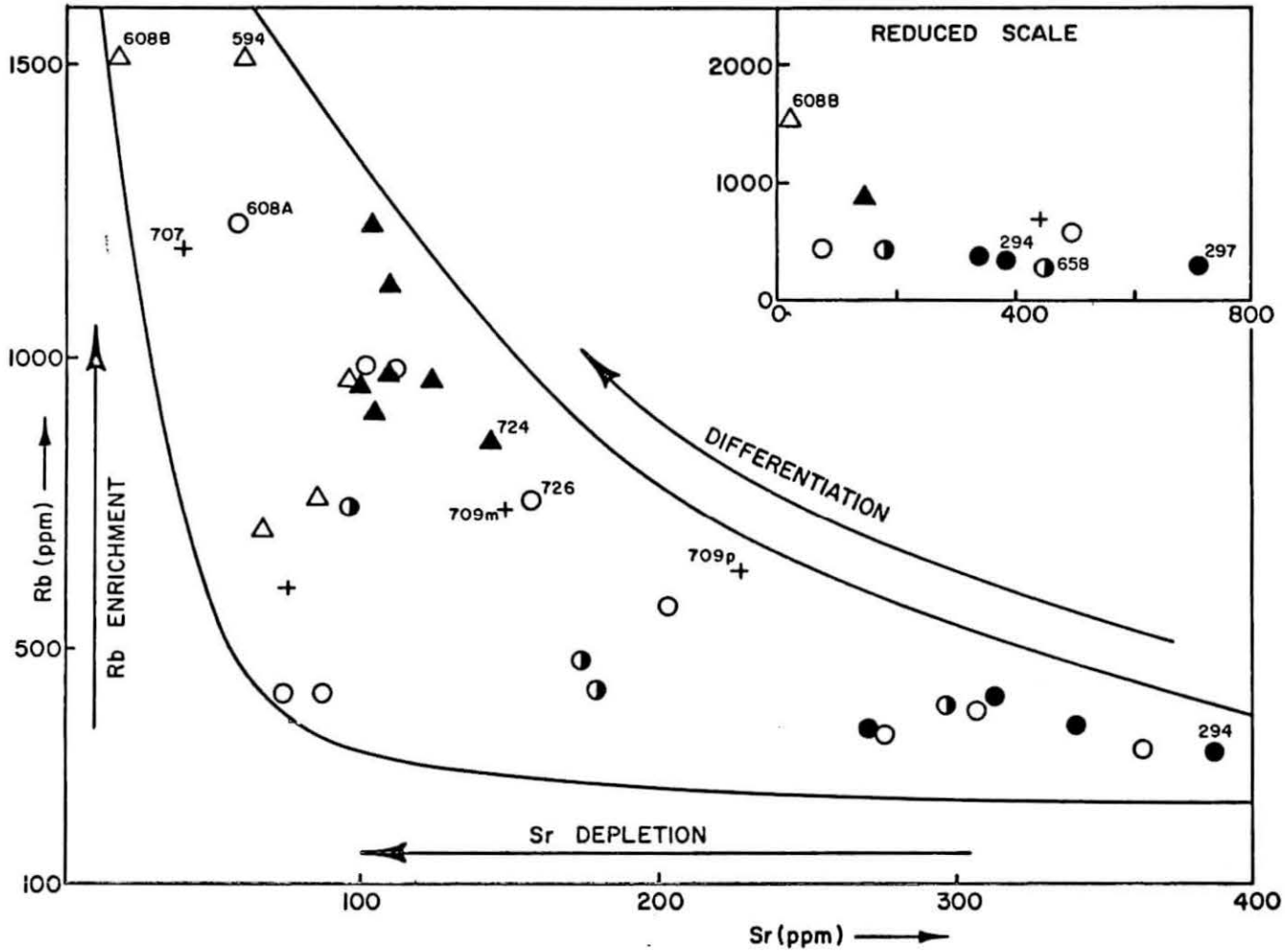


Figure 12. Rb and Sr Contents of K-feldspar Separates - Hope and Ida Granites. Inset at Reduced Scale. Selected Samples Numbered. Symbols as in Figure 6.

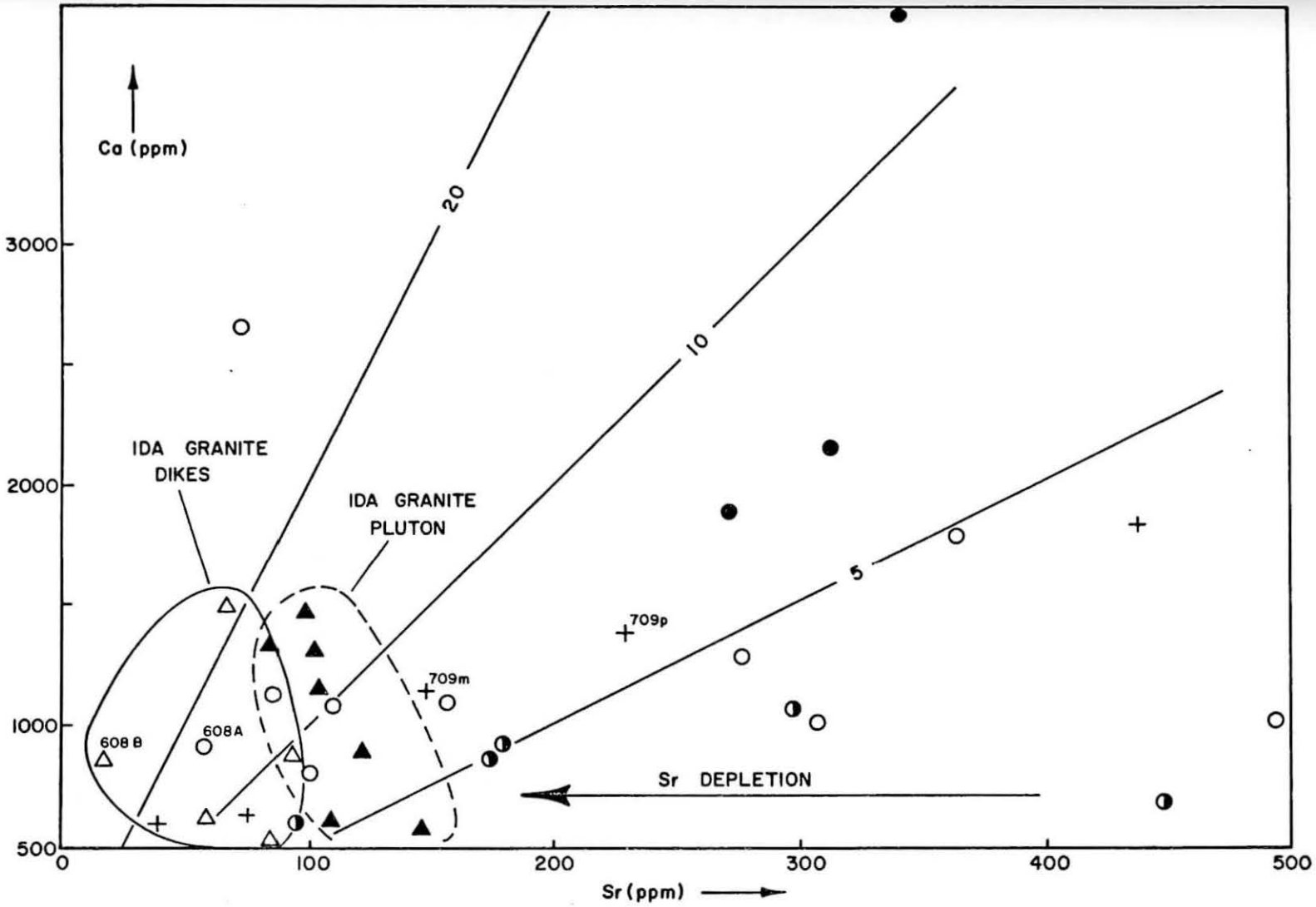


Figure 13. Ca and Sr Contents of K-feldspar Separates - Hope and Ida Granites. Areas of Ida Granite Plutonic and Dike Samples Outlined. Ca/Sr Ratios 5, 10 and 20 Indicated. Selected Samples Numbered. Symbols as in Figure 6.

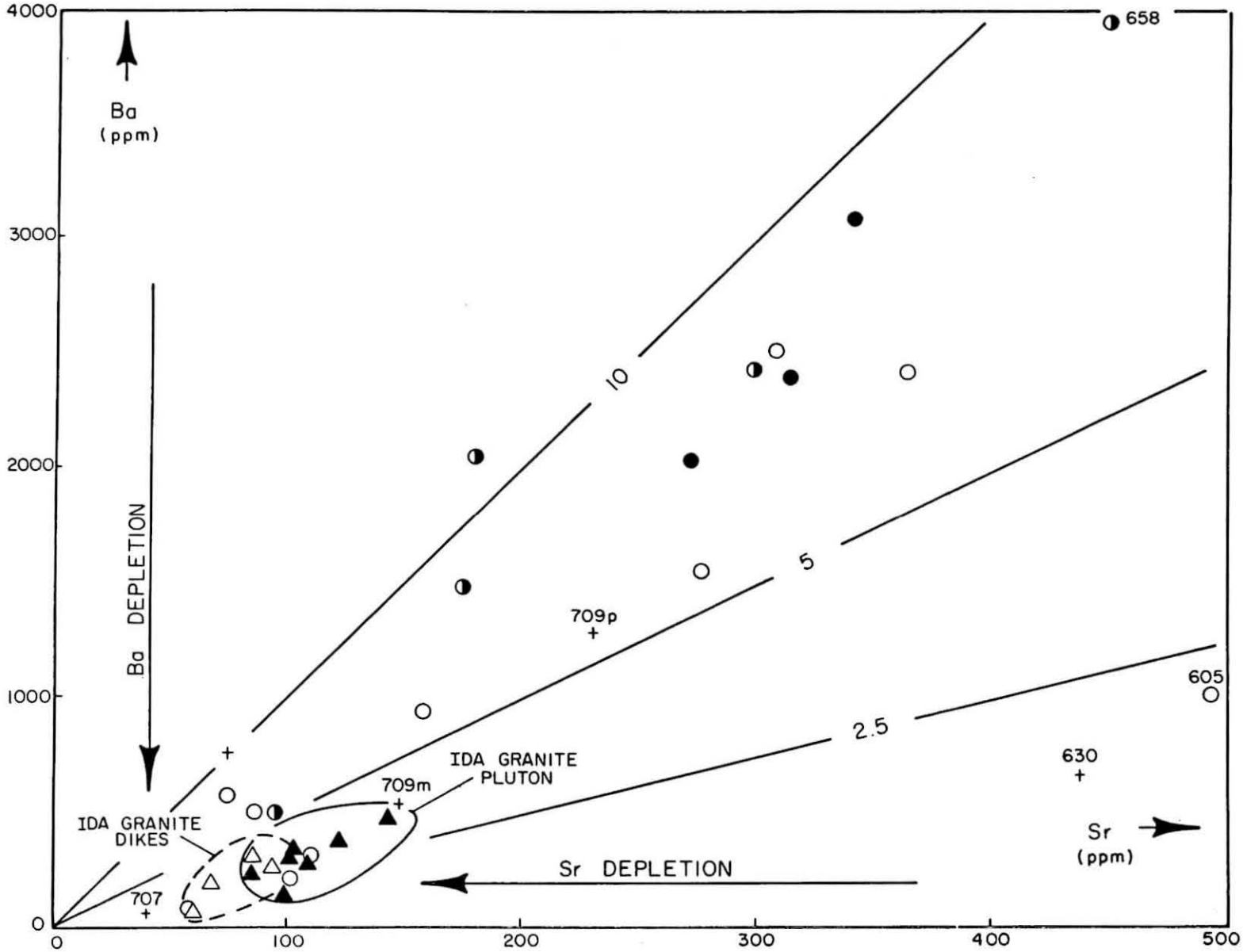


Figure 14. Ba and Sr Contents of K-feldspar Separates - Hope and Ida Granites. Areas of Ida Granite Plutonic and Dike Samples Outlined. Ba/Sr Ratios 2.5, 5 and 10 Indicated. Selected Samples Numbered. Symbols as in Figure 6.

a relatively small area, with low Ca and Sr concentrations, but the Hope Granite samples are scattered throughout the diagram and show no detectable relationship between Ca and Sr. By contrast, the Ba and Sr contents of both Hope and Ida Granite K-feldspar samples are clearly related (Fig. 14). The Ida Granite samples plot in a small area of the diagram and show a strong degree of coherence between Ba and Sr, with an average Ba/Sr ratio of about 3. The Hope Granite samples range much more widely across the diagram, but, except for samples 605 and 630, they also show a significant degree of coherence of Ba and Sr.

### Interpretation

The marked coherence of Ba and Sr in the K-feldspar samples and the similarity of the Rb/Sr and Ba/Rb variation diagrams suggest that Sr and Ba were both progressively depleted in the magma at similar rates during crystallization of the Hope Granite samples. During crystallization of the Ida Granite samples the Ba depletion rate was much slower but Sr continued to be depleted until the Ida Granite aplite and pegmatite dikes were emplaced.

## Ratio Variation Diagrams as Indicators of Differentation Trends

It has been shown that the K-feldspar concentration ratios K/Rb, Ba/Rb and Rb/Sr are sensitive parameters of magmatic differentiation in the Hope and Ida Granites. Figures 15, 16 and 17 are variation diagrams in which these ratios are plotted versus each other. In each diagram the samples plot in a narrow curved band. The patterns shown by individual samples and by lithologic groups of samples are the same in each diagram. The Ida Granite samples are closely spaced near one end of the trend and the least differentiated samples, 292, 587, and 658 for example, plot at the other end.

Each trend therefore represents a liquid line of descent of the magma from which the samples crystallized, and the position of a sample on the trends is a measure of the degree of differentiation of the magma from which it crystallized.

## Individual Samples

A number of samples deserve individual mention because of special features of their chemistry or mineralogy.

Samples 709m and 709p, respectively, the separates of matrix and phenocryst K-feldspar from sample 709, show several chemical differences, as mentioned previously. Sample 709p is significantly richer in Na, Ba and Sr and poorer in K and Rb than sample 709m. The pattern of differences between these two samples in Ba, Sr and Rb is illustrated in

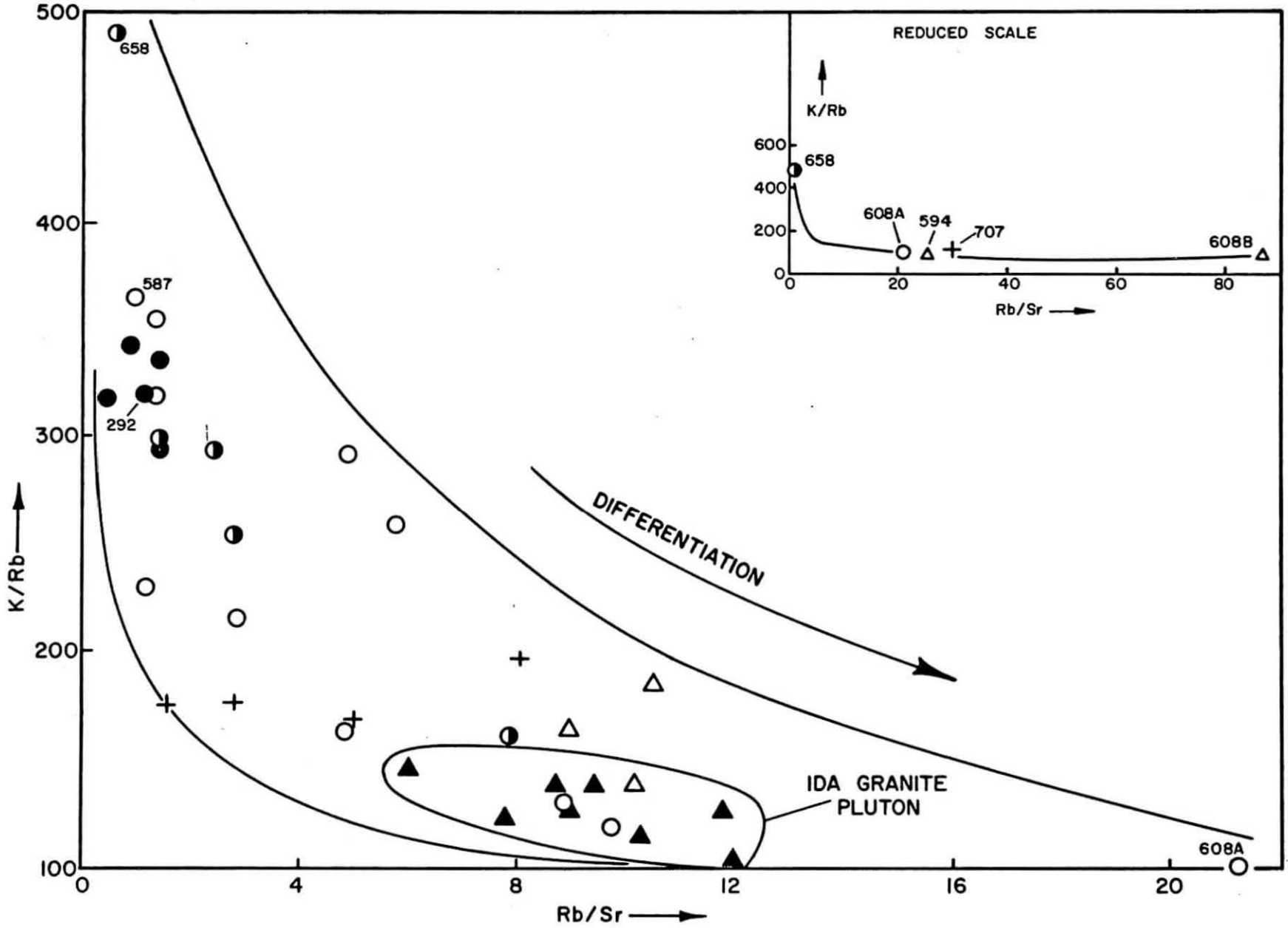


Figure 15. K/Rb and Rb/Sr Ratios in K-feldspar Separates - Hope and Ida Granites. Area of Ida Granite Plutonic Samples Outlined. Inset at Reduced Scale. Selected Samples Numbered. Symbols as in Figure 6.

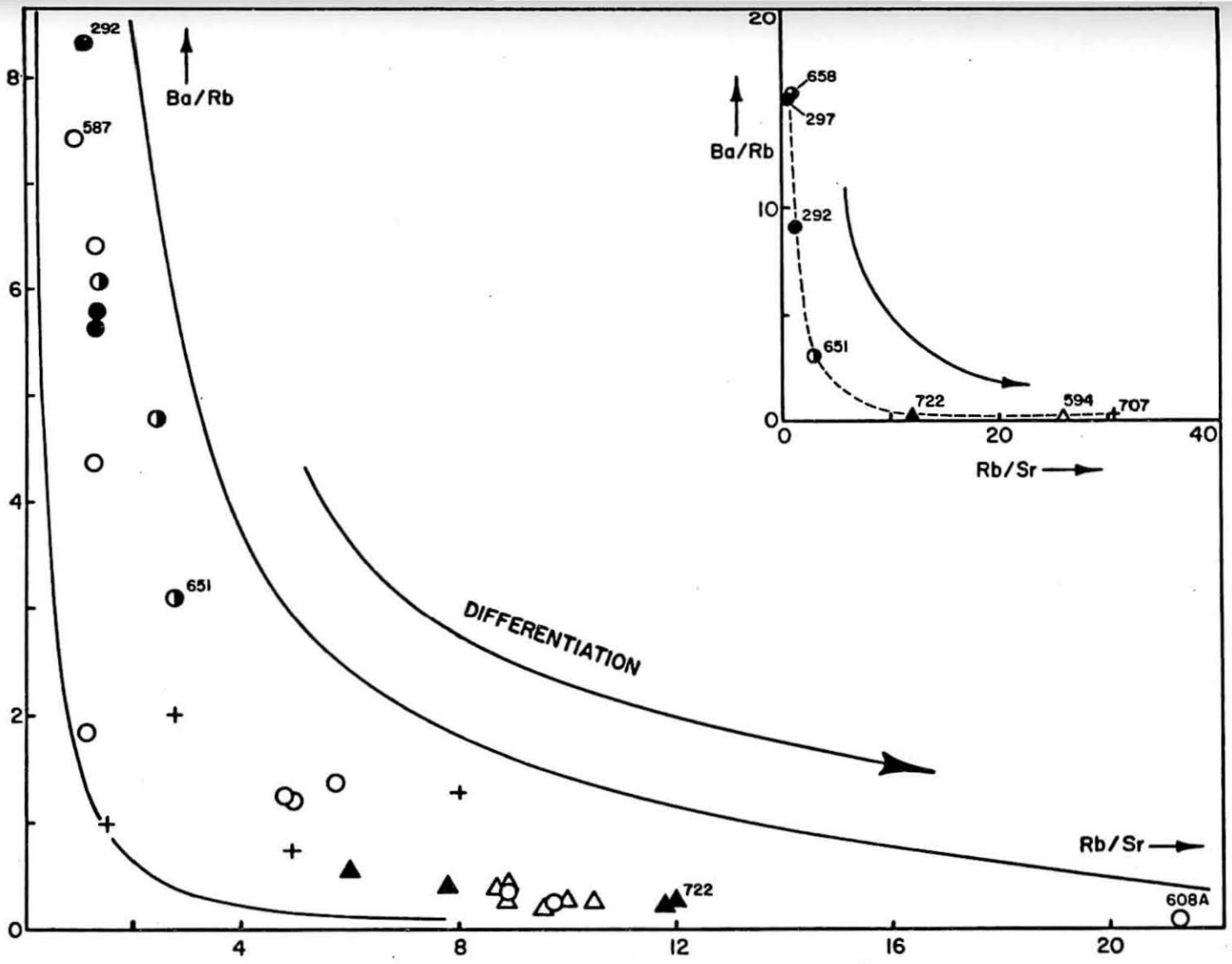


Figure 16. Ba/Rb and Rb/Sr Ratios in K-feldspar Separates - Hope and Ida Granites. Inset at Reduced Scale. Selected Samples Numbered. Symbols as in Figure 6.

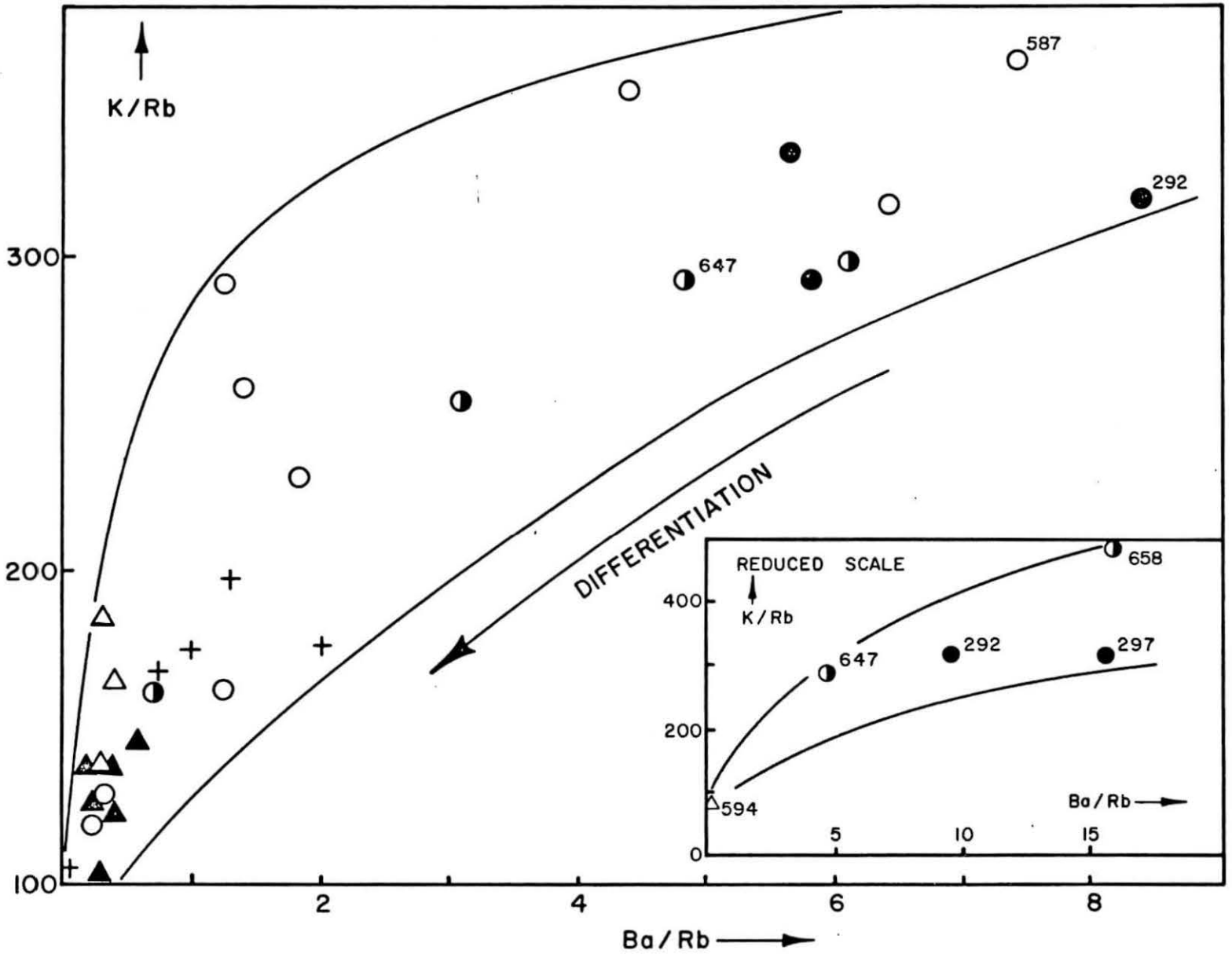


Figure 17. K/Rb and Ba/Rb Ratios in K-feldspar Separates - Hope and Ida Granites. Inset at Reduced Scale. Selected Samples Numbered. Symbols as in Figure 6.

Figures 14, 10 and 12. It is consistent with that predicted by Goldschmidt's rules and is therefore probably due to crystallization of the bulk of the phenocrysts in sample 709 before the matrix K-feldspars. The contrast in K and Na contents may be due to initial crystallization of the K-feldspar phenocrysts in a more sodic magma on the Na side of the albite-orthoclase binary eutectic (Bowen and Tuttle, 1950) and their subsequent removal from contact with more potassic later-stage magmas either by mantling or by physical movement.

Sample 608B is an aplite dike which was collected in the same hand specimen as the Hope Granite which it intrudes (sample 608A). The proximity of samples 608A and 608B on the K/Rb, Ca/Sr and Rb/Sr K-feldspar variation diagrams (Figs. 6, 13) reflects a similarity in K-feldspar content of K, Ca, Rb, and Sr. It is therefore possible that exchange of these elements took place between sample 608A and the dike from which sample 608B was collected.

A similar exchange may have affected samples 724 and 726, which were collected from the contact zone between the Ida Granite pluton and the Mt. Hope pluton (Fig. 18). As described in Chapter III of Gunner (1971), the contact at this locality is diffuse and suggests that the Ida Granite pluton was intruded before the Hope Granite had completely solidified. Sample 726 is coarser-grained, richer in mafic minerals and has plagioclase which is more calcic than in sample 724. However, the proximity of the two samples on the K/Rb and Rb/Sr K-feldspar variation diagrams (Figs. 6 and 12) suggests that sample 726 exchanged Rb and Sr with the Ida Granite magma at the time of its emplacement.

## Geographic Variation of K-feldspar Chemistry of Hope and Ida Granite Samples

Samples were collected on traverses across the Mt. Hope, Mt. Ida and East Beardmore plutons for a comparison of the crystallization histories of different parts of these bodies. The K/Rb, Ba/Rb and Rb/Sr ratios of K-feldspars from 34 samples are plotted on Figure 18.

Heier and Taylor (1959) showed that in a cylindrical body of granitic magma which crystallized from the margins inward, the K/Rb ratios of K-feldspars show a progressive decrease from the margins to the center of the pluton, where the last portions of the magma crystallized. In such an intrusion, contours of equal K-feldspar K/Rb ratio should form a concentric pattern. The same should be true of other parameters of differentiation, such as K-feldspar Ba/Rb and Rb/Sr ratios, plagioclase composition and biotite mode.

It is clear from Figure 18 that the Mt. Hope, Mt. Ida and East Beardmore plutons do not conform to a simple model. Because of the low density of sample distribution and the uncertainty of the exact locations of some of the pluton margins, no attempt to contour the data has been made. However certain general conclusions can be drawn.

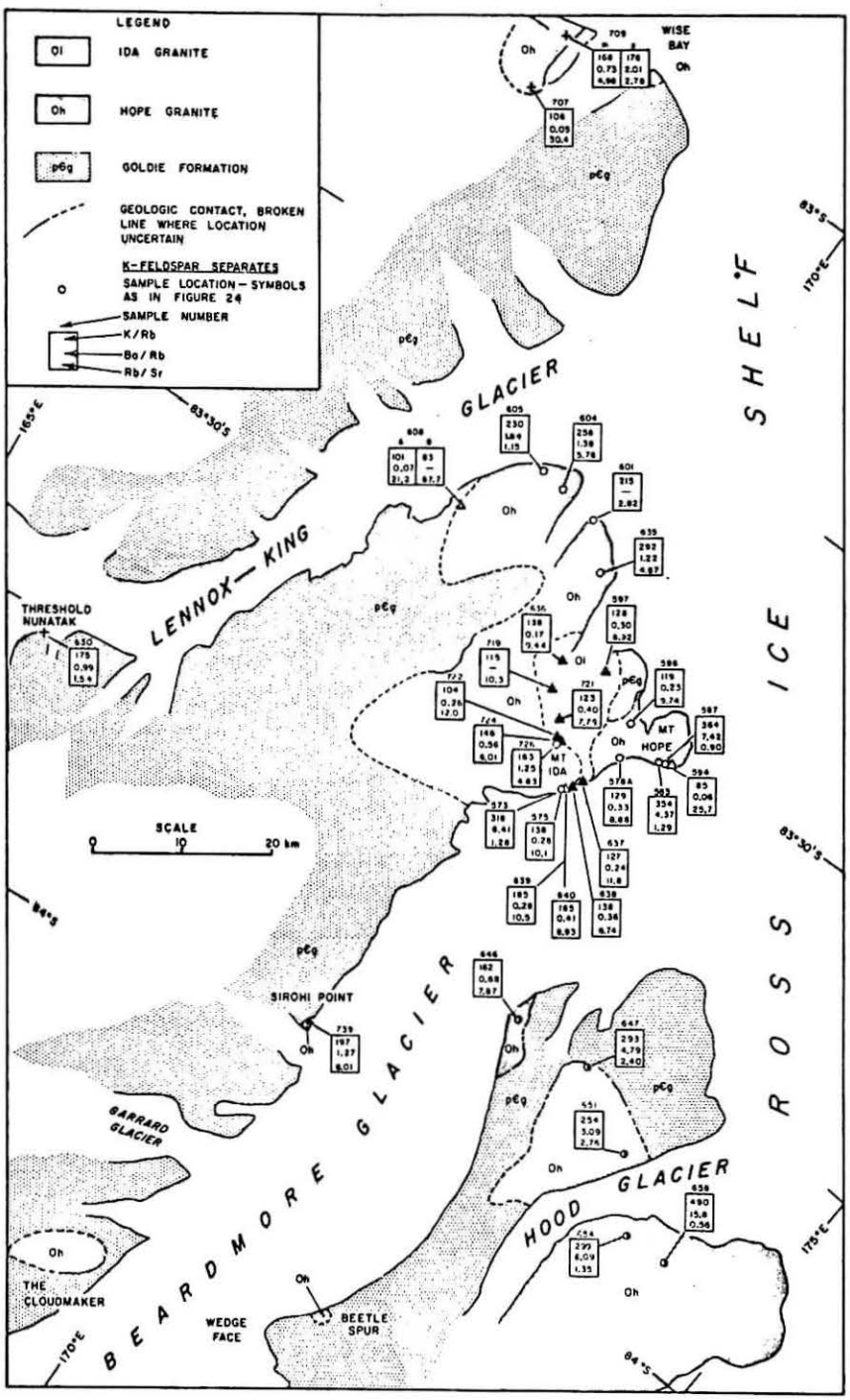


Figure 18. Shackleton Coast, Geologic Sketch Map. Locations of Hope and Ida Granite Samples and K/Rb, Ba/Rb and Rb/Sr Ratios of K-feldspar Separates Indicated.

The data on the East Beardmore pluton are insufficient for detailed interpretation. The K-feldspar K/Rb, Ba/Rb and Rb/Sr ratios in the five samples do not appear to be related to distance from the pluton margin. However there seems to be a distinct increase in differentiated character of the K-feldspars from east to west. It is possible that this pattern is due to a sequence of intrusion of separate bodies of progressively differentiated magma from east to west.

The Mt. Hope pluton has more complex K-feldspar chemical patterns. The limited data allow a tentative subdivision of the samples into three areas, as shown in Figure 19. The ranges of K/Rb, Ba/Rb and Rb/Sr K-feldspar ratios in the samples from each area are listed in Table 9.

Table 9: Mt. Hope pluton: Ranges of K-feldspar K/Rb, Ba/Rb, and Rb/Sr ratios in Areas I, II and III

| Area | Location | K/Rb | Ba/Rb | Rb/Sr |
|---|---|---|---|---|
| I | Granite Pillars - Mt. Hope | High 318-364 | High 4.37-7.42 | Low 0.90-1.29 |
| II | Lower Beaver Glacier | Intermediate 215-292 | Intermediate 1.22-1.84 | Intermediate 1.15-5.76 |
| III | The Gateway - Cape Allen | Low 119-129 | Low 0.23-0.33 | High 8.88-9.74 |

Area I includes outcrops of the pluton along the Beardmore Glacier, sampled at Mt. Hope and Granite Pillars. K-feldspars from this area have the highest K/Rb and Ba/Rb and the lowest Rb/Sr ratios obtained from the Mt. Hope pluton. Area II, around the mouth of the Beaver Glacier, has rocks with intermediate values of the three parameters. In Area III, which includes Cape Allen and the west side of the Gateway, the two samples have the lowest K/Rb and Ba/Rb K-feldspar ratios recorded from the pluton. Samples 608A and 726 have been excluded from this consideration because they may have been contaminated, as discussed previously.

This geographic pattern of K/Rb, Ba/Rb and Rb/Sr ratios in K-feldspars suggests that the Hope Granite rocks in areas I, II and III represent a sequence of increasingly differentiated magmas. It is suggested that the magmas in these three areas were tapped from the same body of differentiating magma and were emplaced in separate episodes in the sequence I, II, III. Since no contacts between any of these hypothetical intrusions have been seen, it seems likely that each was emplaced before the previous intrusion had completely solidified. By the time of emplacement of the Mt. Ida pluton, Intrusion I had crystallized sufficiently for a sharp contact to be formed against it at Granite Pillars.

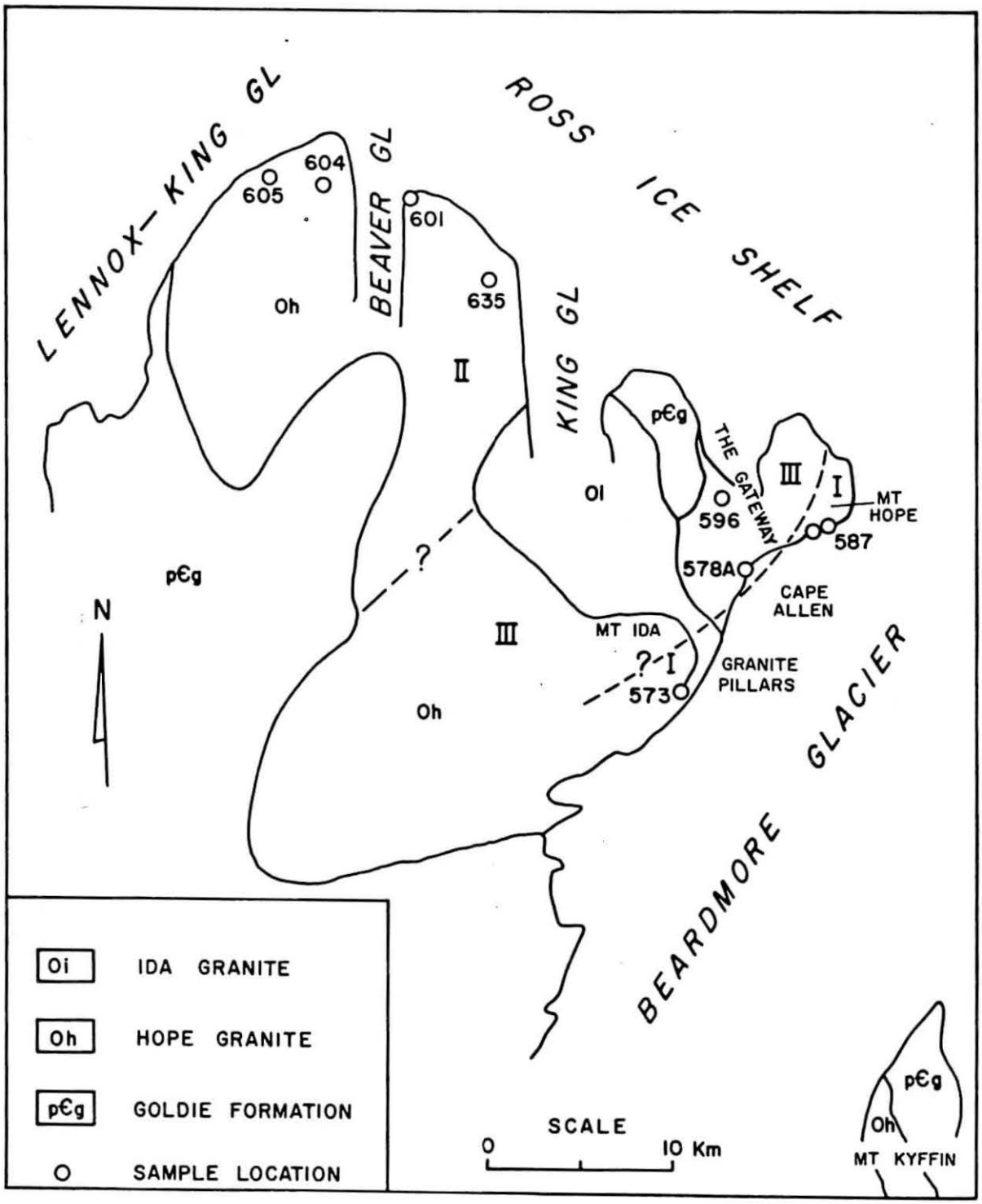
LENNOX-KING GL
BEAVER GL
ROSS ICE SHELF
KING GL
BEARDMORE GLACIER
604
605
601
635
Oh
II
pεg
THE GATEWAY
III
I
MT HOPE
596
587
578A
CAPE ALLEN
Ol
?
N
III
MT IDA
?
I
573
GRANITE PILLARS
Oh
Oi IDA GRANITE
Oh HOPE GRANITE
pεg GOLDIE FORMATION
SAMPLE LOCATION
SCALE
0
10 Km
pεg
Oh
MT KYFFIN

Figure 19

The evidence that the Hope Granite at the north ridge of Mt. Ida was still partly molten at the time of intrusion of the Ida Granite, as discussed previously, suggests that the Hope Granite at this locality belonged to a later intrusion, probably II or III. This would provide an alternative explanation for the low K/Rb and Ba/Rb and the high Rb/Sr ratios in the K-feldspar of sample 726.

The K-feldspars sampled from the Mt. Ida pluton show relatively small variations in K/Rb, Ba/Rb and Rb/Sr ratios. These can be accounted for by local heterogeneities in a generally homogeneous magma which crystallized over a small temperature range. The K/Rb, Ba/Rb and Rb/Sr ratios in Ida Granite K-feldspars are comparable to those in samples from Area III, and are consistent with the field evidence that the Ida Granite was the latest intrusion in this sequence of magmatism. Its finer average grain size suggests that the Ida Granite cooled more rapidly than the Hope Granite. This may have been due to a regional lowering of the geo-isotherms, corresponding to the close of the magmatic phase of the Ross Orogeny and to the exhaustion of the supply of granitic magma. There is no evidence that the Mt. Ida pluton was emplaced during more than one episode.

The sparse data available on the East Beardmore pluton and the outlying intrusions of Hope Granite at Wise Bay, Threshold Nuntak and Sirohi Point allow only a speculative attempt at comparing the stages of differentiation of their magmas with those of the Mt. Hope pluton. The most easterly sample (658) from the East Beardmore pluton contains K-feldspars whose chemistry suggests that the most basic Hope Granite magma sampled was present in this area. The remaining samples from the East Beardmore pluton and three of the four samples from the other outlying plutons have K-feldspar chemistries which suggest that the stage of differentiation of their magmas was comparable to that of Intrustion II of the Mt. Hope pluton. Sample 707 from Wise Bay has K-feldspar chemistry comparable to that of the most extremely differentiated aplite and pegmatite dikes. This indicates that the magma of the Wise Bay intrusion underwent considerable differentiation.

The K-feldspars in the six Hope Granite samples from the Martin Dome pluton have K/Rb, Ba/Rb and Rb/Sr ratios which show relatively little variation and have values that suggest that the K-feldspars crystallized from a relatively undifferentiated magma. However the concentrations of K, Ca and Sr in these K-feldspars show a systematic pattern of change, as Figures 6, 12 and 13 illustrate. The samples are progressively depleted in Ca, Sr and, to a lesser extent, Na in the order 297, 294, 292, 314, 315. Their K, Ca and Sr contents are plotted on a location diagram in Figure 20. Although the data are limited, they indicate that the samples at Macdonald Bluffs crystallized from a less differentiated magma than those at Kreiling Mesa. It is tentatively suggested that the magma from which the Macdonald Bluff samples (292, 294 and 297) formed was intruded first. Then a separate body of magma was intruded, and samples 314 and 315, whose K-feldspars have lower Ca and Sr and higher K concentrations crystallized from it. The southward increase

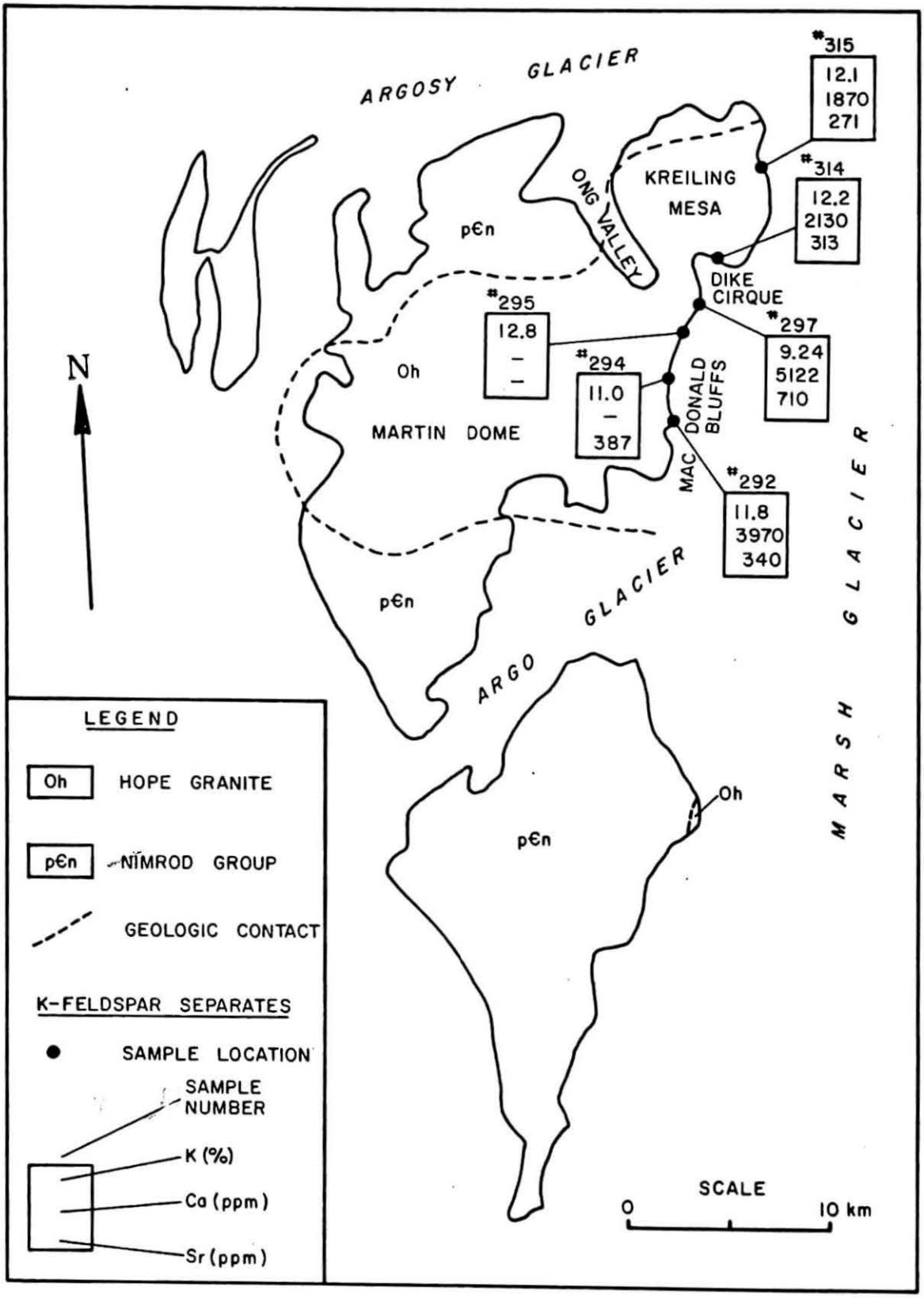


Figure 20. Southern Miller Range. Geologic Sketch Map, Showing Concentrations of K, Ca and Sr in K-feldspar Separates from Hope Granite Samples.

in differentiated character of the K-feldspars in samples 297, 294 and 292 may indicate a southward trend towards increased magmatic differentiation at Macdonald Bluffs.

Although no analytical data on other parts of the Martin Dome pluton are available, it is suggested that the Martin Dome massif if formed of a single intrusion. Thus Ong Valley and Dike Cirque, which separate Kreiling Mesa from Martin Dome, may mark the contact zone between two intrustions which make up the Martin Dome pluton.

## Conclusions

The chemical study of the magmatic development of the Hope and Ida Granites, combined with the evidence of a common initial $^{87}Sr/^{86}Sr$ ratio presented in the preceding paper of this report, has verified the two hypotheses which were stated at the beginning of this Chapter:

(1) The Hope and Ida Granite intrusions in the Shackleton Coast region crystallized from a common parent magma;

(2) Differentiation of this magma caused the chemical and mineralogical variations observable within and between the intrusions.

The main conclusions of the chemical phase of this study are summarized as follows:

(1) The data presented clearly demonstrate the magmatic origin of the Hope and Ida Granites.

(2) K-feldspar samples from both rock units fit a single set of simple patterns on variation diagrams of K/Rb, Ba/Rb, Ba/Sr, Rb/Sr. This strongly supports the strontium isotope evidence presented in the previous paper that all the intrusions studied in the Shackleton Coast were derived from the same parent magma.

(3) The chemical variations in the K-feldspars and plagioclases and the modal variations in the rocks are best explained in terms of magmatic differentiation.

(4) There is evidence that the Mt. Hope pluton was emplaced in more than one episode. A closely-spaced sequence of three intrusions of Hope Granite, followed by the Mt. Ida pluton and the pegmatite and aplite dikes, is suggested.

(5) Geochemical and petrographic comparisons with the Mt. Hope pluton suggest that the Hope Granite intrustions at Wise Bay, Threshold Nunatak, Sirohi Point and the East Beardmore pluton crystallized from magmas which were at similar stages of differentiation to that of the Mt. Hope pluton.

## References


Bowen, N. L. and Tuttle, O. F., 1950, The system $NaAlSi_3O_8$-$KAlSi_3O_8$-$H_2O$. Jour. Geol., 58, 489-511.

Goldschmidt, V. M., 1937, The principles of distribution of chemical elements in minerals and rocks. Jour. Chem. Soc., 655-673.

Gunner, J. D., 1971, Age and origin of The Nimrod Group and of the Granite Harbour Intensives, Beardmore Glacier Region, Antarctica. Ph.D. dissertation, Dept. of Geology, The Ohio State University, 231p.

Heier, K. S. and Taylor, S. R., 1959, The distribution of Li, Na, K, Rb, Cs, Pb and Tl in southern Norwegian Precambrian alkali feldspars. Geochim. Cosmochim. Acta, 15, 284-304.

Nockolds, S. R. and Allen, R., 1953, The geochemistry of some igneous rock sines. Geochim. Cosmochim. Acta, 4, 105-142.

Van der Kaaden, G., 1951, Optical studies on natural plagioclase feldspars with high and low-temperature optics. Thesis, State University, Utrecht, 150p.

Van der Plas, L. and Tobi, A. C., 1965, A chart for judging The reliability of point counting results. Amer. Jour. Sci., 263, 87-90.

Williams, H., Turner, F. J. and Gilbert, C. M., 1954, Petrography. W. H. Freeman and Co., San Francisco, 406p.

Wright, L. T., 1968, X-ray and optical study of alkali feldspars II. An X-ray method for determining the composition and structural state from measurement of $2\theta$ values for three reflections. Amer. Mineral, 53, 88-104.

# THE INITIAL $^{87}Sr/^{86}Sr$ RATIOS AND SILICA CONTENT OF MESOZOIC BASALT FROM ANTARCTICA

(Excerpts from a M.Sc. thesis by John R. Bowman submitted to the Department of Geology in 1971)

Thirteen samples of tholeiitic basalt rocks from Mountain "B" on Kirwan Escarpment in western Queen Maud Land and ten samples of tholeiitic basalt (Kirkpatrick Basalt) from Storm Peak in the Queen Alexandra Range of the central Transantarctic Mountains were studied in this project. [Locations of these areas can be found in Figure 1 (Storm Peak) and Figure 2 (Kirwan Escarpment and Mountain "B").] Sample positions within the stratigraphic sections of Mountain "B" and Storm Peak are shown in Figures 3 and 4, respectively.

These basalt samples were analyzed for Rb, Sr, and $SiO_2$ concentrations, the Rb/Sr ratio, and for the isotopic composition of Sr. Rb and Sr concentrations were measured by x-ray fluorescence spectrometry. $SiO_2$ concentrations were obtained commercially by standard wet chemical techniques (A. S. McCreath and Sons, Inc.). All measured $^{87}Sr/^{86}Sr$ ratios were corrected for fractionation, assuming a $^{86}Sr/^{88}Sr$ ratio of .1194. The initial $^{87}Sr/^{86}Sr$ isotope ratio was calculated for each sample from the relationship:

$$\left(\frac{^{87}Sr}{^{86}Sr}\right)_o = \left(\frac{^{87}Sr}{^{86}Sr}\right)_p - \left(\frac{^{87}Rb}{^{86}Sr}\right)\lambda t$$

using a value of $1.39 \times 10^{-11}$ $yr^{-1}$ for the decay constant of $^{87}Rb$, and an age of 170 million years for both suites of basalts. Extensive K-Ar age data available on the Kirkpatrick Basalt average 170 million years (Wade, et al., 1965; Elliot, 1969). Deposition of the Kirkpatrick Basalt was perhaps not simultaneous over the whole of the central Transantarctic Mountains. The presence of weathering horizons and sedimentary interbeds indicate deposition of this basalt over an extended time interval, the length of which is not known. This time interval evidently is not resolved by the K-Ar dates and does not significantly affect the calculated initial $^{87}Sr/^{86}Sr$ ratios of the basalt samples. The only radiometric age available for the Kirwan Escarpment Basalts is 172 ± 10 m.y. (Sample T-1-1, K-Ar, whole-rock).

Analytical data for the 13 basalt samples from the Kirwan Escarpment are presented in Tables 1 and 2. Average Sr and Rb concentrations are compiled in Table 1. Sr concentrations range from 141.2 to 258.5 ppm, averaging 174.0 ppm. Rb concentrations also vary widely from 2.7 to 18.1 ppm, averaging 9.8 ppm. There is a significant range of Sr concentrations, but given the relatively poorer precision of the Rb analysis for these basalts, only the extreme values of the Rb concentrations are definitely significantly different. The Rb and Sr concentrations are

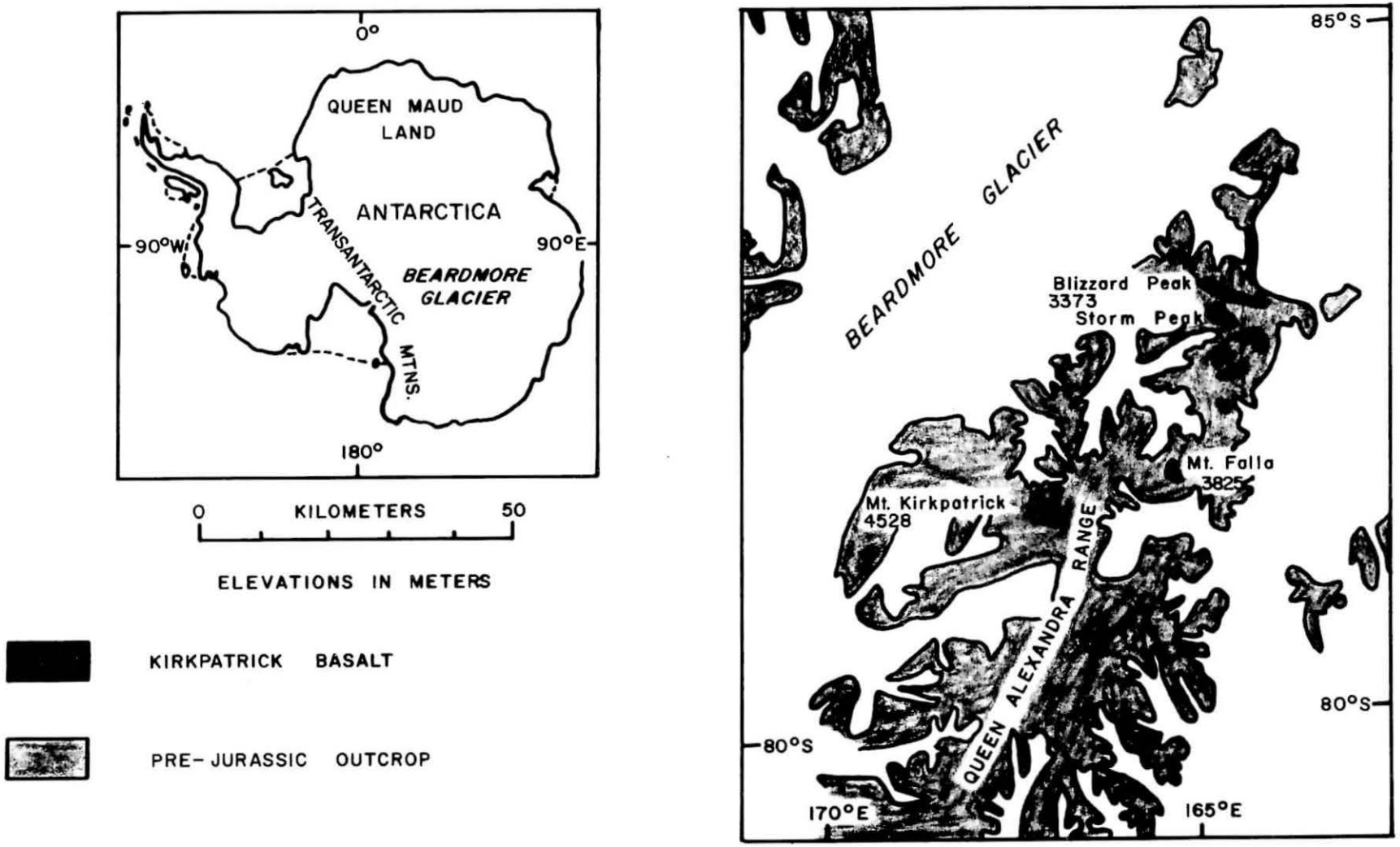


Figure 1. Queen Alexandra Range Map

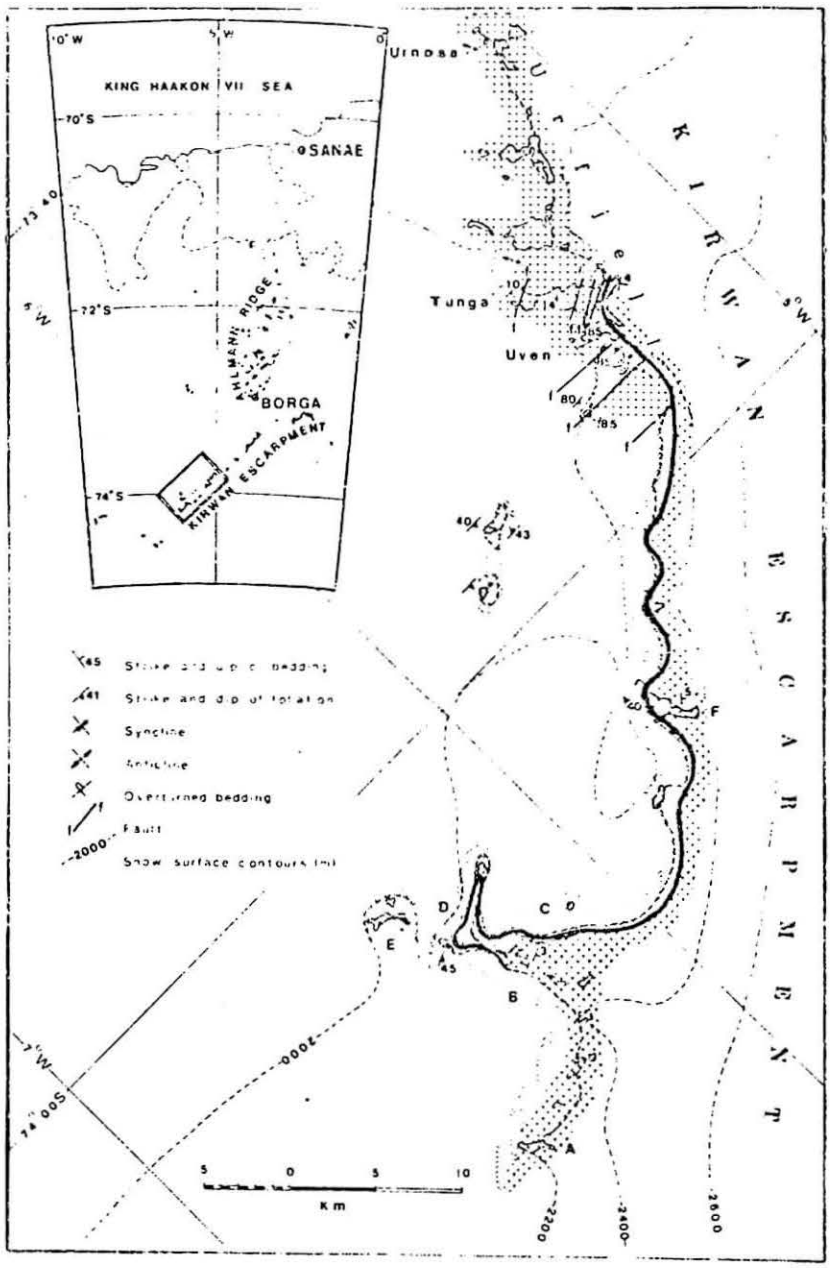


Figure 2. Geologic Map of the Kirwan Escarpment Area, Western Queen Maud Land.

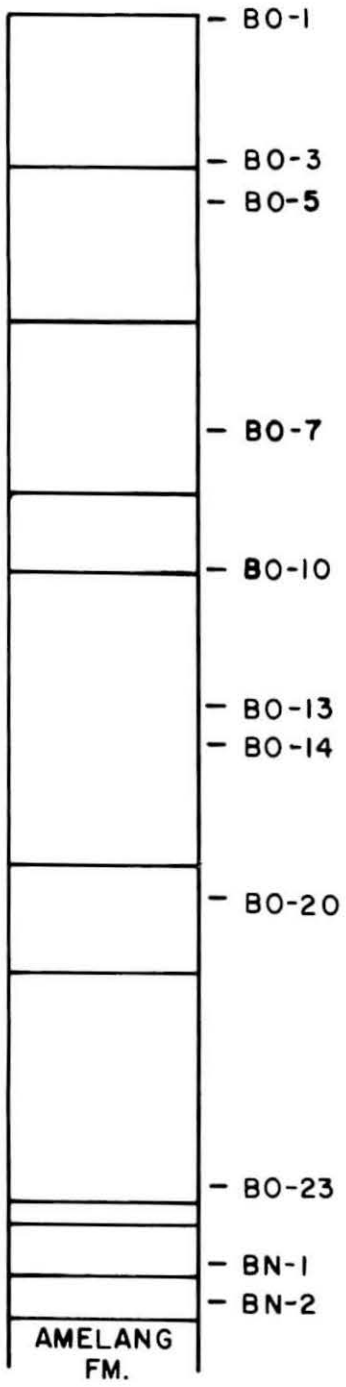


Figure 3. Kirwan Volcanics Stratigraphic Section, Mountain "B", Kirwan Escarpment.

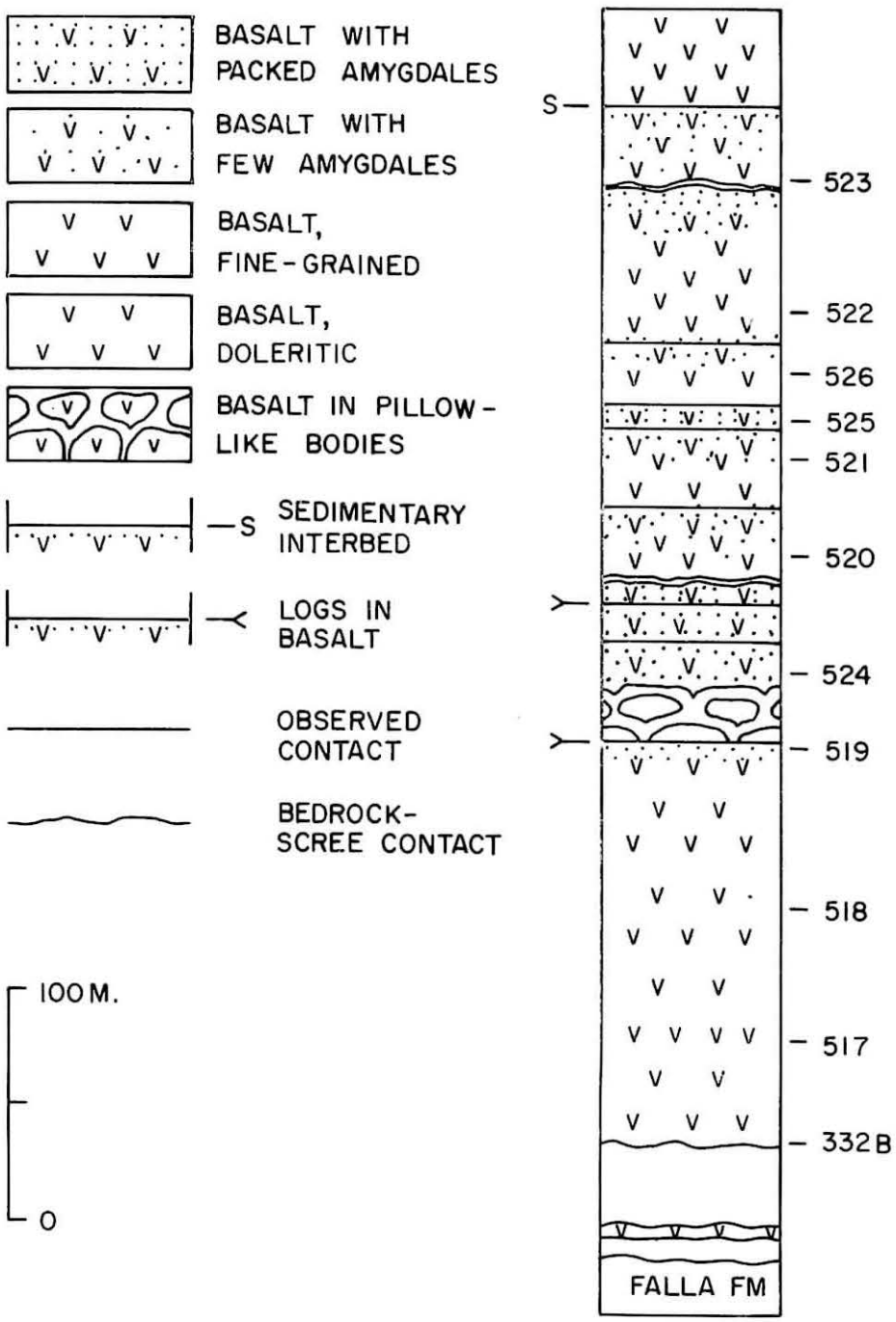


Figure 4. Kirkpatrick Basalt Stratigraphic Section, Storm Peak, Queen Alexandra Range.

Table 1

Whole-Rock Rb-Sr Analyses, Kirwan Escarpment

| Sample | Sr, ppm | Rb, ppm | Rb/Sr |
|---|---|---|---|
| BN-1 | 141.2 ± 5.7 | 5.5 ± 1.0 | 0.038 |
| BN-2 | 155.1 ± 4.6 | 5.1 ± 2.0 | 0.033 |
| BO-1 | 144.4 ± 1.3 | 6.1 ± 1.4 | 0.042 |
| BO-3 | 147.5 ± 5.1 | 5.9 ± 1.8 | 0.040 |
| BO-4 | 146.1 ± 4.7 | 16.3 ± 4.8 | 0.111 |
| BO-5 | 215.2 ± 10.3 | 2.7 ± 2.0 | 0.013 |
| BO-7 | 157.0 ± 5.6 | 2.8 ± 2.2 | 0.018 |
| BO-10 | 156.7 ± 5.7 | 13.1 ± 3.5 | 0.084 |
| BO-13 | 161.4 ± 4.9 | 12.9 ± 2.7 | 0.080 |
| BO-14 | 164.3 ± 4.5 | 12.8 ± 3.9 | 0.084 |
| BO-20 | 245.9 ± 7.2 | 15.0 ± 2.4 | 0.061 |
| BO-23 | 168.1 ± 4.7 | 18.1 ± 2.7 | 0.108 |
| T-1-1 | 258.5 ± 8.5 | 12.0 ± 2.9 | 0.046 |

Table 2

Whole-Rock Rb-Sr and $SiO_2$ Analyses,
Kirwan Escarpment Basalts

| Sample No. | $\left(\frac{Sr^{87}}{Sr^{86}}\right)$ corr. | $\frac{Sr^{86}}{Sr^{88}}$ | $\frac{Rb^{87}}{Sr^{86}}$ | $\frac{Sr^{87}}{Sr^{86}}$ initial | $SiO_2$ % |
|---|---|---|---|---|---|
| BN-1 | 0.7027±0.0004<br>0.7032±0.0004<br>0.7029±0.0004 | 0.1178<br>0.1194 | 0.116 | 0.7026 | 50.29 |
| BN-2 | 0.7036±0.0003 | 0.1175 | 0.088 | 0.7034 | 49.51 |
| BO-1 | 0.7032±0.0005 | 0.1175 | 0.121 | 0.7030 | 50.22 |
| BO-3 | 0.7044±0.0008 | 0.1179 | 0.117 | 0.7041 | 49.99 |
| BO-4 | 0.7048±0.0004 | 0.1186 | 0.316 | 0.7040 | 50.16 |
| BO-5 | 0.7067±0.0006 | 0.1169 | 0.026 | 0.7066 | 50.05 |
| BO-7 | 0.7043±0.0002 | 0.1196 | 0.052 | 0.7042 | 49.95 |
| BO-10 | 0.7035±0.0004 | 0.1176 | 0.237 | 0.7030 | 51.02 |
| BO-13 | 0.7049±0.0002 | 0.1191 | 0.240 | 0.7043 | 51.10 |
| BO-14 | 0.7048±0.0003 | 0.1184 | 0.226 | 0.7042 | 51.13 |
| BO-20 | 0.7058±0.0006 | 0.1193 | 0.177 | 0.7054 | 49.57 |
| BO-23 | 0.7053±0.0003 | 0.1185 | 0.306 | 0.7046 | 51.73 |
| T-1-1 | 0.7056±0.0002 | 0.1192 | 0.135 | 0.7053 | 50.32 |

within the range of values recorded for normal basaltic rocks (Prinz, 1967; Engel, et al., 1965). The Rb/Sr ratios for the basalt samples vary from 0.009 to 0.109, averaging 0.057. These ratios are consistent with average values reported for normal basaltic rocks (Faure and Hurley, 1963; Prinz, 1967).

$SiO_2$ concentrations expressed as dry weight percent (%) and Sr isotopic data for the basalt samples from the Kirwan Escarpment are presented in Table 2. $SiO_2$ concentrations vary from 49.51 to 51.73% averaging 50.39%, and consistent with values of normal continental tholeiite bassalts (Manson, 1967). The present $^{87}Sr/^{86}Sr$ ratios range from 0.7029 to 0.7066, averaging 0.7046, while the initial $^{87}Sr/^{86}Sr$ ratios range from 0.7026 to 0.7066, averaging 0.7042. These values are compatible with those reported for basaltic rocks elsewhere especially continental thoeiite basalts (Faure and Hurley, 1963; Hedge and Walthall, 1963; Lessing and Catanzara, 1964). These data confirm previous analyses which indicate the presence of a Jurassic basalt province characterized by normal initial $^{87}Sr/^{86}Sr$ ratios and Rb, Sr, and $SiO_2$ concentrations in western Queen Maud Land (Juckes, 1968; Faure and Elliot, 1970). The Kirwan Escarpment basalts are compared to other basalts in Table 3.

Geochemically and with respect to the isotopic composition of Sr, these basalts are similar to normal continental tholeiite basalts. However, the range of initial $^{87}Sr/^{86}Sr$ ratios is too great to be explained by analytical error alone, given the low Rb/Sr ratios of the samples. The basalt flows are either not the same age, were inhomogeneous isotopically at the time of crystallization, or have not remained closed to Rb and Sr since crystallization. The lowest $^{86}Sr/^{87}Sr$ ratio (BN-1) was duplicated, giving it an average initial $^{87}Sr/^{86}Sr$ ratio of 0.7029.

The analytical data for the ten Kirkpatrick Basalt samples from Storm Peak in the Queen Alexandra Range are listed in Tables 4 and 5. The Sr concentrations range narrowly from 118.3 to 136.3 ppm, averaging 131.8 ppm. The Rb concentrations vary from 42.8 to 86.1 ppm, averaging 66.4 ppm. These values are in good general agreement with earlier Rb-Sr analyses on the Kirkpatrick Basalt and Ferrar Dolerite (Compston, et al., 1968; Hill, 1969; Faure, et al., 1970). The high Rb concentrations are a peculiar characteristic of the Kirkpatrick Basalt, setting it apart from normal tholeiitic basalt values (Engel, et al., 1965; Prinz, 1967). Sr concentrations are lower than those of average basalt and continental tholeiites (Faure and Hurley, 1963; Gast, 1960) but not much lower than typical oceanic tholeiites (Engel, et al., 1965. The Rb/Sr range from 0.350 to 0.631 and average 0.494. These unusually high ratios again emphasize the anomalous chemical compositions of the Kirkpatrick Basalt, because tholeiitic basalts normally have Rb/Sr of $\sim$ 0.06.

$SiO_2$ concentrations, $^{87}Rb/^{86}Sr$ ratios, and Sr isotopic data for the Storm Peak basalts are presented in Table 5. These samples are characterized by abnormally high $SiO_2$ contents, ranging from 55.05% to

Table 3: Comparison of Antarctic and Tasmanian Tholeiites with Oceanic and Hawaiian Tholeiites

| | Tholeiitic Basalt Queen Maud Land[a] | Kirkpatrick Basalt Queen Alexandra Range[b] | Tasmanian Dolerite[c] | Oceanic Tholeiites[d] | Hawaiian Tholeiites[e] |
|---|---|---|---|---|---|
| $SiO_2$ | 49.2 | 56.34 | 53.18 | 49.34 | 49.36 |
| $TiO_2$ | -- | 1.28 | 0.65 | 1.49 | 2.50 |
| $Al_2O_3$ | 12.7 | 13.12 | 15.37 | 17.04 | 12.94 |
| $Fe_2O_3$ | 3.72 | 4.50 | 0.76 | 1.99 | 3.03 |
| FeO | 8.95 | 7.52 | 8.33 | 6.82 | 8.53 |
| MnO | -- | 0.22 | 0.15 | 0.17 | 0.16 |
| MgO | 8.93 | 3.54 | 6.71 | 7.19 | 8.44 |
| CaO | 9.51 | 7.84 | 11.04 | 11.72 | 10.30 |
| $Na_2O$ | 2.15 | 2.34 | 1.65 | 2.73 | 2.13 |
| $K_2O$ | 0.66 | 1.37 | 1.03 | 0.16 | 0.38 |
| $H_2O$ | 1.85 | 1.62 | 0.67 | 0.69 | -- |
| $H_2O^+$ | 0.14 | 0.51 | 0.45 | 0.58 | -- |
| $P_2O_5^-$ | 0.22 | 0.16 | 0.08 | 0.16 | 0.26 |
| Sr | 174 | 132 | 130 | 115 | 250 |
| Rb | 10 | 66 | 33 | 1.2 | 10 |
| Rb:Sr | 0.057 | 0.494 | 0.25 | 0.01 | 0.04 |
| K:Rb | -- | 205 | 200 | 1400 | 500 |
| $^{87}Sr:^{86}Sr$ | 0.7042 | 0.7113 | 0.711 | 0.702 | 0.703 |

[a](Neethling, 1970; this study).
[b](Elliot, 1970; this study).
[c](Heier et al., 1965; McDougall, 1962).
[d](Engel et al., 1965; Tatsumato, 1965).
[e](MacDonald and Katsura, 1964; Hedge and Walthall, 1963; Lessing et al., 1963, Heier et al., 1964).

Table 4

Whole-Rock Rb-Sr Analyses, Storm Peak
Queen Alexandra Range

| Sample | Sr, ppm | Rb, ppm | Rb/Sr |
|---|---|---|---|
| 517 | 134.4 ± 4.3 | 68.8 ± 3.5 | 0.512 |
| 518 | 130.8 ± 4.2 | 66.0 ± 4.0 | 0.504 |
| 519 | 133.8 ± 3.3 | 75.3 ± 6.2 | 0.562 |
| 520 | 136.6 ± 4.4 | 70.0 ± 3.3 | 0.512 |
| 521 | 136.3 ± 4.4 | 51.8 ± 1.8 | 0.380 |
| 522 | 118.3 ± 3.6 | 42.8 ± 2.8 | 0.362 |
| 523 | 135.1 ± 4.8 | 86.1 ± 2.5 | 0.637 |
| 524 | 132.6 ± 5.2 | 83.2 ± 3.0 | 0.627 |
| 525 | 130.5 ± 5.1 | 67.3 ± 5.8 | 0.516 |
| 526 | 129.4 ± 5.3 | 52.8 ± 3.4 | 0.408 |

Table 5

Whole-Rock Isotope and $SiO_2$ Analyses, Storm Peak

| Sample | $\frac{^{87}Sr}{^{86}Sr}$ corr, | $\frac{^{86}Sr}{^{88}Sr}$ | $\frac{^{87}Rb}{^{86}Sr}$ initial | $\frac{^{87}Sr}{^{86}Sr}$ | $SiO_2$ % |
|---|---|---|---|---|---|
| 517 | 0.7158±0.0004<br>0.7155±0.0002<br>0.7161±0.0003<br>0.7158±0.0003 | 0.1181<br>0.1190<br>0.1174 | 1.437 | 0.7124 | 58.37 |
| 518 | 0.7153±0.0002<br>0.7154±0.0005<br>0.7154±0.0004 | 0.1193<br>0.1181 | 1.458 | 0.7118 | 58.13 |
| 519 | 0.7150±0.0003 | 0.1185 | 1.540 | 0.7114 | 57.61 |
| 520 | 0.7148±0.0002<br>0.7165±0.0005<br>0.7157±0.0004 | 0.1190<br>0.1192 | 1.423 | 0.7123 | 58.49 |
| 521 | 0.7146±0.0002 | 0.1193 | 1.013 | 0.7121 | 57.94 |
| 522 | 0.7119±0.0002 | 0.1183 | 1.161 | 0.7091 | 55.05 |
| 523 | 0.7160±0.0005 | 0.1194 | 1.829 | 0.7117 | 57.85 |
| 524 | 0.7147±0.0004<br>0.7148±0.0004<br>0.7148±0.0004 | 0.1179<br>0.1190 | 1.773 | 0.7106 | 57.51 |
| 523 | 0.7140±0.0003 | 0.1178 | 1.504 | 0.7103 | 56.27 |
| 526 | 0.7136±0.0003 | 0.1182 | 1.169 | 0.7107 | 56.16 |
| 332B | 0.7153±0.0003 | 0.1190 | -- | 0.7122 | -- |

58.49% and averaging 57.34%. Present $^{87}Sr/^{86}Sr$ ratios range from 0.7118 to 0.7160, averaging 0.7147. Initial $^{87}Sr/^{86}Sr$ ratios for these samples range from 0.7091 to 0.7124, averaging 0.7113. These values are unusually high for basalts, and agree with earlier analyses (Compston, et al., 1968; Hill, 1969; Faure, et al., 1970). Basaltic rocks almost always have initial $^{87}Sr/^{86}Sr$ ratios of 0.702-0.706 (Faure and Hurley, 1963; Hedge and Walthall, 1963; Lessing and Catanzaro, 1964). Mesozoic continental tholeiite basalts from South America and South Africa have ratios of 0.705-0.706 (Manton, 1968; Compston, et al., 1968). Only the Jurassic continental tholeiitic dolerites from Tasmania have comparable initial $^{87}Sr/^{86}Sr$ ratios (Heier, et al., 1965).

The observed range of initial $^{87}Sr/^{86}Sr$ ratios for the Kirkpatrick Basalt samples from Storm Peak is too great to be explained solely by analytical error. As in the case of the Kirwan Escarpment basalts, the Storm Peak samples must be of different age, have different initial $^{87}Sr/^{86}Sr$ ratios, or not have remained closed to Rb and Sr since crystallization. Time intervals of unknown length between eruptions are evident in the Storm Peak section, but were apparently of insufficient duration to be detected by the available K-Ar dates.

All analytical data presented in this study are consistent with previous data from the Kirkpatrick Basalt in this and other areas (Compston, et al., 1968; Hill, 1969; Faure, et al., 1970) and serve to re-emphasize the quite unusual nature of these basalts. A comparison of the chemical and Sr isotopic characteristics of the Kirkpatrick and other basalts is presented in Table 3.

Table 6 is a compilation of major oxide analyses for Kirkpatrick Basalt samples from Storm Peak (Elliot, 1969, 1970, 1971, written communication). Five of these basalt samples have been analyzed for Rb, Sr and the isotopic composition of Sr. K/Rb ratios for these five samples are listed in Table 6 and range from 129 to 297, averaging 187, slightly lower than the 211-314 range reported by Hill (1969) for the Kirkpatrick Basalt and Ferrar Dolerite in the Queen Alexandra Range. These ratios are consistent with others reported for Jurassic tholeiitic basalts from Tasmania and the central Transantarctic Mountains in Antarctica (Heier, et al., 1965; Gunn, 1965; Compston, et al., 1968).

The K/Rb ratios of these rocks are remarkably low for basaltic rocks. Ocean tholeiites usually exhibit K/Rb ratios of 1000-2000 (Lessing, et al., 1963; Gast, 1965; Tatsumoto, et al., 1963). Normal continental tholeiites exhibit K/Rb ratios primarily in the 400-600 range, the South African Karoo Dolerities and South American Serra Geral Tholeiites being typical examples (Erlank and Hofmeyr, 1966, 1968).

Table 6

Chemical Analyses for 12 Kirkpatrick Basalts, Storm Peak Section, Queen Alexandra Range

| Sample No. This study / Elliot(1970) | 27.45 | 27.28 | 332B 26.1 | 27.13 | 27.17 | 27.22 |
|---|---|---|---|---|---|---|
| $SiO_2$ | 53.14 | 52.88 | 57.75 | 57.16 | 57.12 | 57.52 |
| $TiO_2$ | 0.63 | 1.00 | 1.44 | 11.43 | 1.47 | 0.50 |
| $Al_2O_3$ | 13.98 | 15.88 | 12.23 | 12.84 | 12.30 | 13.78 |
| $Fe_2O_3$ | 4.40 | 5.05 | 3.26 | 6.91 | 2.77 | 6.08 |
| FeO | 5.11 | 5.21 | 8.93 | 6.28 | 9.37 | 5.88 |
| MnO | 0.36 | 0.18 | 0.32 | 0.17 | 0.32 | 0.17 |
| MgO | 7.58 | 5.24 | 2.78 | 2.75 | 3.40 | 2.59 |
| CaO | 9.72 | 9.46 | 7.11 | 6.50 | 7.92 | 6.55 |
| $Na_2O$ | 2.06 | 2.28 | 1.98 | 2.32 | 1.70 | 2.56 |
| $K_2O$ | 0.51 | 1.45 | 1.54 | 1.90 | 1.31 | 2.05 |
| $H_2O^+$ | 2.12 | 1.36 | 1.84 | 1.79 | 1.59 | 1.32 |
| $H_2O^-$ | -- | -- | -- | -- | -- | -- |
| $P_2O_5$ | 0.07 | 0.12 | 0.18 | 0.17 | 0.14 | 0.18 |
| $CO_2$ | 0.03 | 0.08 | 0.02 | 0.13 | 0.02 | 0.37 |
| K/Rb | -- | -- | 240 | -- | -- | -- |

| | 523 27.36 | 27.41 | 524 27.51 | 27.56 | 525 27.64 | 526 27.67 |
|---|---|---|---|---|---|---|
| $SiO_2$ | 57.85 | 56.20 | 57.51 | 56.51 | 56.27 | 56.16 |
| $TiO_2$ | 1.05 | 2.33 | 1.40 | 1.48 | 1.40 | 1.27 |
| $Al_2O_3$ | 12.24 | 11.56 | 12.90 | 13.02 | 13.40 | 13.38 |
| $Fe_2O_3$ | 4.75 | 5.56 | 4.13 | 4.00 | 2.56 | 4.50 |
| FeO | 8.41 | 9.75 | 7.98 | 8.23 | 8.65 | 6.48 |
| MnO | 0.22 | 0.23 | 0.17 | 0.19 | 0.19 | 0.17 |
| MgO | 2.74 | 2.19 | 2.67 | 3.00 | 3.51 | 3.98 |
| CaO | 7.00 | 6.40 | 7.66 | 8.42 | 8.59 | 8.79 |
| $Na_2O$ | 2.70 | 2.70 | 2.62 | 2.36 | 2.52 | 2.26 |
| $K_2O$ | 1.07 | 2.05 | 1.08 | 0.92 | 0.98 | 1.57 |
| $H_2O^+$ | 1.55 | 1.29 | 1.65 | 1.85 | 1.76 | 1.30 |
| $H_2O^-$ | -- | -- | 0.43 | 0.67 | 0.36 | 0.58 |
| $P_2O_5$ | 0.20 | 0.26 | 0.167 | 0.158 | 0.158 | 0.144 |
| $CO_2$ | 0.01 | 0.02 | 0.02 | 0.01 | 0.02 | 0.06 |
| K/Rb | 124 | -- | 130 | -- | 146 | 297 |

Source: Elliot (1969, 1970, 1971).

## Chemical and Sr Isotope Homogeneity within the Kirwan Volcanics

The extent of geochemical and Sr isotopic homogeneity over a distance of a few inches in flow No. 6 at the Kirwan Escarpment can be inferred from analytical data from powders of two different hand specimens of sample BO-14. These data are listed in Table 7. The results for the two samples are statistically indistinguishable. Homogeneity over a ten-meter stratigraphic interval in this same flow can be estimated by comparison of samples BO-13 and BO-14. Analytical data for these samples are also statistically indistinguishable.

Significant lateral variation in the isotopic composition of Sr may be indicated on a large scale (on the order of kilometers) by data from samples BN-1 and T-1-1. Sample T-1-1 was collected 25 km ENE of Mountain "B" at Tunga near the base in the second flow of the Kirwan Escarpment, while BN-1 was collected from the second flow at Mountain "B". The values of the initial $^{87}Sr/^{86}Sr$ ratio are quite different. It is not known whether or not these two flows are in fact equivalent, and much more field correlation and Sr isotope analyses are needed to determine the extent of homogeneity of the Sr isotope composition with the basalt sequence on the Kirwan Escarpment.

Table 7

Small-Scale Homogeneity within Flow 6, Kirwan Escarpment

| Analysis | $BO\text{-}14_a$ | $BO\text{-}14_b$ | Diff. |
|---|---|---|---|
| $Y_{Sr}$* | 1.0826 ± 0.0160 | 1.0910 ± 0.0290 | 0.0084 |
| $Y_{Rb}$ | 0.4445 ± 0.1665 | 0.4678 ± 0.1127 | 0.0233 |
| Rb/Sr | 0.080 ± 0.022 | 0.076 ± 0.013 | 0.004 |
| $SiO_2$ | 51.16% | 51.09% | 0.07% |
| $^{87}Sr/^{86}Sr$ | 0.7046 ± 0.0003 | 0.7049 ± 0.0003 | 0.0003 |

$$*Y_{Sr} = \left( \frac{\frac{\text{SrK}\alpha \text{ net}}{\text{MoK}\alpha \text{ compton}}}{\frac{\text{SrK}\alpha \text{ net}}{\text{MoK}\alpha \text{ compton}}} \right)_{\text{Spl.}}^{\text{Std.}}$$

## Comparison of the Kirwan Escarpment and Kirkpatrick Basalt Suites

A comparison of the analytical data in Tables 1-2 and 4-5 indicate the existence of significant differences between the Kirwan Escarpment basalt suite and the Kirkpatrick Basalt sequence at Storm Peak and confirm the conclusions of Faure and Elliot (1970) and Faure, et al. (1970) that two distinct Jurassic basalt provinces exist on this continent. The chemical and Sr isotopic characteristics of these two basalt suites are illustrated and contrasted in a series of plots of chemical parameters and $^{87}Sr/^{86}Sr$ ratios.

The first obvious difference between the two sequences is their greatly different initial $^{87}Sr/^{86}Sr$ ratios, graphically summarized in the frequency diagram of Figure 5.

Figure 6 is a plot of the initial $^{87}Sr/^{86}Sr$ ratio versus the $SiO_2$ concentration for the basalt samples from the Kirwan Escarpment and Storm Peak. The two basalt sequences form two widely separated and distinct data clusters within the diagram.

The initial $^{87}Sr/^{86}Sr$ ratios for the basalt samples from the Kirwan Escarpment do not seem to be related in any systematic manner to $SiO_2$ content. Three of the samples have initial $^{87}Sr/^{86}Sr$ ratios greater than 0.7050, however these samples do not have abnormally high Rb/Sr ratios. Sample BO-5 has the highest initial $^{87}Sr/^{86}Sr$ ratio (0.7066) and the lowest Rb/Sr ratio (0.009). Variations in both parameters are significant and indicate that the individual flows of the basalt sequence have either been derived from different sources with respect to the isotopic composition of Sr and subsequently differentiated to varying degrees, or have been subjected to varying degrees of contamination during ascent from the source area, or both.

The Kirkpatrick Basalt samples from Strom Peak show a positive, well-developed correlation of the initial $^{87}Sr/^{86}Sr$ ratio and the $SiO_2$ content. This is the most significant and striking geochemical and Sr isotope characteristic of the Kirkpatrick Basalt to arise from this study.

Two facts cannot be overemphasized. First, the initial $^{87}Sr/^{86}Sr$ ratios of these samples are significantly different and cannot be attributed solely or even primarily to analytical error or age differences between flows. Second, no known physical process associated with magmatic differentiation has ever been demonstrated to fractionate isotopes of Sr within the magma, the crystallizing phases, or between liquid and solid phases. If differentiation processes were solely responsible for the observed range of $SiO_2$ concentrations in the Storm Peak Kirkpatrick Basalt samples, no correlation between the initial $^{87}Sr/^{86}Sr$ ratio and the $Si_2$ content should exist. If the basalt magma was originally isotopically homogeneous and had remained closed with regards to Rb and Sr since time of crystallization, the initial $^{87}Sr/^{86}Sr$ ratios of the

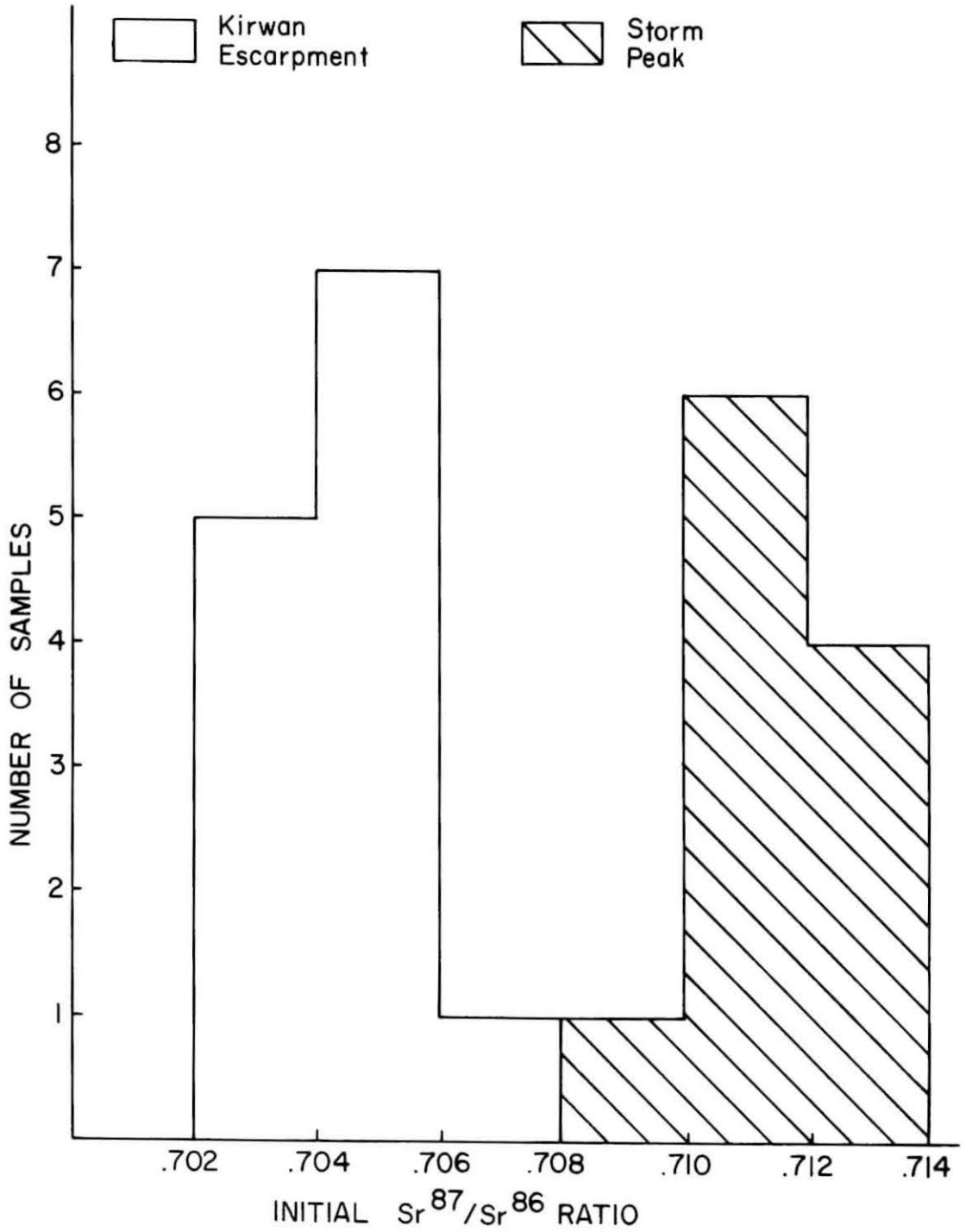


Figure 5. Initial $Sr^{87}/Sr^{86}$ in the Kirkpatrick (Storm Peak) and Kirwan Escarpment Basalts.

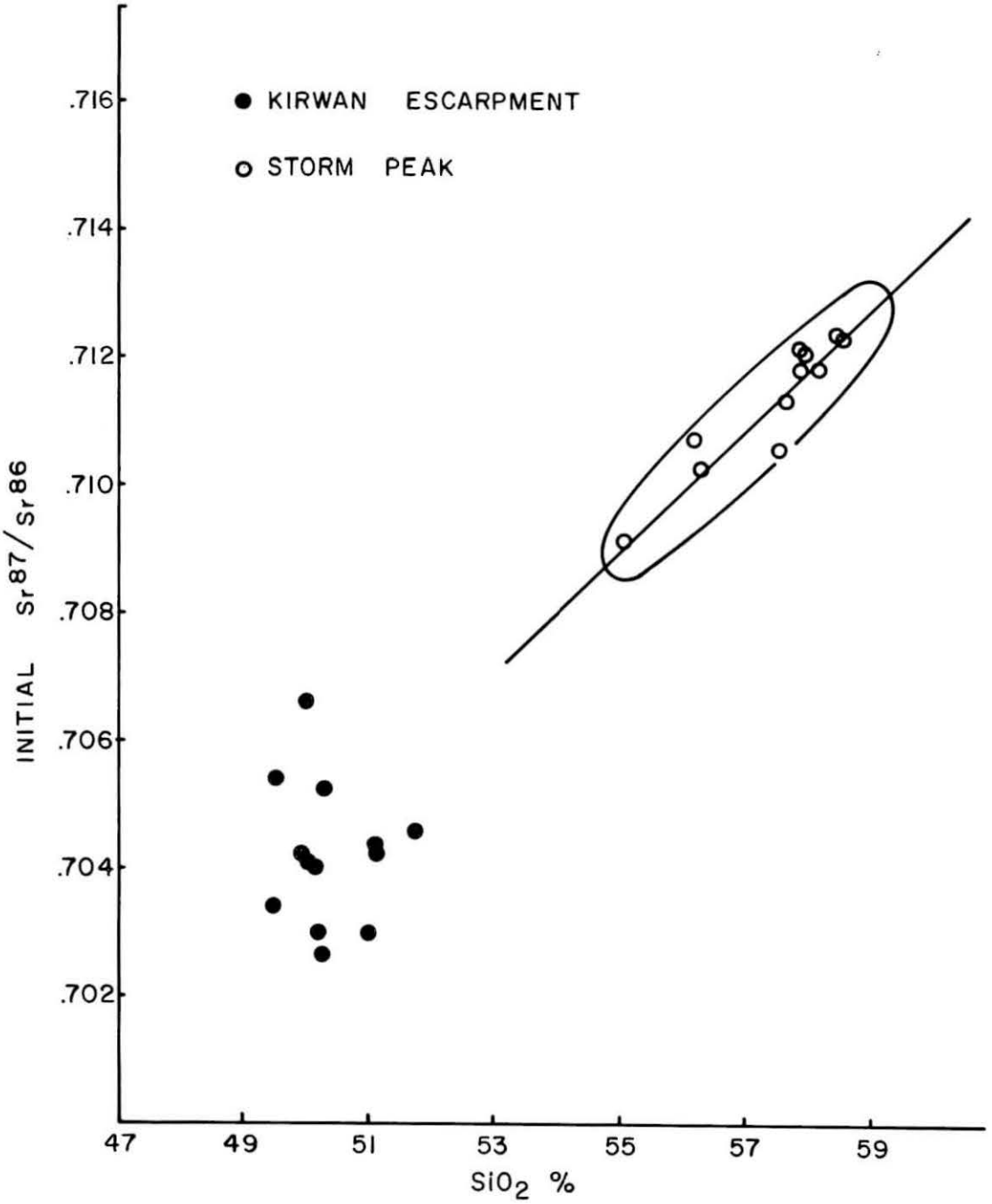


Figure 6. Initial $Sr^{87}/Sr^{86}$ vs. $SiO_2$ Content for the Kirkpatrick Basalt at Storm Peak and the Kirwan Escarpment Basalt. Symbols are consistent in Figures which compare the two suites.

basalt flows, regardless of $SiO_2$ content or other geochemical parameter, should be identical, within analytical error.

The presence of the $SiO_2$ - initial $^{87}Sr/^{86}Sr$ ratio correlation in the flow sequence at Storm Peak confirms the preliminary discovery of such a correlation by Faure, et al. (1970). A combined plot of samples analyzed in this project and those analyzed by Faure, et al. (1970) from the same stratigraphic section at Storm Peak is shown in Figure 7. It is apparent from this plot that, although each set of analytical results exhibits a distinct and well-developed positive correlation, the slopes of the two lines are different. The different sets of samples apparently are not related in any systematic stratigraphic or chemical manner, so it is believed that the differences in slopes are due to a systematic analytical error in the determination of the Rb/Sr or $^{87}Sr/^{86}Sr$ ratios for one of the suite of samples. Duplication of analyses is in progress and we expect to be able to reconcile the two sets of data.

Other geochemical and Sr isotope correlations exist within the Storm Peak basalt sequence. Plots of the $K_2O$, $Na_2O$, CaO, and MgO content and the initial $^{87}Sr/^{86}Sr$ for five basalt samples from different flows at Storm Peak are shown in Figure 8. Good positive correlation of the initial $^{87}Sr/^{86}Sr$ and $K_2O$ content is present, with some scatter. A good negative correlation of the initial $^{87}Sr/^{86}Sr$ and CaO, and a less well-defined negative correlation with MgO, is also found. No systematic relationship seems to exist between the initial $^{87}Sr/^{86}Sr$ ratio and $Na_2O$ content. These correlations are based on only five samples and so are preliminary in nature, but they confirm those found by Faure, et al. (1970) in other Kirkpatrick Basalt samples from Storm Peak.

These correlations of the initial $^{87}Sr/^{86}Sr$ ratio with $K_2O$, MgO, and CaO are geochemically consistent with previously discussed positive correlations with $SiO_2$ to the extent that CaO and MgO are both segregated from $K_2O$ and $SiO_2$ in normal igneous processes. It is apparent that whatever processes are enriching the Storm Peak basalt samples in $K_2O$ and $SiO_2$ and depleting them in MgO and CaO are also enriching these samples in radiogenic $^{87}Sr$.

These correlations are quite significant, because as emphasized previously, no magmatic differentiation process is known to fractionate Sr isotopes. If the observed variations in $K_2O$, MgO, and CaO concentration were due solely to differentiation processes, there would be no correlation of the initial $^{87}Sr/^{86}Sr$ ratio with these parameters, positive or negative.

Figure 9 is a plot of Rb versus Sr concentration, in which the great geochemical separation of these two suites is again illustrated by a total lack of overlap of Rb and Sr values. These differences in Rb and Sr concentrations are similar to those found by Faure, et al. (1970) for basalt from western Queen Maud Land and from the Transantarctic Mountains.

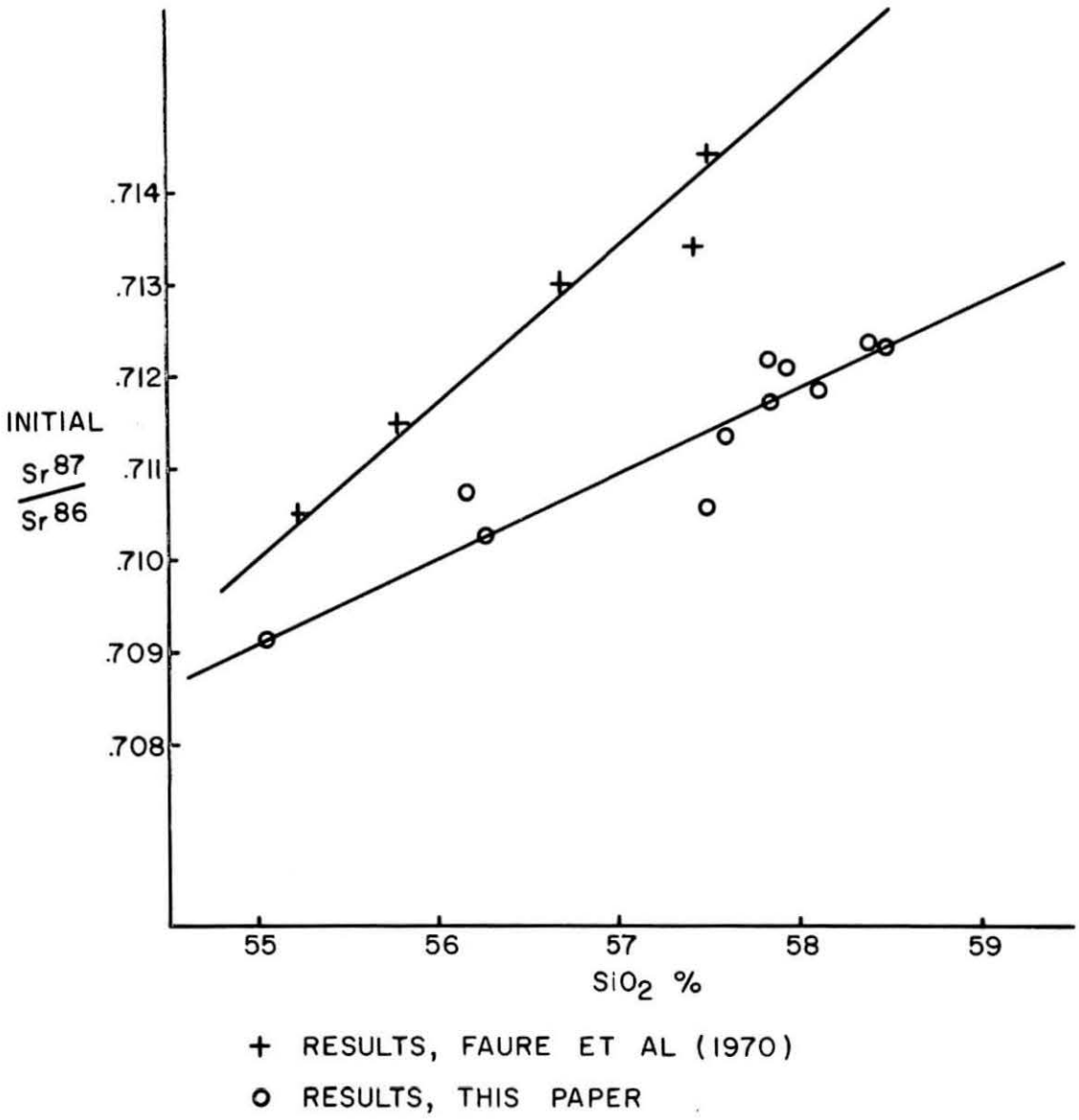


Figure 7. Initial $Sr^{87}/Sr^{86}$ vs. $SiO_2$ Content for the Kirkpatrick Basalt at Storm Peak Utilizing Data from Faure et al. (1970) and This Study.

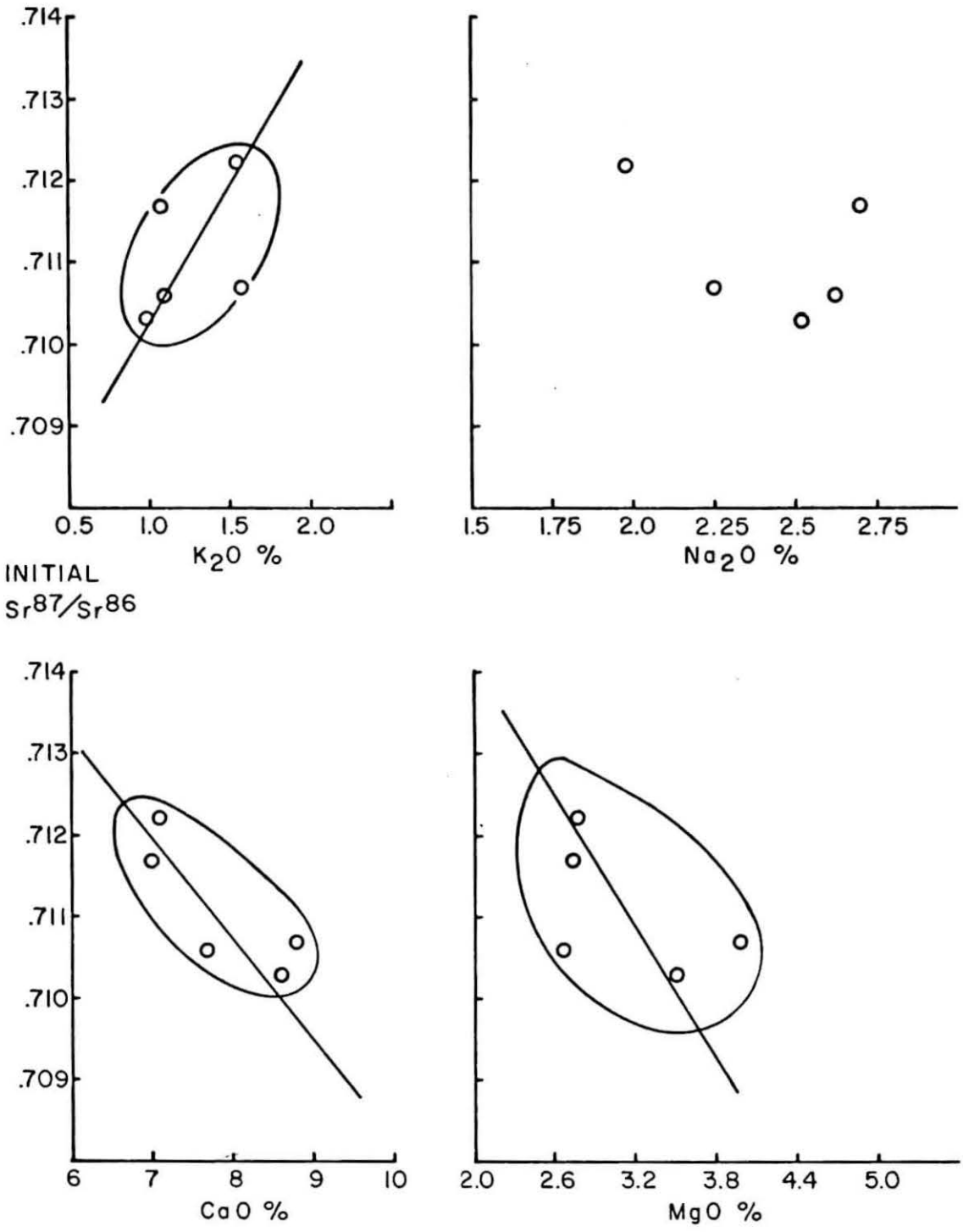


Figure 8. Initial $Sr^{87}/Sr^{86}$ vs. $K_2O$, $Na_2O$, CaO, and MgO Content for Five Kirkpatrick Basalt Samples from Storm Peak.

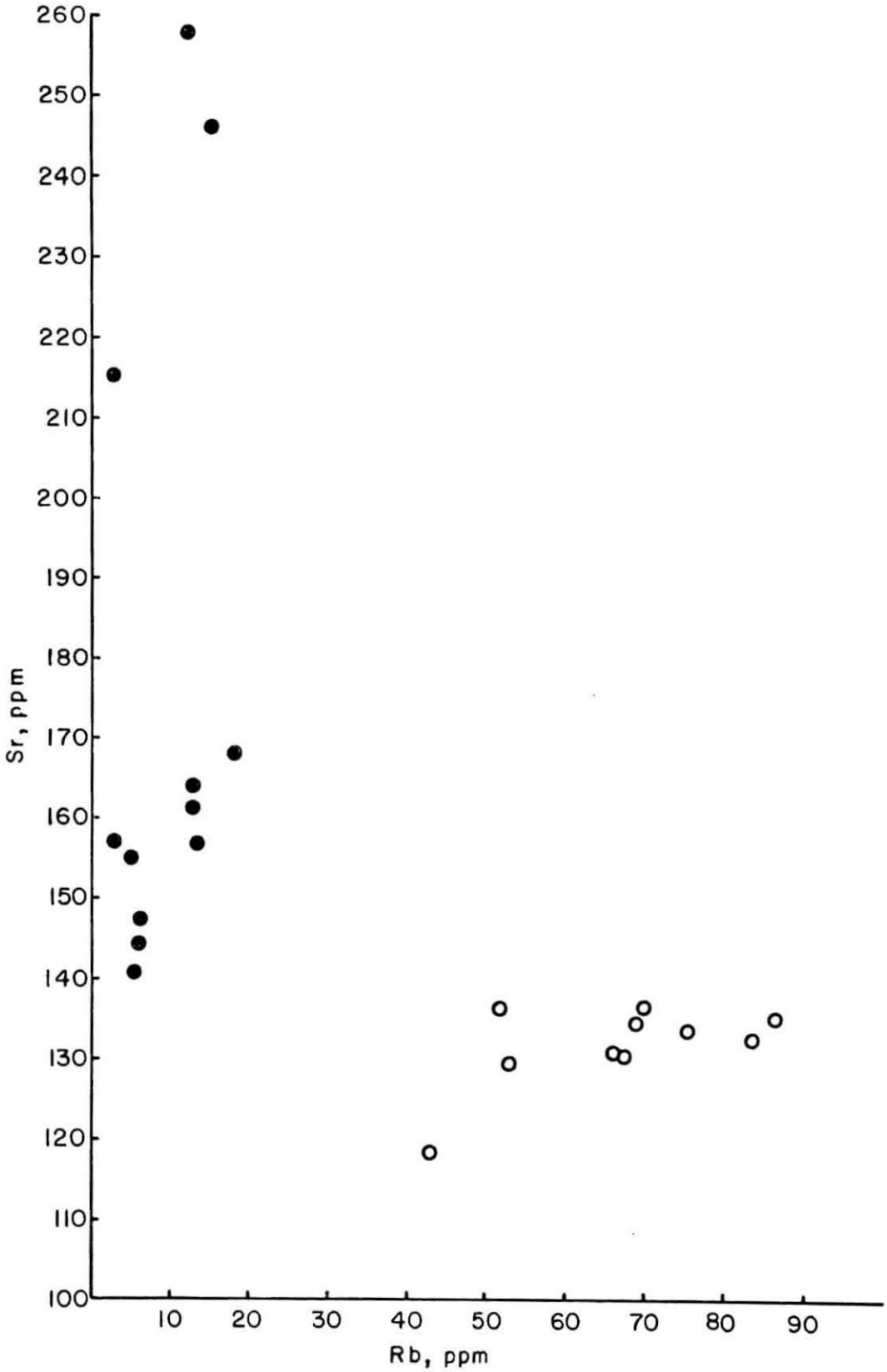


Figure 9. Sr vs. Rb Content for the Kirwan Escarpment and Storm Peak Basalts.

From the previous discussion, it is clear that the basalt sequences from the Kirwan Escarpment and Storm Peak are distinctly different in terms of $SiO_2$, Rb, and Sr concentrations, and the Rb/Sr and initial $^{87}Sr/^{86}Sr$ ratios. The Kirwan Escarpment basalts are characterized by chemical compositions and Sr isotope ratios typical of basaltic rocks (Lessing, et al., 1963; Faure and Hurley, 1963; Engel et al., 1965; Gast, 1965). There is significant variability of values for the above parameters in the basalt samples from this sequence of flows but no definite systematic relationships between them are exhibited.

In complete contrast, the Kirkpatrick Basalt flow sequence on Storm Peak is characterized by high $SiO_2$, Rb, and $K_2O$ contents, low MgO, CaO, and Sr contents, low K/Rb ratios, and high Rb/Sr and initial $^{87}Sr/^{86}Sr$ ratios. These characteristics are completely atypical for normal basalts and continental tholeiites (Heier, et al., 1965; Compston, et al., 1968; Hill, 1969; Faure, et al., 1970). In addition, definite and significant correlations exist between the initial $^{87}Sr/^{86}Sr$ ratio and $SiO_2$, $K_2O$, CaO, MgO, and Rb contents.

In order to gain insight into the origin of these two suites of basalts, and in particular to investigate the peculiar characteristics of the Kirkpatrick Basalt at Storm Peak, it is instructive to examine the variations of the chemical and isotopic compositions of Sr within each sequence of flows.

In the preliminary investigation of the Storm Peak basalt samples, Faure, et al. (1970) noted that there was a systematic relationship between the value of the initial $^{87}Sr/^{86}$ ratio, the $SiO_2$ content, and stratigraphic position within the flow sequence; the initial $^{87}Sr/^{86}Sr$ ratio and $SiO_2$ content decreased from the bottom of the sequence toward the top. Analyses of ten additional basalt samples in this study make possible a plot of initial $^{87}Sr/^{86}Sr$ ratio vs. stratigraphic position in the section at Storm Peak. This plot is shown in Figure 10. It can be seen that three cycles appear to be present. The cycles are marked by discontinuities in the initial $^{87}Sr/^{86}Sr$ ratio and have been numbered from the bottom up: cycle I includes flows 2-4, cycle II includes flows 5-10, cycle III includes flows 11 and 12. The extent of the development of these cycles varies, with cycle II being most complete. Flow 2 forms most of the stratigraphic thickness of Cycle I. There is some variation of the initial $^{87}Sr/^{86}Sr$ ratio within this flow which conforms to the general decrease in this ratio for the cycle as a whole. Most of this apparent variation is not real, however, but is probably due to analytical uncertainty.

The Sr isotope data from this study confirms the general conclusion resulting from the earlier data of Faure, et al. (1970), but indicate that the situation is more complicated because there are major discontinuities in the initial $^{87}Sr/^{86}Sr$ ratio. The presence of these cycles may indicate (1) change in magma source area, (2) periods of quiescence, (3) changes in rate of magma ascent, or discontinuities of magma development. The flow separating cycles I and II contains logs (Elliot, 1969,

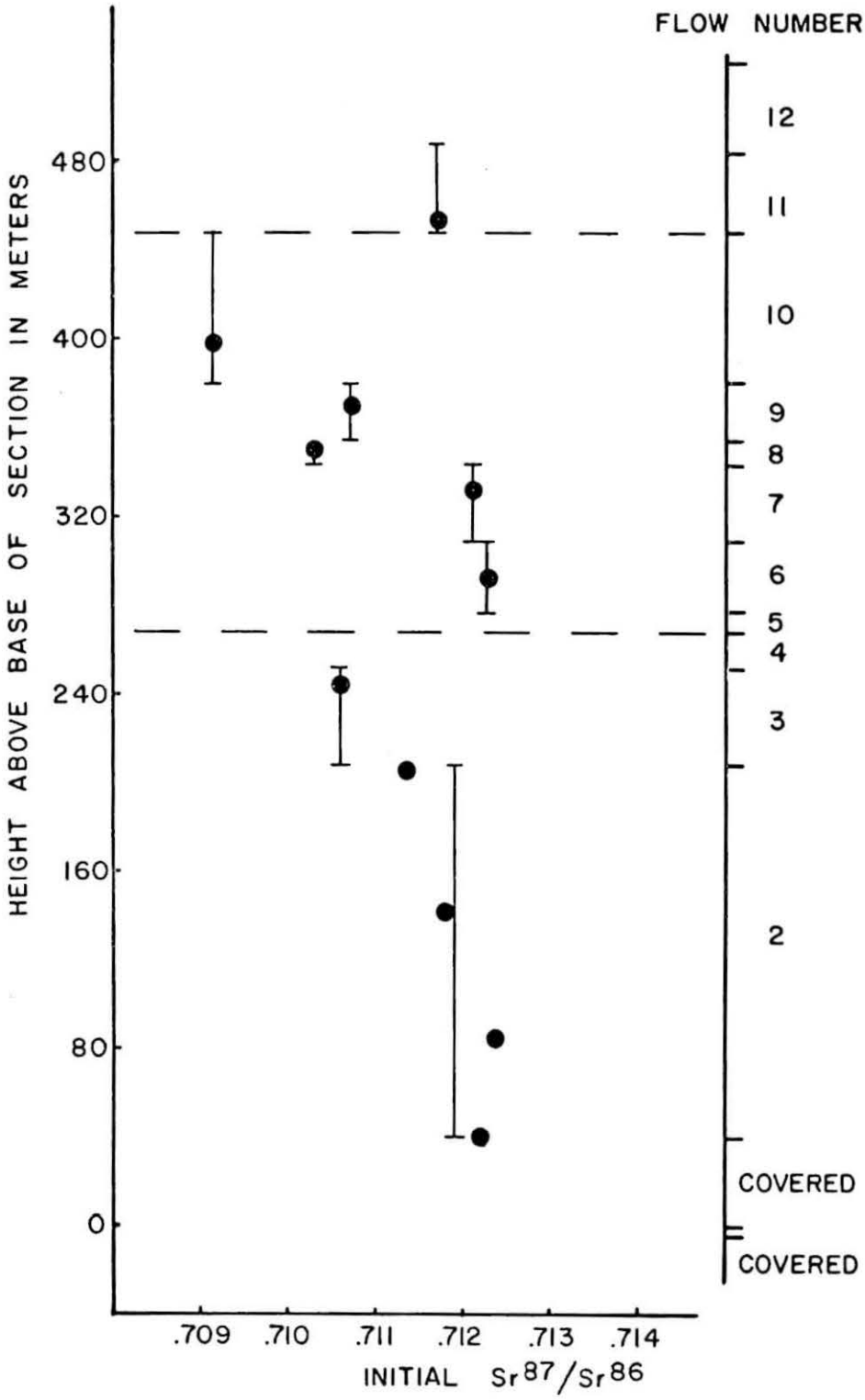


Figure 10. Initial $Sr^{87}/Sr^{86}$ vs. Sample Stratigraphic Position, Storm Peak Section.

1970) which indicates a period of quiescence of unknown length. The flow contact between cycle II and III is covered, and has not yet been examined. Whatever the cause for these Sr-isotope discontinuities and resultant cycles, it must again be emphasized that the significant variation of the initial $^{87}Sr/^{86}Sr$ within each cycle and the discontinuities bounding the cycles cannot be explained by processes of magmatic differentiation alone.

Because of the presence of the three volcanic cycles, the initial $^{87}Sr/^{86}Sr$ ratios basalt from cycles I and II were replotted versus their $SiO_2$ contents. Since the hypothetical cycle III is defined by only one sample, it was omitted. The plots for cycle I and II are shown in Figure 11. The correlation of the initial $^{87}Sr/^{86}Sr$ ratios with $SiO_2$ within each cycle is striking. The differences in slope for each cycle are also significant. The explanation of this phenomenon is not yet clear.

The discontinuities in the initial $^{87}Sr/^{86}Sr$ ratio of the basalt sequence at Storm Peak is also reflected by other geochemical parameters with which the initial $^{87}Sr/^{86}Sr$ ratio has been shown to display some of correlation. Figure 12 is a plot of Rb, Sr, and $SiO_2$ concentrations for samples from this study plus the six samples analyzed by Faure, et al. (1970) vs. position within the stratigraphic section of the samples. The lines connecting each sample position on the diagram are only intended to assist in the visualization of the mutual relationships of these parameters and do not imply that there is continuous variation of these parameters between the flows. Several striking facts are apparent.

Rb, Sr and $SiO_2$ content all reflect the presence of the three cycles by major discontinuities in their respective concentrations. The stratigraphic positions of the discontinuities indicated by Rb and $SiO_2$ are very nearly coincident with those defined by the initial $^{87}Sr/^{86}Sr$ ratios. Figure 13 is a plot of $Na_2O$, $K_2O$, MgO, and CaO concentration vs. sample position within the Storm Peak stratigraphic section. The two discontinuities are quite clearly shown by $K_2O$, CaO, MgO, and less well by $Na_2O$. The coherent variation of the CaO and MgO content is well developed as expected from the geochemical behavior of Mg and Ca. The $K_2O$ concentrations are coherent with $SiO_2$ and Rb concentration variations and moderately consistent with variations in the initial $^{87}Sr/^{86}Sr$ ratio, with some exceptions. No easily identifiable systematic variation exists in $Na_2O$ content within the stratigraphic section. Nevertheless, a fairly well-developed expression of the geochemical discontinuity between cycles I and II can be seen in the $Na_2O$ content.

The Rb/Sr ratios also reflect the presence of three cycles, as shown in Figure 14. Since no systematic relationship exists between the Rb/Sr ratio and the initial $^{87}Sr/^{86}Sr$ ratio, it is surprising that a cyclic increase of Rb/Sr ratio exists. However, except for variations between flows 7, 8, and 9 of cycle II, there is no significant difference

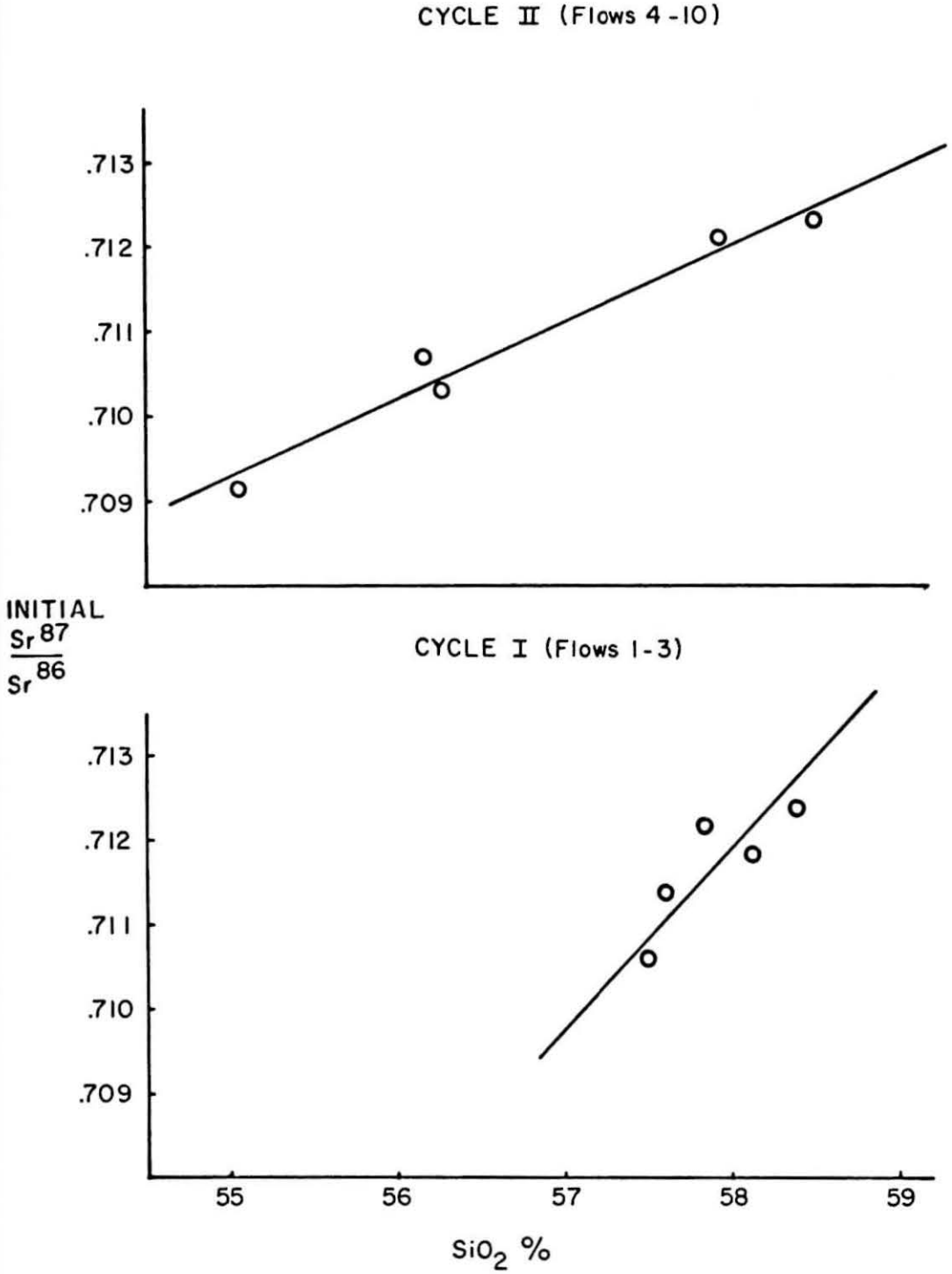


Figure 11. Initial $Sr^{87}/Sr^{86}$ vs. $SiO_2$ Content for Cycles I and II, Storm Peak Section.

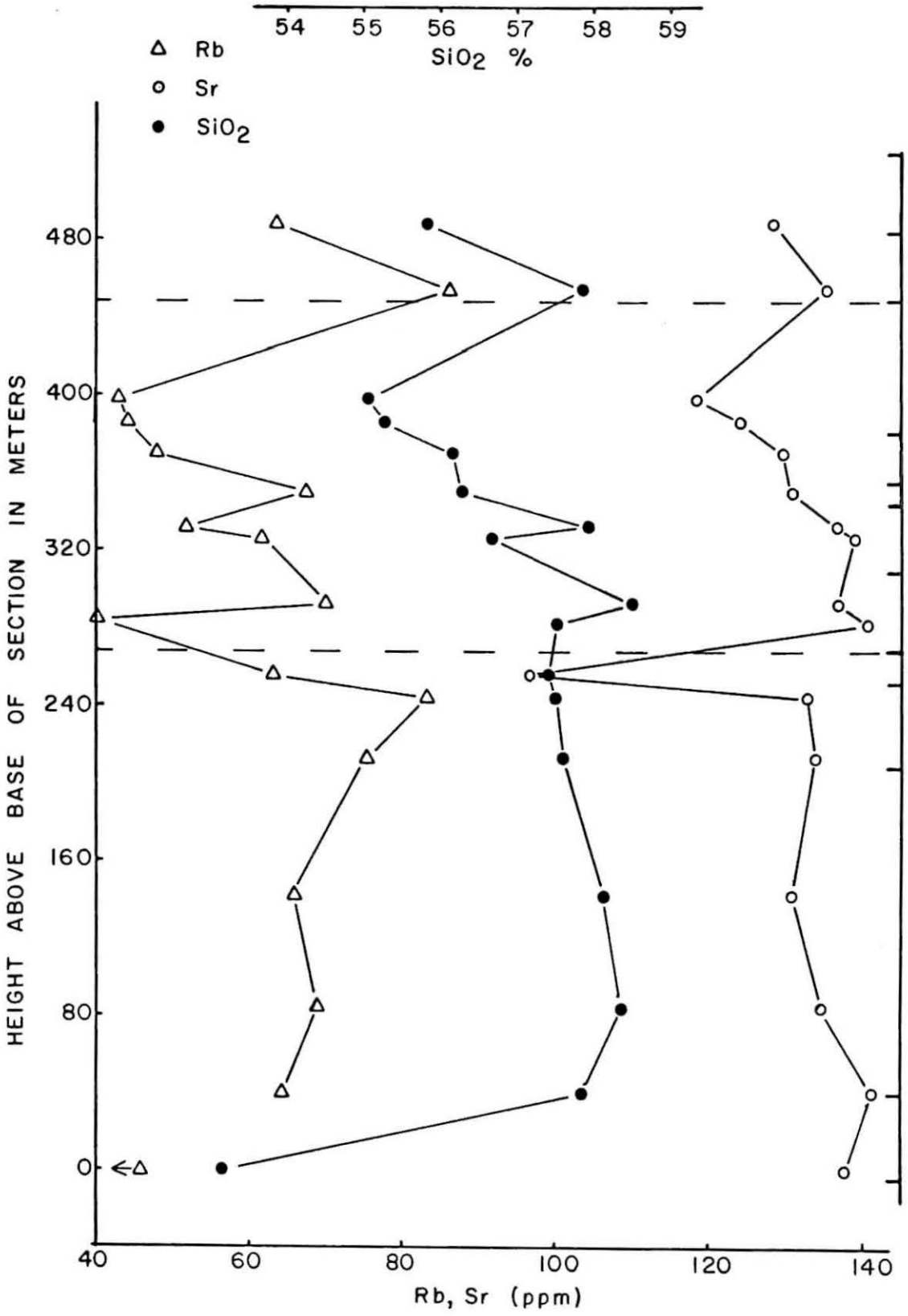


Figure 12. Rb, Sr, and $SiO_2$ Content vs. Sample Stratigraphic Position, Storm Peak Section.

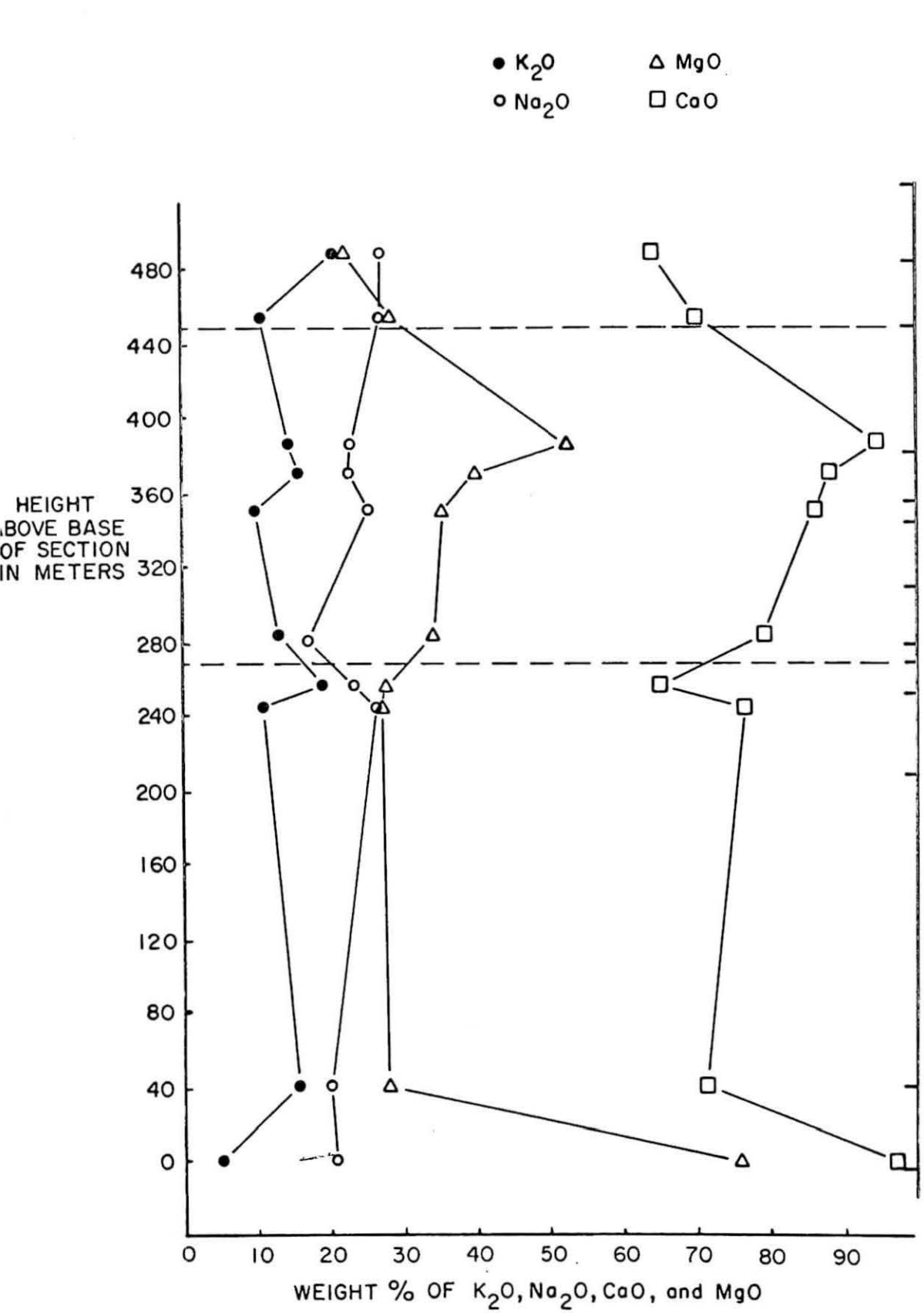


Figure 13. $Na_2O$, $K_2O$, MgO, and CaO Content vs. Sample Stratigraphic Position, Storm Peak Section.

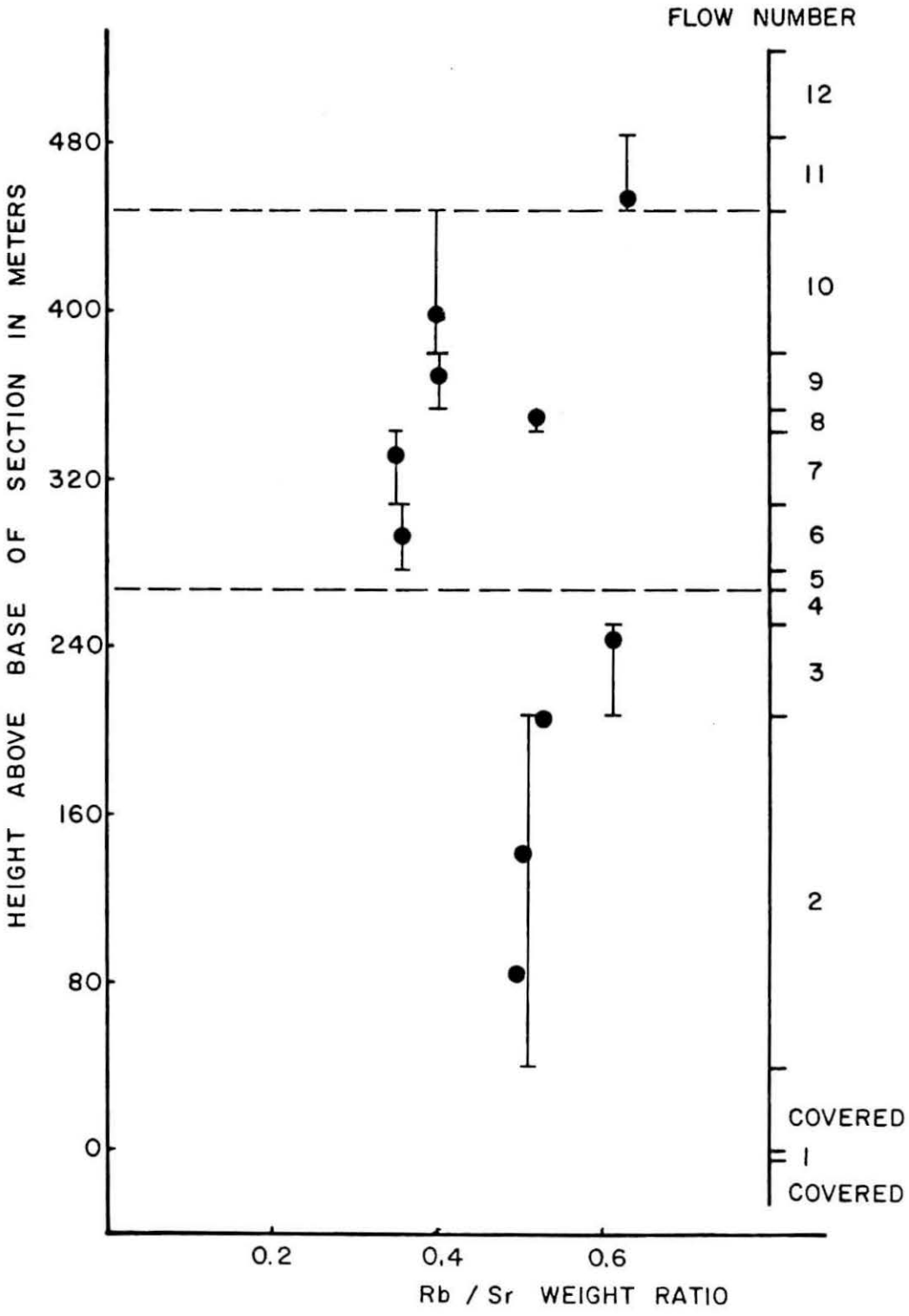


Figure 14. Rb/Sr vs. Sample Stratigraphic Position, Storm Peak Section.

in the Rb/Sr ratios of flows within each cycle, at the 95 percent confidence level. Significant changes do occur at the discontinuities.

Plots of analytical results vs. sample position within the stratigraphic section for the Kirwan Escarpment basalt sequence are shown in Figures 15 and 16. Figure 15 is a plot of the initial $^{87}Sr/^{86}Sr$ ratio vs. stratigraphic position. Sample T-1-1 was taken from the sequence at Tunga, 35 km E-NE from Mountain "B". T-1-1 is shown on the Mountain "B" section at its relative stratigraphic position in meters above base of flow sequence. The initial $^{87}Sr/^{86}Sr$ ratio of these samples display some variation up section. The variation in this ratio is real, but seemingly no major discontinuities exist in this basalt sequence, in contrast to the Kirkpatrick Basalt on Storm Peak.

Figure 16 is a plot of Rb, Sr and $SiO_2$ content versus stratigraphic position for the Kirwan Escarpment basalt samples. Again, the only significance of the lines joining points on the graph is to assist in visualizing the mutual relationships of these chemical parameters, and does not imply continuous variation between samples. There is no readily apparent discontinuity at any stratigraphic position in this section.

## Summary

On the basis of data presented in the previous discussion, the following characteristics of the Kirkpatrick Basalt at Storm Peak and the Kirwan Escarpment basalt can be noted:

1. The Storm Peak basalts are characterized by unusually high $SiO_2$, Rb, and $K_2O$ contents, low MgO, CaO, and Sr contents, abnormally high initial $^{87}Sr/^{86}Sr$ and Rb/Sr ratios, and low K/Rb ratios. These values are completely atypical of normal basaltic rocks.

2. In contrast, the basalts at the Kirwan Escarpment are characterized by initial $^{87}Sr/^{86}Sr$ ratios and Rb, Sr, and $SiO_2$ concentration values more typical of normal continental tholeiites.

3. The Storm Peak basalt samples show significant and well-defined positive correlations of the initial $^{87}Sr/^{86}Sr$ ratio with $K_2O$, Rb, and $SiO_2$, and negative correlation of this ratio with MgO and CaO.

4. In complete contrast, no definite correlation of the initial $^{87}Sr/^{86}Sr$ ratios of the basalt samples from the Kirwan Escarpment with Rb, Sr, or $SiO_2$ content exists.

5. Both basalt sequences were initially inhomogeneous with respect to the isotope composition of Sr, or have been open Rb and/or Sr since time of crystallization.

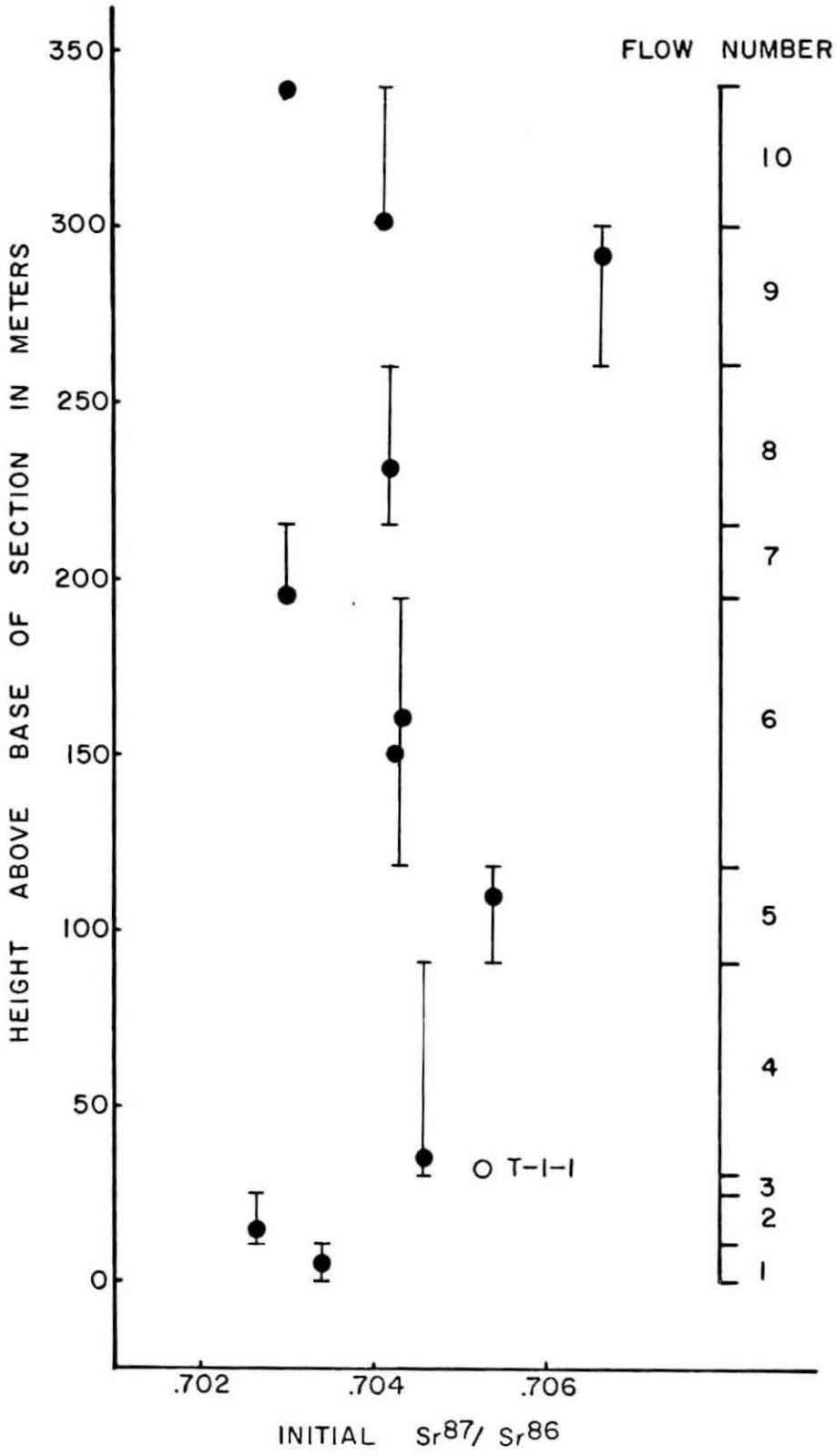


Figure 15. Initial $Sr^{87}/Sr^{86}$ vs. Sample Stratigraphic Position, Kirwan Escarpment Section.

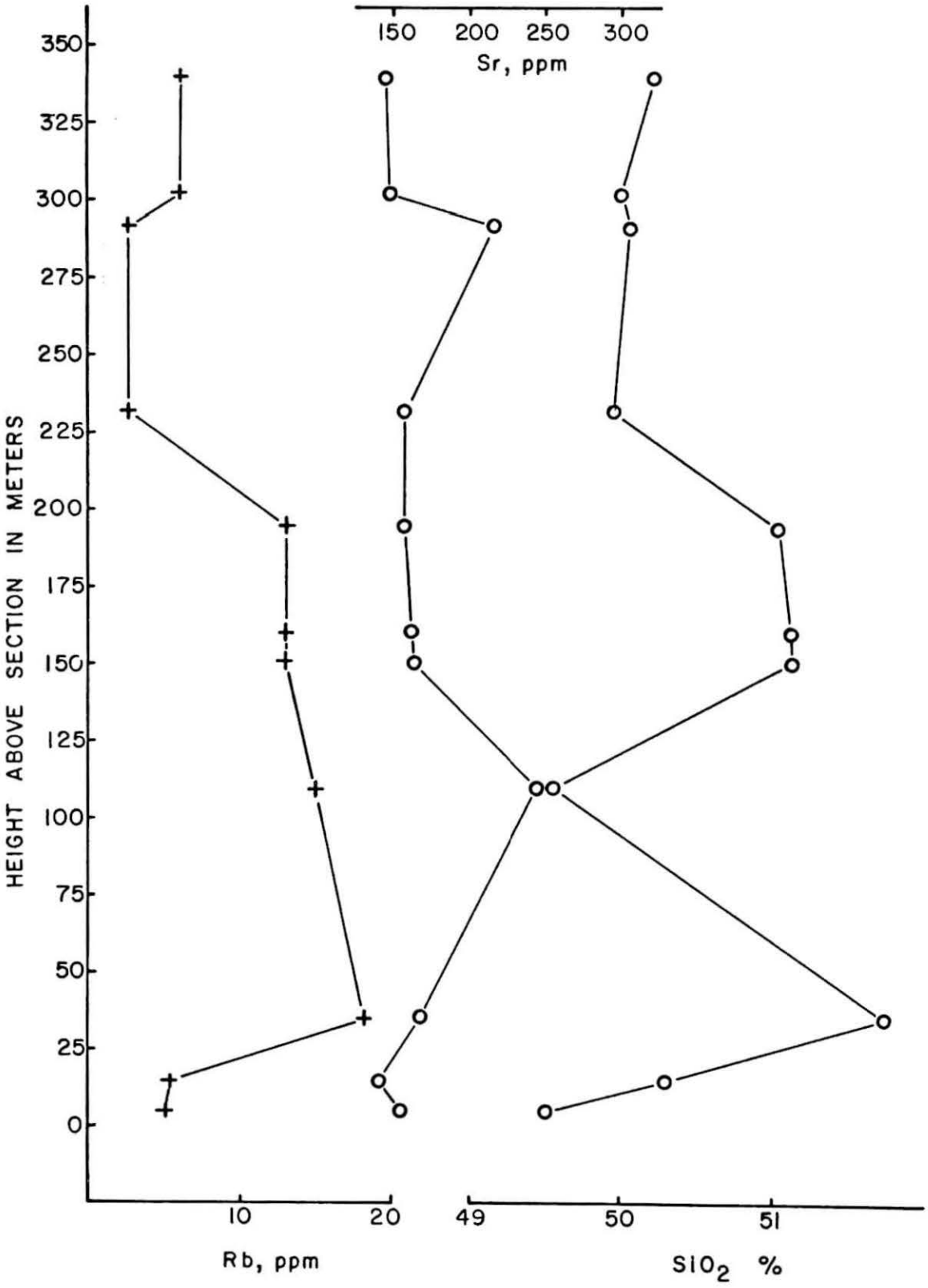


Figure 16. Rb, Sr, and $SiO_2$ Content vs. Sample Stratigraphic Position, Kirwan Escarpment Section.

6. All analytical data for the Kirkpatrick Basalt samples from Storm Peak indicate the existence of significant chemical discontinuities at certain well-defined stratigraphic positions within the flow-sequence which define two, and possibly three, different cycles of eruption. Complicated by these discontinuities, the $SiO_2$ contents and the initial $^{87}Sr/^{86}Sr$ ratios decrease up the section in each of the cycles.

7. The analytical data for the Kirwan Escarpment basalt samples indicate no well-defined and consistent chemical discontinuities. The initial $^{87}Sr/^{86}Sr$ ratio oscillates in value up section. The Sr concentration may also vary coherently with the initial $^{87}Sr/^{86}Sr$, but no precise relationship can be determined at this time.


## Acknowledgments

This research was made possible by the generous cooperation of D. C. Neethling and L. G. Wolmarans of the Geological Survey of South Africa who provided the suite of basalt samples from the Kirwan Escarpment of Queen Maud Land. We are also grateful to D. H. Elliot for sharing with us his collection of Kirkpatrick Basalt from Storm Peak, Transantarctic Mountains


## References


Bowman, J. R., 1971, Use of the isotopic composition of strontium and $SiO_2$ content in determining the origin of Mesozoic basalt from Antarctica. M.Sc. Thesis, Dept of Geology. The Ohio State University, 179p.

Compston, W., McDougall, I., and Heier, K. S., 1968, Geochemical comparison of the Mesozoic basaltic rocks of Antarctica, South Africa, South America, and Tasmania: Geochim. et Cosmochin. Acta, v. 32, No. 2, p. 129-149.

Elliot, D. H., 1969, Jurassic Tholeiites of the central Transantarctic Mountains, Antarctica: Proceedings of the Second Columbia River Basalt Symposium, Cheney, Washington, U.S.A.

Elliot, D. H., 1970, Major oxide chemistry of the Kirkpatrick Basalt, central Transantarctic Mountains, Antarctica: SCAR/IUGS Symposium on Artarctic Geology and Solid Earth Geophysics, Oslo.

Engel, A. E. J., Engel, C. G., and Havens, R. G., 1965, Chemical Characteristics of Oceanic Basalts and the Upper Mantle: GSA Bull. 76, p. 719-734.

Erlank, A. J. and Hofmeyr, P. K., 1966, K/Rb and K/Cs ratios in Karoo dolerites from South Africa: Jour. of Geophys. Res., v. 71, p. 5439.

Erlank, A. J. and Hofmeyr, P. K., 1968, K/Rb ratios in Mesozoic tholeiites from Antarctica, Brazil, and India: Earth and Planetary Sci. Letters, v. 4, p. 33.

Faure, G. and Hurley, P. M., 1963, The isotopic composition of Strontium in oceanic and continental basalts: Application to the origin of igneous rocks: Jour. Petrology, v. 4, p. 31-50.

Faure, G., and Elliot, D. H., 1970, Isotope composition of strontium in Mesozoic basalt and dolerite from Dronning Maud Land: Contribution 11, Laboratory for Isotope Geochemistry, Ohio State University, Columbus, Ohio.

Faure, G., Hill, R. L., Jones, L. M., and Elliot, D. H., 1970, Isotope composition of strontium and silica content of Mesozoic Basalt and Dolerite from Antarctica: SCAR/IUGS Symposium on Antarctic Geology and Solid Earth Geophysics, Oslo.

Gast, P. W., 1960, Limitations of the composition of the upper mantle: Jour. Geophys. Res., v. 65, p. 1287-1297.

_____, 1965, Terrestrial ratio of potassium to rubidium and the composition of the earth's mantle: Science, v. 147, p. 858-860.

Gunn, B. M., 1965, K/Rb and K/Ba ratios in Antarctic and New Zealand tholeiites and alkali basalts: Jour. Geophys. Res., v. 70, No. 24, p. 6241.

Hedge, C. E. and Walthall, F. G., 1963, Radiogenic Strontium-87 as an index of geological processes: Science, v. 140, No. 3572, p. 1214.

Heier, K. S., Compston, W., and McDougall, I., 1965, Thorium and Uranium Concentrations, and the Isotopic Composition of Strontium in the Differentiated Tasmanian Dolerites: Geochim. et. Cosmochim, Acta, v. 29, No. 6, p. 643-659.

Hill, R. L., 1969, Strontium Isotope Composition of Basaltic Rocks of the Transantarctic Mountains, Antarctica: unpublished M.Sc. Thesis, The Ohio State University, Columbus, Ohio.

Juckes, L. M., 1968, The geology of Mannefallknausane and part of Vestfjella, Dronning Maud Land: British Antarct. Survey Bull. 18, pp. 65-78.

Lessing, P. and Catanzaro, E. J., 1964, $^{87}Sr/^{86}Sr$ in Hawaiian lavas: Jour. Geophys. Res., v. 69, p. 1599.

Lessing, P., Decker, R. W., and Reynolds, R. C., Jr., 1963, Potassium and rubidium distributions in Hawaiian lavas: Jour. Geophys. Res., v. 68, p. 5851.

Manson, V., 1967, Geochemistry of Basaltic Rocks: Major Elements: In Basalts: The Poldervaart Treatise on Rocks of Basaltic Composition, v. I, H. H. Hess and A. Poldervaart, ed., New York, Interscience Publishers, p. 215-269.

Manton, W. I., 1968, The origin of associated basic and acid rocks in the Lebombo-Nuanetsi igneous province, Southern Africa, as implied by strontium isotopes: Jour. Petrology, v. 9, p. 23.

McDonald, G. A. and Katsura, T., 1964, Chemical composition of Hawaiian lavas: Jour. Petrol., v. 5, p. 82.

Neethling, D. C., 1970a, Age and correlation of the Ritscher Supergroup and other precambrian rock units, Queen Maud Land, Antarctica: SCAR/IUGS Symposium on Antarctic Geology and Solid Earth Geophysics, Oslo.

Neethling, D. C., 1970b, Comparative Geochemistry of Proterozoic and Paleozoic Tholeiites of western Queen Maud Land: SCAR/IUGS Symposium on Antarctic Geology and Solid Earth Geophysics, Oslo.

Printz, M., 1967, Geochemistry of Basaltic Rocks: Trace Elements: In Basalts: The Poldervaart Treatise on Rocks of Basaltic Composition, v. I. H. H. Hess and A. Poldervaart, ed. New York, Interscience Publishers, p. 271-324.

Tatsumoto, M., Hedge, C. E., and Engel, A. E. J., 1965, Potassium, rubidium, strontium, thorium, uranium and the ratio of strontium-87 to strontium-86 in oceanic tholeiitic basalt: Science, v. 150, p. 886.

Wade, F. A., Yeats, V. L., Everett, J. R., Greenlee, D. W., LaPrade, K. E., and Shenk, J. C., 1965. The geology of the central Queen Maud Range, Transantarctic Mountains, Antarctica. Texas Tech. Coll. Research Rept. Ser., Antarctic Ser., 65-1, 54 p.